12-14-2014

Nitrogen Isotopes in the Measurement of N2-Fixation and the Estimation of Denitrification in the Global Ocean

Richard Dabundo
University of Connecticut - Avery Point, richard.dabundo@uconn.edu

Nitrogen Isotopes in the Measurement of N_2-Fixation and the Estimation of Denitrification in the Global Ocean

Richard Dabundo

B.S. Pennsylvania State University, 2014

A Thesis

Submitted in Partial Fulfillment of the

Requirements for the Degree of

Master of Science

At the

University of Connecticut

2014

APPROVAL PAGE

Masters of Science Thesis

Nitrogen Isotopes in the Measurement of N_2-Fixation and the Estimation of Denitrification in the Global Ocean

Presented by

Richard Dabundo, B.S.

Major Advisor_____
Julie Granger

Associate Advisor_____
Craig R. Tobias

Associate Advisor_____
Pieter T. Visscher

University of Connecticut

2014

Acknowledgements

I would like to thank everyone at the University of Connecticut who has assisted me in the pursuit of my MS. Julie Granger, who was essential in providing support, the initial ideas behind the research projects, and continued guidance throughout the research process. Lija Treibergs, who helped to both provide important insights and to keep our laboratory moving. Craig Tobias for his patience and assistance even though he always seemed to have too much to do. Pieter Visscher, for sharing his in-depth knowledge of microbiology. David Cady, for his help whenever we had problems, and his uncanny knowledge of seemingly every scientific instrument. Claudia Koerting, who provided my introduction to the Avery Point laboratory environment. The Dam lab for help with my excursion into the growth of phytoplankton. And, finally, George McManus for readily providing access to his equipment and assistance in its use.

Table of Contents

List of Tables

List of Figures

Chapter 1

Environmental controls on the isotope effect of denitrification in *Paracoccus denitrificans* and its implications for the global oceanic nitrogen budget

Introduction

Nitrogen (N) is an essential nutrient for all living organisms, as well as a major limiting nutrient of primary production in the ocean. As a limiting nutrient, fixed N, which consists of all organic N and inorganic N compounds that are more biologically accessible than N_2, exhibits significant control over ocean productivity, thus influencing food web dynamics and oceanic carbon sequestration (Vitousek and Howarth 1991; Gruber and Galloway 2008). While fixed nitrogen undergoes numerous biological and chemical reactions within the environment, there exist few marine inputs and outputs. N inputs to the ocean consist of both natural and anthropogenic fixed N added via terrestrial runoff (river and groundwater fluxes), atmospheric deposition, and microbial N_2 fixation. N_2 fixation is the biological reduction of gaseous N_2 to ammonium (NH_4^+), which is subsequently incorporated into organic matter. Its activity in the surface ocean constitutes the dominant oceanic input of fixed N. Outputs from the marine system consist of water-column and benthic denitrification, anaerobic ammonium oxidation (anammox), and sedimentary burial (Gruber and Galloway 2008). Denitrification is the biological conversion of nitrate (NO_3^-) to N_2 via the enzymatic reduction of NO_3^- to nitrite (NO_2^-), NO_2^- to nitrous oxide (N_2O), and finally N_2O to N_2 gas. It is an important respiratory process that occurs only in the near or total absence of oxygen (Stouthamer et al. 1982). Anammox is a more recently discovered route for the conversion of reactive N to N_2 gas, reducing NO_2^- to N_2 using ammonium (NH_4^+) as the reductant (van de Graaf et al. 1996). Both denitrification and anammox are inhibited by oxygen, and thus, within the marine environment, these processes predominately take place within oxygen minimum zones and sediments where the decomposition of organic matter has depleted ambient oxygen (Gruber 2008).

Estimates of total oceanic N inputs and outputs (i.e. nitrogen budgets) have been developed using a variety of techniques, resulting in a wide range of estimates (Table 1), and leading to much debate. While direct measurement of N flux processes is the best way to obtain accurate rates, financial and temporal restrictions render the complete measurement of inputs and outputs impractical. The formulation of an overall nitrogen budget thus requires indirect calculations, such as extrapolations from semi-conservative, nutrient based tracers (such as N*, Gruber and Sarmiento 1997) and/or from isotopic tracers. N* is a term used to estimate local net N flux, and is derived from the concept of the Redfield ratio. Based on the premise that the remineralization of plankton material in the ocean's subsurface yields inorganic nitrogen and phosphorous (P) in a ratio of nearly 16:1, given the stoichiometry of phytoplankton nutritional requirements (Redfield et al. 1963; Anderson and Sarmiento 1994), local or regional deviations from the 16:1 ratio in subsurface nutrients can be interpreted as the integrated magnitude of local inputs and/or outputs of N (Gruber and Sarmiento 1997). Net nitrogen input is assumed to be a result of biological N_2 fixation and net output a result of water-column or benthic denitrification, including anammox (Dalsgaard et al. 2003; Lam et al. 2009; Dalsgaard et al. 2012). While useful, N* is biased by non-Redfield N:P remineralization fluxes (Deutsch et al. 2012), and requires the extrapolation of patterns derived from finite measurements to the entire ocean. Moreover, N* is insensitive to nutrient fields that integrate concomitant regional N_2 fixation and denitrification (Gruber 2004). Nitrogen isotopic tracers can provide complimentary constraints in this respect. This is done using knowledge of the isotopic composition of environmental N pools (reported as $\delta^{15}N$) and the isotope effect (ε) of different N cycle processes (explained in detail below). The isotope effect of a process affecting N isotopic ratios ($^{15}\varepsilon$) is a function of the relative reaction rates of ^{14}N and ^{15}N in said process (^{14}k and ^{15}k, respectively), where a positive

isotope effect indicates preferential use of the light isotope in a given reaction. $\delta^{15}N$ and $^{15}\varepsilon$ are reported in per mil (‰) units, and are defined by equations 1 and 2, respectively:

$$(1)\ \delta^{15}N_{sample} = \left[\frac{^{15}N_{sample}/^{14}N_{sample}}{^{15}N_{reference}/^{14}N_{reference}} - 1\right] * 1{,}000$$

$$(2)\ ^{15}\varepsilon = \left(\frac{^{14}k}{^{15}k} - 1\right) * 1{,}000$$

Where the $^{15}N/^{14}N$ reference is atmospheric N_2.

Nitrogen budget estimates have not been consistent over the past few decades. The most disputed N budget terms are N_2 fixation and sedimentary denitrification. N_2-fixation rate estimates have grown considerably over time as the number of field measurements have been expanded and techniques have evolved, from 15 Tg N yr^{-1} (Codispoti and Christensen 1985) to 120 ± 50 Tg N yr^{-1} (Gruber 2004). However, the more recent N_2 fixation rate estimates cover a narrow range relative to the wide range of estimated denitrification rates, which are on the order of 165 to 450 Tg yr^{-1} (Table 2). While the lowest estimated denitrification rates have led to overall nitrogen budgets that are approximately in balance, many are massively out of balance - with outputs far outweighing inputs (Table 1). Whether or not the marine N budget is in balance is unknown, however, the predicted imbalances appear excessive. If the disproportionately high magnitude of N loss deemed possible by some of these nitrogen budgets is real, it has significant implications for oceanic productivity and carbon sequestration through time. For example, a net 200 Tg N yr^{-1} loss leads to depletion of oceanic N in about 3,000 years, and, barring a temporal change in the Redfield Ratio, would release about 0.1 Gt CO_2 yr^{-1} to the atmosphere due to lost productivity (Brandes and Devol, 2002). CO_2 generation of this magnitude is not seen during the Holocene (Barnola et al. 1995; Indermühle et al. 1999). Furthermore, the N budgets predicting large-scale net N loss are potentially flawed. For example, it has been argued by Gruber (2008)

that the N budget of Codispoti et al. (2001) greatly over estimates open ocean benthic denitrification since the budget requires about 90% of the nitrogen that reaches the sea floor be denitrified, implying that the (commonly oxygenated) waters overlying the sediments perform very little nitrification. Additionally, Brandes and Devol (2002) acknowledge that their N budget, developed using isotopic constraints, is reliant on a high $^{15}\varepsilon$ of water-column denitrification ($^{15}\varepsilon_{denit}$) of ~25‰, while a $^{15}\varepsilon_{denit}$ of 10-15‰ would bring the budget into approximate balance. $^{15}\varepsilon_{denit}$ has been seen to vary from 5 to 30‰ in field and laboratory measurements (Table 3).

The cause(s) of variation in the isotope effect of water-column denitrification are the primary concern of the research outlined herein, as the accuracy of $^{15}\varepsilon_{denit}$ is essential to the formulation of a valid isotopically constrained N budget. An N isotopic budget is constructed by pairing known mass fluxes with their isotopic composition to determine the remaining unknown term using a mass balance calculation. As the average $\delta^{15}N$ of oceanic fixed N is expected to have changed negligibly from 5‰ during the Holocene (Kienast 2000), isotopic steady state can be assumed – meaning that the $\delta^{15}N$ of input and output fluxes must be equivalent. The N budget constructed by Brandes and Devol (2002) used the following mass flux and isotopic constraints, as determined from the compilation of numerous reported values: Terrestrial runoff and atmospheric deposition each represent a 25 Tg N yr^{-1} input, and have opposite $\delta^{15}N$ values of +4‰ and -4‰ respectively, thus constituting a net $\delta^{15}N$ input of 0‰. The greatest input, nitrogen fixation, has an estimated rate of 110 Tg N yr^{-1} and a $^{15}\varepsilon$ of about -1‰. Since the substrate of N_2-fixation is dissolved atmospheric N_2 gas, with a $\delta^{15}N$ of 0‰, N_2-fixation generates NH_3 with a $\delta^{15}N$ of about -1‰. Hence, inputs, and consequently outputs, have a net $\delta^{15}N$ of approximately -1‰. With respect to N sinks, sedimentary burial accounts for 25 Tg N yr^{-}

[1], and has a $\delta^{15}N$ of +6‰. As denitrification in the water-column and in the sediments have different isotope effects, they must be considered separately. The cellular level isotope effect of water-column denitrification in this exercise was considered to be 25‰, with an estimated rate of 75 Tg N yr^{-1}. Water-column denitrification thus removed nitrogen with a $\delta^{15}N$ of -20‰. The isotope effect exhibited by sedimentary denitrification is much lower than that of water-column denitrification since the majority of nitrate that enters the sediments is denitrified, and thus little remains to reflect the resulting fractionation. Sedimentary denitrification was estimated to have an isotope effect of 1.5‰, meaning that it results in N losses with a $\delta^{15}N$ slightly below that of the ocean, at 3.5‰. From these numbers, a mass balance calculation then yields a sedimentary denitrification rate of 278 Tg N yr^{-1}, resulting in a net loss of about 218 Tg N yr^{-1} from the ocean (Figure 1, Brandes and Devol 2002).

A downward shift in the isotope effect of water-column denitrification would decrease the calculated sedimentary denitrification mass flux, as less benthic denitrification would be required to offset the ^{15}N-enrichment induced by water-column denitrification. For example, a $^{15}\varepsilon_{denit}$ of 15‰ results in a ~111 Tg N yr^{-1} benthic denitrification rate, reducing total N losses by ~167 Tg N yr^{-1}. The 25‰ $^{15}\varepsilon_{denit}$ value used in the N budget of Brandes and Devol (2002) is supported by $^{15}\varepsilon_{denit}$ estimates derived from measurements of $\delta^{15}N_{NO3}$ in field and in laboratory studies with both marine and freshwater denitrifying organisms (Table 3). However, the value of $^{15}\varepsilon_{denit}$ has been observed to fall well below the presumed 25‰ in several of the culture experiments and field measurements. In addition, field approximations may be over-estimated due to uncertainties in accounting for lateral transport of NO_3^- along isopycnals into oxygen minimum zones (Deutsch et al. 2010).

ε_{denit} is controlled by the physiological regulation of respiratory nitrate reduction and its effect on the ratio of cellular nitrate uptake to efflux. The current understanding of this fractionation mechanism, dubbed the "efflux model", is derived from the study of nitrate reduction during both bacterial denitrification and the analogous process of nitrate assimilation by unicellular marine algae. In both processes, the dominant nitrate isotope fractionating step occurs during intracellular enzymatic reduction of nitrate to nitrite - by assimilatory nitrate reductase (NR) during nitrate assimilation, or by respiratory nitrate reductase (NAR) during denitrification. Other paths by which nitrate isotopic ratios could potentially be altered are by fractionation during nitrate transport, which has been shown to be relatively minor or absent (Granger et al. 2004; Needoba et al. 2004; Granger et al. 2008; Karsh et al. 2012; Karsh et al. 2014), or by the re-oxidation of product NO_2^- back to NO_3^-, which is not observed during bacterial denitrification (Wunderlich et al. 2012). The intracellular reduction of nitrate to nitrite enriches the cytoplasm in $^{15}N_{NO3}$ and $^{18}O_{NO3}$ due to the preferential reduction of $^{14}N_{NO3}$ and $^{16}O_{NO3}$ to nitrite. It thus follows that export of nitrate from the cell is necessary for the isotope effect of NR or NAR (ε_{enzyme}) to be expressed in the external medium (Figure 2), resulting in the measured cellular level isotope effect (referred to as "ε_{cell}" here to encompass both denitrification and nitrate assimilation). As the rate of nitrate efflux approaches the rate of uptake ε_{enzyme} is more completely expressed and ε_{cell} is maximized, yielding the qualitative equation:

(3) ε_{cell} = efflux/uptake * ε_{enzyme}

Presuming the magnitude of nitrate efflux increases in conjunction with the intracellular nitrate concentration, efflux/uptake must increase in response to an increase in nitrate uptake, as, upon the saturation of enzymatic nitrate reduction, nitrate reduction constitutes a smaller proportion of total nitrate outputs from the cell.

Several lines of evidence from the study of nitrate assimilation in unicellular phytoplankton support the validity of the efflux model outlined above. (1) The highest observed $^{15}\varepsilon_{cell}$ values (~30‰) in laboratory and field experiments (Table 3) are approximately the same as the *in vitro* isotope effect of purified NR (27-30‰) (Schmidt and Medina, 1991; Karsh et al. 2012). A maximum $^{15}\varepsilon_{cell}$ value equivalent to $^{15}\varepsilon_{enzyme}$ implies that the isotope effect of enzymatic reduction is indeed expressed to the extracellular medium, invoking nitrate efflux as essential for $^{15}\varepsilon_{enzyme}$ expression. (2) In a cultured marine diatom the magnitude of the difference between the $\delta^{15}N$ of internal nitrate vs. external nitrate was found to be inversely proportional to the measured $^{15}\varepsilon_{cell}$ (Needoba et al. 2004). Since a high efflux rate minimizes the difference between intra- and extracellular nitrate $\delta^{15}N$ values, it was implied that a greater efflux to uptake ratio increases the expression of $^{15}\varepsilon_{enzyme}$. (3) The ratio of efflux to reduction was increased via the partial inhibition of nitrate reductase activity with tungstate, resulting in an elevated $^{15}\varepsilon_{cell}$. (Shearer et al. 1991). (4) Phytoplankton cultures' intracellular and extracellular nitrate were found to have a co-varying change in $\delta^{18}O_{NO3}$ to change in $\delta^{15}N_{NO3}$ ratio ($\Delta\delta^{18}O$:$\Delta\delta^{15}N$) of ~1:1 across a range of $^{15}\varepsilon_{cell}$ magnitudes during nitrate assimilation (Granger et al. 2004; Needoba et al. 2004). Coherently, purified NR fractionates nitrate oxygen and nitrogen isotopes with the same constant $\Delta\delta^{18}O$:$\Delta\delta^{15}N$ ratio of ~1:1 (Karsh et al. 2012). This suggests that nitrate reduction is the dominant fractionating step, as uptake and efflux exhibit a $\Delta\delta^{18}O$:$\Delta\delta^{15}N$ of 1.4 ± 0.4‰ and 2.3 ± 0.9‰, respectively (Karsh et al. 2014). If fractionation were significant during transport, isotopic discrimination during transport would have to result in fractionation with an equivalent $\Delta\delta^{18}O$:$\Delta\delta^{15}N$ ratio to maintain equal values between the intra- and extracellular nitrate pools.

Evidence that denitrification fractionates with a mechanism analogous to nitrate assimilation by macroalgae includes: (1) NAR and NR have equivalent molybdenum (Mo)

reaction centers, which are considered likely to induce similar relative rates of isotopic fractionation (Melander and Saunders 1980). (2) Like NR, purified NAR has been observed to fractionate nitrate with a $^{15}\varepsilon$ of 27-30‰ (Treibergs *personal communication*) (3) Denitrifying organisms fractionate nitrate O and N with the same co-varying extracellular $\Delta\delta^{18}O{:}\Delta\delta^{15}N$ of ~1:1 as nitrate assimilation (Granger et al. 2008; Kritee et al. 2012; Wunderlich et al. 2012). (4) $^{15}\varepsilon_{cell}$ approaches zero when nitrate uptake becomes the rate limiting step during denitrification at low nitrate concentrations (Granger et al. 2008; Kritee et al. 2012). The absence of an isotope effect at low substrate concentrations indicates that nitrate transport did not noticeably contribute to the observed $^{15}\varepsilon$ of denitrifying microorganisms.

The intraspecific isotope effect of denitrification displays a broad range (Granger et al. 2008, Kritee et al. 2012), implicating environmental conditions, rather than exclusively differences between organisms, as a major driver of variation in $^{15}\varepsilon_{denit}$. The environmental conditions that control this relationship have not yet been resolved. The physiological mechanism by which denitrifying bacteria regulate nitrate respiration in response to the presence of oxygen provides clues as to factors that can influence the magnitude of ε_{denit}, granting insight with respect to the controls of variability in the cellular nitrate uptake and respiration rates. Exposure of most denitrifiers to sufficient oxygen concentrations results in the complete termination of cellular nitrate reduction (John 1977, Robertson and Kuenen 1985, Hernandez and Rowe 1988, Baumann et al. 1996). The best supported mechanism by which oxygen inhibits cellular nitrate respiration is via the cessation of nitrate uptake into the cell, rather than by the inhibition of intracellular nitrate reduction. For one, inside-out membrane vesicles of *Paracoccus denitrificans* have been observed to reduce oxygen and nitrate simultaneously (John 1977), and the permeabilization of the *P. denitrificans* plasma membrane by treatment with Triton X-100

detergent allowed nitrate reduction under aerobic conditions (Alefounder and Ferguson 1980). In both studies, nitrate respiration occurred when the cytoplasmic face of the plasma membrane, the location of NAR (John 1977), was made accessible to nitrate without the need for active uptake – despite the presence of oxygen. Due to the possibility that Triton X-100 addition allowed aerobic nitrate respiration because of an unknown side-effect, two other detergents (cetyltriethylammonium bromide and lauryldimethylamine oxide) were tested in *P. denitrificans* cultures, and, similarly, were found to release the regulation of nitrate respiration by oxygen (Alefounder et al. 1983). Second, cellular nitrate respiration in the presence of oxygen is not stimulated by durohydroquinone, a compound capable of directly reducing NAR, suggesting that oxygen prevents nitrate from contacting NAR. Inhibition of nitrate uptake by oxygen as the mechanism for oxygen regulation of nitrate respiration has been extended beyond *P. denitrificans* to a variety of denitrifying bacteria, as Hernandez and Rowe (1988) demonstrated that, in 11 of 12 species, cell free extracts were capable of nitrate reduction in the presence of oxygen, while nitrate respiration was completely inhibited by oxygen in whole cells. Since oxygen regulates nitrate uptake, and nitrate uptake controls ε_{denit} (as per the efflux model), the physiological mechanism by which oxygen regulates nitrate uptake may yield essential insights in the understanding of the magnitude of ε_{denit}.

Several studies implicate oxidation of the electron transport chain (ETC) as the mechanism by which oxygen regulates nitrate uptake (Alefounder et al. 1981, Kucera et al. 1981; Alefounder et al. 1983; Kucera et al. 1983). The rate of electron flow in the ETC and nitrate respiration were first linked by the use of the antimycin to inhibit electron flow through cytochrome c (Alefounder et al. 1981; Kucera et al. 1981). In *P. denitrificans*, cytochrome c leads to nitrite reductase, nitrous oxide reductase, and two cytochrome oxidases (*co* and aa_3) -

but not to a third cytochrome oxidase, cytochrome *o* (Stouthamer et al. 1991). As it blocks electron flow to two of three cytochrome oxidases, antimycin inhibits aerobic respiration by up to 50%, while simultaneously allowing aerobic nitrate reduction (Alefounder et al. 1981; Kucera et al. 1981). In these studies, decreasing the number of outlets for the passage of electrons to oxygen may have reduced the ETC by slowing electron flow. This expectation was supported by correlation between the inhibition of nitrate respiration and slight changes in the redox state of the ubiquinone pool, which lies upstream of cytochrome c in the ETC. Oxygen and nitrous oxide were found to induce complete or near complete inhibition of nitrate reduction, respectively, while nitrite did not cause inhibition (Alefounder et al. 1983) or caused significantly weaker inhibition (Kucera et al. 1983). The degree of nitrate respiration inhibition corresponded with the extent of ETC oxidation, which was measured directly, while oxidation of the ETC was purportedly caused by the greater rate of electron consumption by nitrous oxide and oxygen than nitrite, as determined from the relative rates of substrate reduction. In summary, oxygen prevents nitrate respiration by inhibiting uptake (John 1977; Alefounder and Ferguson 1980; Alefounder et al. 1983; Hernandez and Rowe 1988), and the magnitude of nitrate respiration inhibition by oxygen, nitrous oxide, and nitrite has been correlated with their relative effects on the oxidation state of the ETC (Alefounder et al. 1981; Kucera et al. 1981; Alefounder et al. 1983; Kucera et al. 1983).

It is important to make the distinction that the inhibition of nitrate respiration by oxygen and other compounds is not always complete. If inhibition were always either complete or entirely absent, it would not be possible for fluctuations in the oxidation state of the ETC to result in a range of nitrate uptake rates. As per the efflux model, a range of nitrate uptake rates is necessary for the cell to express intermediate values of $^{15}\varepsilon_{denit}$. Indeed, in *P. denitrificans*

cultures, nitrate respiration in the presence of oxygen or nitrous oxide was found to increase concomitantly with the concentration of antimycin (Alefounder et al. 1981; Kucera et al. 1981, Alefounder 1983), and the presence of trace oxygen has been observed to decrease denitrifying organisms' cell specific nitrate respiration rate and average $^{15}\varepsilon_{denit}$ without abolishing nitrate respiration all-together (Kritee et al. 2012). Furthermore, direct reduction of the ETC can relieve inhibition of nitrate reduction. The inhibition of NAR activity by nitrite and nitrous oxide was progressively released in proportion to the concentration of N,N,N',N'-tetramethyl-p-phenylenediamine (TMPD) added to *P. denitrificans* cultures (Kucera et al. 1983). TMPD donates electrons directly to cytochrome c, which is located upstream of nitrite and nitrous oxide reductases, but does not lead to NAR. Therefore, increased reduction of cytochrome c may alleviate the electron demand of nitrite and nitrous oxide reductases, diminishing the oxidative effects of these enzymes on the redox state of the ETC, and elevating nitrate uptake.

Concluding that a high rate of nitrate uptake increases $^{15}\varepsilon_{denit}$, and that nitrate uptake is, in turn, elevated as the ETC is reduced, we hypothesize that the redox state of the carbon substrate used in a *P. denitrificans* culture will correlate with $^{15}\varepsilon_{denit}$ – with more reduced carbon substrates resulting in a greater $^{15}\varepsilon_{denit.}$ While oxygen oxidizes the ETC by increasing the rate of electron consumption, more reduced carbon substrates may reduce the ETC by increasing the rate at which electrons are supplied. Conceivably, this would occur because more reduced carbon sources have a greater potential to produce reducing equivalents (e.g. NADH), forcing cells to dissipate more electrons per atom of carbon obtained. Analogously, the redox state of carbon sources have been observed to correlate with the rate of periplasmic nitrate reductase (NAP) activity in aerobic *Paracoccus pantotrophus* cultures (Richardson and Ferguson 1992). NAP activity rose when the carbon redox state decreased, ostensibly to consume electrons and

maintain redox balance. Furthermore, the role of carbon substrates in controlling the amplitude of $^{15}\varepsilon_{denit}$ has been suggested by Kritee et al. (2012). Cultures were grown on complex organic matter until the complete consumption of nitrate. Then, upon the re-amendment of nitrate to spent cultures, these cultures expressed a lower $^{15}\varepsilon_{denit}$. It is likely that the more energetically favorable carbon from the complex organic source was consumed first, contributing to the increased reduction of the ETC during initial growth, then, after the second nitrate amendment, the degraded carbon contributed to a lower $^{15}\varepsilon_{denit}$.

In order to clarify the relationship between carbon substrates and $^{15}\varepsilon_{denit}$, in this study, *P. denitrificans* will be grown upon carbon sources exhibiting a range of oxidation states in otherwise identical batch cultures.

Methods

Strain – Cultures were initiated with the strain *Paracoccus denitrificans* (American Type Culture Collection [ATCC] 19367). *P. denitrificans* is a facultatively aerobic, chemotrophic bacterium capable using nitrate as its terminal electron acceptor in anaerobic conditions. It is a model organism commonly used in the study of denitrification. Respiratory nitrate reduction occurs through the use of respiratory nitrate reductase (NAR), which is bound on the cytoplasmic face of the plasma membrane. Two other nitrate reducing enzymes may be expressed, assimilatory nitrate reductase (NR) and periplasmic nitrate reductase (NAP). NR activity can be repressed by providing *P. denitrificans* cultures with excess ammonium (Warnecke-Eberz and Friedrich 1993). NAP may be used to dissipate excess electrons generated from carbon oxidation (Richardson and Ferguson 1992; Ellington et al. 2002), but its activity was unknown in cultures herein.

Growth conditions and sampling – Freshwater medium was prepared using high purity water (HPW) amended with 250 µM KNO_3, 250 µM NH_4Cl, 5 mM KH_2PO_4, 5 g K_2HPO_4, 304 µM $MgSO_4*7H_2O$, 136 µM $CaCl_2*2H_2O$, 68.4 µM sodium ethylenediaminetetraacetic acid (EDTA), 1 mL L^{-1} Teknova T1001 trace metal mixture, and 5 mL L^{-1} Sigma-Aldrich RPMI 1640 vitamins solution. The trace metal mixture contains 50 mM ferric chloride, 20 mM calcium chloride, 10 mM manganese chloride, 2 mM cobalt chloride, 2 mM cupric chloride, 2 mM nickel chloride, 2 mM sodium molybdate, 2 mM sodium selenite, 2mM boric acid. The media was further amended with 0.2 g/L of a carbon substrate, either malate, succinate, acetate, glucose, pyruvate, citrate, or ethanol. The medium was sterilized by autoclave following the addition of KNO_3, NH_4Cl, KH_2PO_4, K_2HPO_4, $MgSO_4*7H_2O$, $CaCl_2*2H_2O$, and EDTA, and was then supplemented with filter sterilized solutions of the trace metal mixture, vitamin solution, and carbon substrate. A single culture set, one of two batches using acetate as the carbon source, had a NO_3^- concentration of 500 µM instead of 250 µM.

P. denitrificans was initially grown upon solid medium plates containing 15 g L^{-1} Fisher Scientific Agar and 5 g L^{-1} Bacto™ Tryptic Soy Broth produced with artificial freshwater. Artificial freshwater consisted of HPW amended with 304 µM $MgSO_4*7H_2O$, 136 µM $CaCl_2*2H_2O$, and 68.4 µM sodium ethylenediaminetetraacetic acid (EDTA). Aerobic precultures were then inoculated with cells grown on the solid medium plates to acclimate the cells to the freshwater medium and the carbon substrate associated with their destined final batch cultures. Upon reaching visible cellular concentrations, 0.5 to 8 mL preculture was used to inoculate the final cultures. Final cultures consisted of acid washed tri-laminate, polyethylene lined, TEDLAR™ gas tight bags containing 200 mL aerobic freshwater medium. Cultures were held within a Fisher Scientific Isotemp incubation chamber or a University of Connecticut

Department of Marine Sciences environmental chamber at a constant temperature of 20°C, and were sampled periodically to test for the onset of denitrification, resulting from eventual anaerobiosis. Denitrification was determined to have begun upon the accumulation of nitrite, which was detected colorimetrically using Greiss reagents (Parsons et al. 1984). Concurrent measurement of the cultures' total NO_3^- + NO_2^- concentration (explained below) ensured that a lack of nitrite accumulation did not cause the onset of denitrification to be missed. Upon the detection of denitrification, samples were collected at 30 minute to several hour intervals, with more frequent sampling at higher denitrification rates, and stored in acid washed polypropylene bottles. Subsamples were obtained anaerobically by extracting the medium using a Henke Sass Wolf NORM JECT Luer Lock syringe fitted to Leur Lock connectors, and were then placed in ice. Their nitrate concentration was immediately measured, and the samples were subsequently frozen in a -10°C freezer for later analysis of nitrate N and O isotopes. Subsamples taken for picogreen growth analysis (described below) were flash frozen in liquid nitrogen or with dry ice, then stored in a -80°C freezer. Subsamples from ethanol and citrate grown cultures were preserved in a 2% formaldehyde solution (final concentration) in preparation for direct cell counts.

Prior to isotopic analyses, accumulated nitrite in the subsamples was removed using sulfamic acid (Granger and Sigman, 2009), to prevent the measurement of nitrite isotopic ratios through use of the denitrifier method (see below). Moreover, the decomposition of nitrite to nitric oxide and nitrogen dioxide followed by oxidation to nitrate can interfere with nitrate isotope values after long term storage at low nitrate concentrations (Granger et al. 2008).

Nitrate and nitrite analysis – Nitrate + nitrite concentrations were measured by their simultaneous reduction to nitric oxide in hot vanadium (III) solution, and the subsequent

detection of nitric oxide by a chemiluminescence using an NO_x analyzer (model T200 Teledyne Advanced Pollution Instrumentation; Braman and Hendrix 1989). Nitrite was removed from samples using N-(1-naphthyl)ethylenediamine dihydrochloride and sulfanilamide (Parsons et al. 1984), allowing for the acquisition of nitrate concentrations.

Respiration and growth monitoring – The specific respiration rate (h^{-1}) of *P. dentrificans* cultures corresponds to the linear slope of the natural logarithm of the respired nitrate concentration *vs.* time (e.g. Figure 3), where respired nitrate is equivalent to the nitrate drawdown at a given point. Direct cell counts were performed for cultures grown on ethanol and citrate. For these two culture sets, formaldehyde preserved samples were gathered on 0.2 µm polycarbonate track etched membrane filters and stained with a 0.1 g L^{-1} acridine orange solution using the techniques of Hobbie et al. 1977. Cells were then counted using an Olympus BX50 epifluorescence microscope. Alternatively, growth was measured using the Quant-iT Picogreen dsDNA reagent. Picogreen is a fluorescent probe, which binds to dsDNA, allowing for the determination of cellular concentration by spectrofluorometric analysis (Tranvik, 1997). This was done using an AJN Scientific Inc. f-2500 Fluoresence Spectrophotometer using 480 nm excitation and 525 nm emission wavelengths.

Nitrate N and O isotope analyses – The $^{15}N/^{14}N$ and $^{18}O/^{16}O$ isotopic ratios of nitrate samples were measured using the "denitrifier method" (Sigman et al. 2001; Casciotti et al. 2002). The denitrifier method consists of the bacterial conversion of sample nitrate (and any present nitrite) to nitrous oxide by a denitrifying strain lacking nitrous oxide reductase, in our case, *Pseudomonas chlororaphis* f. sp. *aureofaciens* (ATCC 13985). The isotopic composition of the resulting N_2O was then measured using a Delta V Advantage Isotope Ratio Mass Spectrometer (IRMS) pre-empted by a front-loading Gas Bench II gas chromatograph (Thermo Fisher) purge

and trap system. The isotope ratio measurements are reported in the conventional delta (δ) notation in per mille (‰) units, defined for N in equation 1 and O by the following equation:

$$(4)\ \delta^{18}O_{sample} = \left[\frac{^{18}O_{sample}/^{16}O_{sample}}{^{18}O_{reference}/^{16}O_{reference}} - 1\right] * 1{,}000$$

The $^{18}O/^{16}O$ reference is Vienna standard mean ocean water (V-SMOW). The analyses will be standardized via reference to a N_2O gas injections. Individual analyses on the GC-IRMS were referenced to injections of N_2O from a pure N_2O gas cylinder, and then standardized through comparison to the international nitrate standards USGS-34 ($\delta^{15}N$ of -1.8‰ *vs.* air; $\delta^{18}O$ of -27.9‰ *vs.* V-SMOW), USGS-32 ($\delta^{15}N$ of +180‰ *vs.* air; $\delta^{18}O$ of +25.7‰ *vs.* V-SMOW), and IAEA-NO-3 ($\delta^{15}N$ of +4.7‰ *vs.* air; $\delta^{18}O$ of +25.6‰ *vs.* V-SMOW; see Gonfiantini et al. 1984, Böhlke et al. 1995, Böhlke et al. 2003), using standard bracketing techniques. Isotopic measurements had an average standard deviation of 0.1‰ between replicate measurements for both $\delta^{15}N$ and $\delta^{18}O$.

The isotope effect on N and O isotopes of nitrate ($^{15}\varepsilon$ and $^{18}\varepsilon$, respectively) was derived from the Rayleigh Model linearization of isotope ratios versus the logarithm of the nitrate remaining in the medium, in which the resulting slope approximates ε (Mariotti et al. 1981). The isotope effect of denitrification is thus the slope of the following linear equations, which were calculated using Model II geometric mean linear regression analysis:

$$(5)\ \ln\left(\delta^{15}N + 1\right) = \frac{^{15}\varepsilon_{denit}}{1000} * \ln(f) + \ln\left(\delta^{15}N + 1\right)$$

$$(6)\ \ln\left(\delta^{18}O + 1\right) = \frac{^{18}\varepsilon_{denit}}{1000} * \ln(f) + \ln\left(\delta^{18}O + 1\right)$$

Where "f" is the fraction of initial nitrate remaining in the medium ($f = [NO_3^-]/[NO_3^-]_{initial}$).

Results

Following initial growth on oxygen, cultures of *P. denitrificans* began anaerobic respiration of nitrate. The amplitude of the nitrate nitrogen isotope effect ($^{15}\varepsilon_{denit}$), derived from Equation 5, was found to span a broad range during growth on a variety of carbon substrates. $\delta^{15}N$ enrichment vs. $\ln([NO_3^-]/[NO_3^-]_{initial})$ for each individual culture can be seen in Figure 4, where the slope of the linear regression of the data series is the value of $^{15}\varepsilon_{denit}$. Cells grown on citrate displayed the minimum observed $^{15}\varepsilon_{denit}$, of 12.9 ± 1.4‰, while glucose grown cells displayed the maximum observed $^{15}\varepsilon_{denit}$, of 29.7 ± 0.3‰. $^{15}\varepsilon_{denit}$ values of 23.8 ± 0.7‰, 26.5 ± 0.8‰, and 28.4 ± 1.1‰ were observed for malate, ethanol, and pyruvate cultures, respectively. Two discrete batches of acetate and succinate cultures were grown, referred to hereafter as "*acetate 1*", "*acetate 2*", "*succinate 1*", and "*succinate 2*". $^{15}\varepsilon_{denit}$ values of 24.0 ± 0.2‰, 22.1 ± 2.5‰, 17.0 ± 0.7‰, and 23.6 ± 1.4‰ were measured for *acetate 1*, *acetate 2*, *succinate 1*, and *succinate 2*, respectively (Table 3). While the standard deviation for most treatments is that for $^{15}\varepsilon$ of experimental replicate cultures, only a single ethanol culture was measured, and the reported standard deviation was thus calculated from model II geometric mean linear regression analysis of the ethanol $\delta^{15}N$ vs. $\ln([NO_3^-]/[NO_3^-]_{initial})$ data.

Contrary to the original hypothesis, no clear relationship was observed between $^{15}\varepsilon_{denit}$ and the oxidation state of a culture's carbon substrate (Figure 5). Nevertheless, the lowest $^{15}\varepsilon_{denit}$ value of 12.9 ± 1.4‰ did correspond to growth on one of the two most oxidized carbon substrates (citrate), although the low $^{15}\varepsilon_{denit}$ may have been the result of the limited ability of *P. denitrificans* to grow upon citrate under anaerobic conditions, rather than direct correlation to the oxidation state of citrate. Nitrate respiration was inordinately slow in citrate cultures, with replicate cultures taking approximately 24 hours to remove 100 µM nitrate after the onset of

denitrification, a feat which took cultures grown on other carbon sources 1.5 to 4 hours at comparable cell densities. Additionally, direct cell counts revealed that cells grown upon citrate were apparently dying off during nitrate respiration (Figure 6). *P. denitrificans* has been reported to be incapable of growth upon citrate under anaerobic conditions (Robertson and Kuenen 1983). Furthermore, at the same carbon oxidation state, malate grown cultures exhibited a much higher $^{15}\varepsilon_{denit}$ of 23.8 ± 0.7‰, thus suggesting that oxidation state, in and of itself, does not control the value of $^{15}\varepsilon_{denit}$. As the carbon oxidation state decreased from the 1.0 value of citrate and malate to 0.67 (pyruvate), $^{15}\varepsilon_{denit}$ increased to 28.4 ± 1.1‰. Proceeding to the 0.5 oxidation state of succinate, however, $^{15}\varepsilon_{denit}$ was found to then decrease, varying from 17.0 ± 0.7‰ (*succinate 1*) to 23.4 ± 0.1‰ (*succinate 2*). At an oxidation state of 0 the greatest isotope effect was measured, at 29.7 ± 0.3‰ (glucose), but reached as low as 22.1 ± 2.5‰ in *acetate 2* cultures. $^{15}\varepsilon_{denit}$ then declines slightly from the glucose value to 26.8 ± 0.8‰ at the lowest tested oxidation state of -2.0 (ethanol).

In contrast to the oxidation state of carbon, the specific respiration rate (h^{-1}) of nitrate was positively correlated to the measured $^{15}\varepsilon_{denit}$ of respective cultures (Figure 7, Table 3). The specific respiration rate is used as an estimate of the specific growth rate. Equivalence between the specific respiration and specific growth rate requires that the rate of respiration remains constant throughout exponential growth phase, which has been observed in *Escherichia coli* (Andersen and Meyenburg 1980). Ethanol and citrate cultures were excluded from this comparison of $^{15}\varepsilon_{denit}$ and specific respiration rate, as they were not in exponential growth phase during denitrification, meaning a specific respiration rate could not be calculated. The specific respiration rate ranged from 0.44 ± 0.08 (hr^{-1}) for growth on succinate to 1.06 ± 0.07 (hr^{-1}) for growth on glucose, with the minimum rate associated with the lowest $^{15}\varepsilon_{denit}$ (17.0 ± 0.7‰,

succinate 1), and the greatest rate associated with the greatest $^{15}\varepsilon_{denit}$ (29.7 ± 0.3‰, glucose). Even among cultures grown on a single carbon substrate where $^{15}\varepsilon_{denit}$ can be seen to differ significantly between culture batches (i.e. *succinate 1* and *succinate 2*), $^{15}\varepsilon_{denit}$ remained correlated to the specific respiration rate. The specific respiration rate of *succinate 2* cultures was elevated alongside their $^{15}\varepsilon_{denit}$, at 0.67 ± 0.07 hr^{-1} and 23.6 ± 1.4‰, respectively, relative to the low values measured among *succinate 1* cultures, at 0.44 ± 0.08 (hr^{-1}) and 17.0 ± 0.7‰. The difference between the two acetate batches was less striking. Within *acetate 1* treatments a $^{15}\varepsilon_{denit}$ of 24.0 ± 0.2‰ is associated with a specific respiration rate of 0.72 ± 0.04, while in *acetate 2* treatments a $^{15}\varepsilon_{denit}$ of 22.1 ± 2.5‰ is associated with a specific respiration rate of 0.64 ± 0.02 (Table 3). The difference in $^{15}\varepsilon_{denit}$ between *acetate 1* and *acetate 2* is thus within one standard deviation. A positive relationship between $^{15}\varepsilon_{denit}$ and specific respiration rate extends to all cultures for which a specific respiration rate could be measured, approaching an asymptote of approximately 30‰ (Figure 7).

Direct cell counts of ethanol and citrate cultures allowed for the calculation of the average rate at which a single cell reduced nitrate to nitrite, known as the cell specific nitrate reduction (CSNR) rate. The CSNR rates of two citrate cultures were measured at $6.06 * 10^{-11}$ ± $2.40 * 10^{-11}$ and $4.81 * 10^{-11}$ ± $1.69 * 10^{-11}$ μmol NO_3^- L^{-1} $cell^{-1}$ min^{-1}, while the CSNR rate of the single ethanol culture was approximately an order of magnitude higher, at $3.80 * 10^{-10}$ ± $0.34 * 10^{-10}$ μmol NO_3^- L^{-1} $cell^{-1}$ min^{-1}. As the $^{15}\varepsilon_{denit}$ of the ethanol grown culture (26.5 ± 0.8‰) was much greater than $^{15}\varepsilon_{denit}$ measured between citrate cultures (12.9 ± 1.4‰), $^{15}\varepsilon$ displayed a positive relationship with CSNR within these limited culture sets. However, this may relate to the respective growth phases of the ethanol and citrate cultures, as the ethanol culture appeared to be in stationary phase, with an approximately constant cellular concentration of $1.60 * 10^6$ ±

0.15 * 10^6 cell ml^{-1}, while the citrate culture entered the death phase after the 47 hour mark (Figure 6).

Measurement of culture growth by spectrofluorometric analysis using the picogreen DNA probe was attempted, but largely unsuccessful. After extended periods in a -80°C freezer, ranging from weeks to months, it was found that DNA degraded, leading to inconsistent measurements. This was seen most clearly in malate grown cultures. Growth was measured by picogreen spectrofluorometric analysis for identical malate culture samples in August 2013 and January 2014. The cultures were originally grown in June, and measurement in August yielded erratic changes in fluorescence height (unitless) with time. Repeated measurement of the same samples in January yielded significantly decreased fluorescence, with heights ranging from ~400 to 550 in August, and ~100 to 170 in January (Figure 8a). While the degradation of DNA precludes these measurements from use in the quantification of accurate growth rates, the observed regular increase in fluorescence with time (coinciding with the occurrence of denitrification) detected in succinate, acetate, pyruvate, glucose, and some malate cultures is a qualitative indication that cultures using these carbon sources were in growth phase over the course of denitrification (Figure 8). *Acetate 1* cultures were not analyzed using this method.

The effect of denitrification on the isotopes of O compared to N is examined through the slope of the linear regression of the change in $\delta^{18}O$ vs. the change in $\delta^{15}N$ ($\Delta\delta^{18}O$:$\Delta\delta^{15}N$) of nitrate remaining within the medium as denitrification progresses. The pooled $\Delta\delta^{18}O$:$\Delta\delta^{15}N$ calculated among all cultures was 0.92 ± 0.00 (Figure 9). The $\Delta\delta^{18}O$:$\Delta\delta^{15}N$ relationship was consistent, with a correlation coefficient greater than 0.999 derived from a model II geometric mean linear regression of all data points. The lowest observed $\Delta\delta^{18}O$:$\Delta\delta^{15}N$ of 0.87 ± 0.02 occurred among *succinate 1* cultures, whereas the greatest observed value was measured within

an individual citrate culture, at 1.13 ± 0.04 (Figure 10). Similar to what was seen with respect to $^{15}\varepsilon_{denit}$ vs. specific respiration rate, the varied $\Delta\delta^{18}O{:}\Delta\delta^{15}N$ values between *succinate 1* and *succinate 2* treatments correlated with $^{15}\varepsilon_{denit}$. The average $\Delta\delta^{18}O{:}\Delta\delta^{15}N$ of *succinate 2* cultures, at 0.93 ± 0.01, being much greater than that of *succinate 1*, at 0.87 ± 0.02, vs. their respective $^{15}\varepsilon_{denit}$ values of 23.6 ± 1.4‰ and 17.0 ± 0.7‰. *Acetate 1* and *acetate 2* cultures were, again, found to be relatively similar, with respective $\Delta\delta^{18}O{:}\Delta\delta^{15}N$ ratios of 0.93 ± 0.01 and 0.96 ± 0.00 (Figure 9, Table 3). The maximum reported $\Delta\delta^{18}O{:}\Delta\delta^{15}N$ of 1.13 ± 0.04 is aberrant, as, for a total of 21 measured values, the second greatest $\Delta\delta^{18}O{:}\Delta\delta^{15}N$ ratio in a single culture was 0.96 ± 0.02 (one of two *acetate 2* cultures). The 1.13 ± 0.04 value is, however, heavily reliant on a single data point lying near the inception of nitrate respiration, and the exclusion of this point from the calculation of the culture's $\Delta\delta^{18}O{:}\Delta\delta^{15}N$ results in a reduced ratio of 0.99 ± 0.06. The inflation of $\Delta\delta^{18}O{:}\Delta\delta^{15}N$ during the early stages of denitrification may be related to a slower initial nitrate reduction rate, and thus increased influence from the competing isotope effects of nitrate uptake and efflux (see *Discussion*). Aside from the relatively low $\Delta\delta^{18}O{:}\Delta\delta^{15}N$ ratio observed in *succinate 1* cultures and the high ratio within an individual citrate culture, $\Delta\delta^{18}O{:}\Delta\delta^{15}N$ remained nearly constant across a broad $^{15}\varepsilon_{denit}$ range (Figure 10). Therefore, while $^{18}\varepsilon_{denit}$ and $^{15}\varepsilon_{denit}$ vary significantly between treatments, they remain nearly equal within a given culture.

Discussion

Redox and ε_{denit}

In this study, cultures of *Paracoccus denitrificans* were grown using a variety of carbon sources, and the discrimination of the N and O isotopes of ambient nitrate during denitrification

($^{15}\varepsilon_{denit}$ and $^{18}\varepsilon_{denit}$, respectively) was monitored in each culture. Cultures grown on different carbon sources exhibited distinct ε_{denit} values, which, except for differences between two discrete sets of succinate grown cultures, were consistent among replicate cultures. The variation in ε_{denit} among cultures grown with different carbon substrates was correlated with the culture's specific respiration rate. We hypothesized that the oxidation state of the cultures' carbon source would control ε_{denit}. More oxidized carbon substrates were expected to lead to lower ε_{denit} values. This hypothesis is based on two assumptions: (1) nitrate uptake into the cell is regulated by the redox state of some component(s) of the electron transport chain, and (2) growth fuelled by more oxidized carbon substrates will lead to a more oxidized electron transport chain. Contrary to expectations, however, no clear correlation was found between the carbon substrate oxidation state and the magnitude of ε_{denit} (Figure 5). This result suggests that one or both of the assumptions inherent to the hypothesis could be erroneous, or that nitrate isotope fractionation responds to physiological mechanisms for which we have not accounted.

In regard to the first assumption, experimental evidence indicates that nitrate uptake does not occur when the ETC is overly oxidized, and the extent of ETC reduction has been correlated with nitrate respiration rates (John 1977; Alefounder et al. 1981; Kucera et al. 1981; Alefounder et al. 1983, Kucera et al. 1983). In combination with the failure of alternative hypotheses to explain nitrate respiration inhibition, such as the direct regulation of ETC components or transport proteins by inhibiting compounds (John 1977, Alefounder et al. 1981), these observations strongly suggest that nitrate uptake is modulated through the ETC oxidation state. Nonetheless, the evidence does not preclude the possibility that, while a threshold ETC oxidation state may be required for nitrate uptake to occur, other physiological controls may then contribute to the regulation of the nitrate uptake rate. For instance, evidence that small changes

in the oxidation state of the ETC will result in proportional modifications to the nitrate uptake rate may reflect competition by intermediates of denitrification, nitrite and nitrous oxide, for electrons, rather than direct control over nitrate transport. While inhibition of nitrate reduction by nitrite and nitrous oxide was correlated with the extent to which the respective compounds oxidized the ETC (Alefounder et al. 1983; Kucera et al. 1983), it is not known to what degree inhibition was induced by changes in the ETC redox state vs. competition between these final electron acceptors for electrons.

Redox and ε_{denit} – growth

Supposing that a more reduced ETC will lead to greater nitrate uptake, and thus a higher $^{15}\varepsilon_{denit}$, the hypothesis that growth on more oxidized carbon sources will lead to a more oxidized ETC, does not hold up. The lack of correlation seen in this study between carbon substrate oxidation state and ε_{denit} suggests that a culture's carbon substrate oxidation state does not predominantly control the ETC redox state in and of itself. We had made the simplifying assumption that the reducing power of a given carbon source translates to a proportional electron flux to metabolic processes. This was expected to be the case due to past observations that electron flux to periplasmic nitrate reductase (NAP) increases alongside the reducing power of the carbon substrate (Richardson and Ferguson 1992; Sears et al. 1997; Ellington et al. 2002). This relationship did not extend to NAR, presumably due to the greater influence of factors other than carbon oxidation state in controlling the net oxidation state of the ETC.

The mean oxidation state of the electron transport chain (ETC) is necessarily a function of (a) the rate at which electrons are provided and (b) the rate at which electrons are consumed by the final electron acceptors. Electrons are provided to the ETC by reductants (such as NADH)

produced from the catabolism of carbon compounds, and by the direct oxidation of some carbon substrates (e.g., the conversion of succinate to fumarate by succinate dehydrogenase; Madigan and Martinko 2006). The redox state of the carbon substrate thus offers a first order measure of the potential for electron supply to the ETC. However, a number of additional factors can also affect the rate at which the ETC is supplied with electrons - including the rate of catabolism and alternative routes of electron consumption. Alternative routes include anabolism and the activity of electron sinks, such as NAP. In turn, the potential rate at which electrons can be consumed by respiration is a function of the kinetics of the catalysts and enzymes involved in respiration. The respective kinetics of electron transport catalysts and enzymes are intrinsic to each, and sensitive to the concentration(s) of terminal oxidant(s) (e.g., O_2, nitrate, nitrite, and nitrous oxide).

The fact that a culture's specific respiration rate and $^{15}\varepsilon_{denit}$ value have been seen to be positively correlated in this study (Figure 7) provides evidence that the rate of catabolism is the predominate factor in increasing the electron supply in growing cultures, presuming positive correlation between the specific respiration rate and growth rate. For one, the rate of catabolism must increase to produce a significantly greater growth rate, as catabolism provides the carbon intermediates and energy necessary to construct cellular components. Secondly, if the diversion of reducing equivalents to the ETC were responsible for its decreased oxidation state, it would be drawing electrons from processes like anabolism or periplasmic nitrate reduction. A decline in reducing power provided to anabolic processes would eventually limit growth, and there is little evidence for high NAP activity in this study (see *Redox and nitrate uptake – NAP*). While growth rate and $^{15}\varepsilon_{denit}$ are related, reducing equivalents can be distributed between respiratory processes and biosynthesis (or other oxidative processes) with varying ratios in response to the utilization of different carbon substrates. This is a potential explanation for the variability seen in

the relationship between growth rate and $^{15}\varepsilon_{denit}$, as it could cause a particular growth rate to be associated with a range of respiration rates. The irregular partitioning of reducing equivalents between growth and respiratory processes was observed indirectly in the study of Constantin and Fick (1997), in which the use of ethanol or acetate as the carbon source appeared to result in a different growth to respiration ratio during denitrification in high nitrate industrial wastewater by *Pseudomonas* species. When grown on ethanol, the cultures exhibited greater growth and less nitrate respiration than cultures grown with acetate. Ethanol is much more reduced than acetate (an oxidation state of -2 vs. 0), and thus provides more electrons per molecule of carbon. Nonetheless, ethanol led to the production of more biomass per molecule of respired nitrate.

Disproportionate partitioning of reducing power is a result of growth using different carbon substrates due to the variety of metabolic pathways through which the substrates are processed. In *P. denitrificans* ethanol and acetate are metabolized using the glyoxylate cycle, succinate, malate, citrate, and pyruvate by the citric acid cycle, and glucose by the citric acid cycle preceded by the hexose monophosphate and Entner Douderoff pathways. Ethanol and acetate metabolism are closely related, as ethanol is converted to acetaldehyde, then to acetate via aldehyde dehydrogenase (Dimmer et al. 2012). During the conversion of acetaldehyde to acetate, aldehyde dehydrogenase is capable of reducing NAD^+ to NADH or $NADP^+$ to NADPH (Ghose and Badra 1985). As NADH is used in respiratory processes and NADPH is used in biosynthetic processes (Madigan and Martinko 2006), NADPH production by aldehyde dehydrogenase is a route by which ethanol may have provided biosynthetic processes with a greater proportion of its reducing power relative to acetate in the study of Constantin and Fick (1997). In the current study, however, the ethanol and acetate culture's $^{15}\varepsilon_{denit}$ cannot be compared by their respective assimilatory pathways since the ethanol culture was not growing

measurably during denitrification. The distinction between growth phases is discussed further below.

Compounds metabolized via the citric acid cycle exhibited nearly the full range of $^{15}\varepsilon_{denit}$ values seen in this study. No correlation between oxidation state and $^{15}\varepsilon_{denit}$ was seen within this subset of carbon compounds. However, the citric acid cycle in *P. denitrificans* can produce NADH or NADPH through the decarboxylation of isocitrate via NAD^+ or $NADP^+$ dependent isocitrate dehydrogenase (Kanehisa et al. 2000; Madigan and Martinko 2006, Kanehisa et al. 2014). With the exception of citrate cultures, which did not grow during denitrification, a possible explanation for the range of $^{15}\varepsilon_{denit}$ values seen among carbon substrates metabolized by the citric acid cycle may then be the disproportionate use of $NADP^+$ vs. NAD^+ dependent forms of isocitrate dehydrogenase, both of which are present in *P. denitrificans*. It is, however, unclear what may cause one form of isocitrate dehydrogenase to be used over the other. Glucose grown cultures exhibited the greatest $^{15}\varepsilon_{denit}$ value in this study. This is consistent with the fact that the biosynthesis of polysaccharides requires glucose and its derivatives. As a result, cells grown on the carbon substrates metabolized by the citric acid cycle and the glyoxylate cycle must synthesize glucose via gluconeogenesis in order to grow, consuming reducing equivalents in the process (Madigan and Martinko 2006).

The supposition that an increased growth rate will elevate catabolism and thus increase the electron supply to the ETC, amplifying nitrate uptake and $^{15}\varepsilon_{denit}$, does not apply to organisms that are not growing. Cultures using ethanol or citrate as the carbon source did not exhibit exponential growth phase during denitrification in this study (Figure 6). In the citrate cultures, the cells ceased to grow upon the switch from aerobic to anaerobic conditions, then proceeded to die off, as suggested by direct cell counts. This is explained by the fact that *P. denitrificans* is

incapable of anaerobic growth using citrate (Robertson and Kuenen 1983). Nonetheless, denitrification occurred in anaerobic citrate cultures, but with the lowest measured $^{15}\varepsilon_{denit}$. The reason *P. denitrificans* is unable to grow anaerobically using citrate is not known. However, ineffective metabolism of citrate could conceivably lead to a more oxidized ETC by providing a limited supply of catabolically derived reducing equivalents, with stored citrate derivatives and/or cell lysis products allowing for diminutive catabolic activity. In contrast, the single culture grown on ethanol performed denitrification during stationary phase with a relatively high $^{15}\varepsilon_{denit}$ of 26.5 ± 0.8‰. The high $^{15}\varepsilon_{denit}$ of the ethanol culture is consistent with our expectation that high nitrate uptake results from a more reduced ETC. The total electron supply per metabolized ethanol molecule would have been high due to ethanol's exceptionally low (-2) carbon oxidation state. Furthermore, while the cells in the ethanol culture were not multiplying and exhibited no evidence for elevated NAP activity (discussed below), nitrate drawdown within the culture medium occurred over a time-span comparable to exponentially growing cultures. In other words, the culture exhibited no obvious decline in nitrate respiration, but alternative routes of electron consumption were not active, potentially leaving the ETC reduced. A lower $^{15}\varepsilon_{denit}$ than was seen in the ethanol culture may be typical for organisms in stationary phase as a result of the catabolism of more oxidized carbon sources, high NAP activity, or other unknown reasons. Alternatively, organisms may commonly maintain high nitrate respiration rates while in stationary phase, but only when a carbon source is available (unlike the citrate cultures). The lack of growth in stationary phase cultures could lead to a reduced ETC due to the decreased diversion of reducing equivalents to anabolic processes, while electrons continue to be provided to the respiratory chain to generate energy for living cells. Unfortunately, a detailed understanding of the relationship between growth phase and $^{15}\varepsilon_{denit}$ cannot be reached, as studies

investigating $^{15}\varepsilon_{denit}$ are typically performed under conditions which lead to measurements of $^{15}\varepsilon_{denit}$ during exponential growth phase (e.g., Granger et al. 2008; Kritee et al. 2012; Wunderlich et al. 2012) and due to our small sample size of only one ethanol culture and two citrate cultures.

Since the ETC oxidation state is a function of both electron sinks and sources, the argument may be posed that an increase in electron supply need not be met with a reduction in the oxidation state if the supply is countered by an equally high respiration rate. However, I propose that the greater electron supply imposed by a higher growth/catabolic rate necessarily leads to a more reduced ETC oxidation state until an appropriately high intracellular nitrate concentration is reached, proportional to the size of the electron supply. In other words, initially, the high electron supply reduces the ETC because the concentration of intracellular nitrate cannot sufficiently promote catalysis of nitrate reduction at an equivalent rate. Eventually, enough intracellular nitrate accumulates (and enough NAR is synthesized), that the respiratory consumption of electrons approaches the rate at which electrons are provided. At this point, approximate redox steady state would be achieved in the ETC. If the intracellular nitrate concentration falls too low, the ETC redox state would likewise fall and increase nitrate uptake.

Redox and ε_{denit} – Cell-specific nitrate respiration rate

An alternative explanation to our hypothesis that growth rate drives change in the nitrate uptake rate through ETC oxidation state is that nitrate uptake is driven by NAR activity. The cell-specific nitrate respiration (CSNR) rate has been proposed to be linked to NAR activity due to the energy dependence of uptake upon respiration (Rowe et al. 1994; Kritee et al. 2012), and due to positive correlation between CSNR and $^{15}\varepsilon_{denit}$ (Kritee et al. 2012). This claim is supported by the observation that NarG^{-} mutants, which are impaired in their ability to produce a catalytic

subunit of NAR, had greatly reduced nitrate uptake rates relative to controls (Rowe et al. 1994). Nitrate can be transported into the cell by either a nitrate/nitrite antiporter or a nitrate/H^+ symporter (Boogerd et al. 1983; Goddard et al. 2008). The symporter is reliant upon nitrate respiration to generate energy in the form of a proton gradient across the plasma membrane, and the antiporter is dependent upon nitrate respiration to generate nitrite via nitrate reduction. While the activity of both of these proposed transporters thus requires products of nitrate respiration, they are not necessarily limited by nitrate respiration. The case may be that an increase in cell-specific nitrate respiration is a result of elevated nitrate uptake, rather than its cause. The notion that nitrate respiration is the direct driver of nitrate uptake is incompatible with the view that the uptake rate is a function of the electron transport chain oxidation state. Presuming that a more reduced ETC leads to a higher uptake rate, then, with the electron supply held constant, an elevated nitrate respiration rate would decrease the uptake rate by oxidizing the ETC. A co-occurring process must thus be amplifying the supply of electrons to the ETC (i.e. catabolism).

The relationship between cell-specific nitrate respiration and $^{15}\varepsilon_{denit}$ does, however, provide support for the notion that the magnitude of $^{15}\varepsilon_{denit}$ is a function of the nitrate uptake rate. In the experiments of Kritee et al. (2012) the value of ε_{denit} increased as CSNR rose among three species, *P. denitrificans*, *Pseudomonas chlororaphis*, and *Marinobacter*. The use of different carbon substrates resulted in different ε_{denit} values, but the proportional relationship between ε_{denit} and CSNR remained. Cultures grown on ethanol and citrate in this study behaved consistently with this relationship. The CSNR of the ethanol culture was an order of magnitude higher than citrate cultures, while ethanol and citrate cultures exhibited $^{15}\varepsilon_{denit}$ values of 26.5 ± 0.8‰ and 12.9 ± 1.4‰, respectively. CSNR rates were not obtained for other carbon sources.

The CSNR rate of a cell may be elevated by concentrating more nitrate in the cell and by concentrating the NAR enzyme. The observed proportional relationship between the CSNR rate and ε_{denit} reveals that an increase in intracellular nitrate plays a prominent role in the maximization of the CSNR rate. This is because, in the context of the efflux model, an increase in CSNR will decrease ε_{denit} by lowering a cell's uptake to efflux ratio if its nitrate uptake rate is held constant. Without an increase in uptake, efflux becomes a smaller proportion of the potential nitrate output from the cell. Therefore, the nitrate uptake and efflux rates must rise to a greater extent than the CSNR rate in order to prevent ε_{denit} from falling.

The concentration of enzymatic substrates in the intracellular pool is often preferred to the synthesis of enzymes (Button 1985). This is consistent with the observation that, in *P. denitrificans*, the K_m of nitrate uptake, at <5 μmol L^{-1} (Parsonage et al. 1985), is significantly lower than that of NAR, which has been reported in the range of 13 μmol L^{-1} to 300 μmol L^{-1}. However, it should be noted that a wide range of K_m values have been reported for NAR, which are seemingly dependent on the reductant provided in vitro. The highest K_m values, ranging from 300 μmol L^{-1} in *P. denitrificans* (Craske and Ferguson 1986) to 3.8 mmol L^{-1} in *Pseudomonas stutzeri* (Blumle and Zumft 1991), have been measured using non-physiological reductants, methyl viologen (MV) and benzyl viologen (BV). Lower K_m values for NAR in *P. denitrificans* have been reported using physiological reductants. The use of durohydroquinone or NADH as the reductant resulted in K_m values of 13 μmol L^{-1} (Craske and Ferguson, 1986) and 40-70 μmol L^{-1} (Parsonage et al. 1985), respectively. The values reported for the physiological reductants should be taken as a lower limit for NAR activity, which may have been limited by the enzymatic rate of NADH or durohydroquinone oxidation.

Redox and ε_{denit} – electron consumption by NAP

An alternative sink for electrons, in the form of periplasmic nitrate reduction by the NAP nitrate reductase, bears further consideration, as it provides a potential explanation for the lack of correlation seen between carbon substrate oxidation state and ε_{denit}. NAP is a dissimilatory nitrate reductase present in denitrifying bacteria. It can act as an electron outlet for redox balance, as its activity has been seen to increase in response to growth on more reduced carbon substrates, but, in most strains studied to date, is not linked to the generate of a proton motive force or to growth (Richardson and Ferguson 1992; Sears et al. 1997; Ellington et al. 2002). The use of NAP as an electron outlet is one possible explanation for the lack of correlation seen between the oxidation state of carbon substrates and ε_{denit}, as excess electrons supplied by more reduced carbon sources may have been fed to NAP rather than NAR. The difference between the isotope effect of NAP and NAR on N and O isotopes of nitrate can potentially be used to determine the relative activity of the respective enzymes. In cultures of *Rhodobacter sphaeroides* NAP had a $^{15}\varepsilon$ ranging from 12.6 ± 0.2 to 19.9 ± 0.2 and an $^{18}\varepsilon$ ranging from 7.9 to 13.1. Despite the variation in isotope effects across cultures, the change in $\delta^{18}O$ to change in $\delta^{15}N$ ratio ($\Delta\delta^{18}O$:$\Delta\delta^{15}N$) was consistent, at 0.62 ± 0.2 (Granger et al. 2008). Because NAP is located in the periplasm, the expression of its isotope effect is not reliant upon nitrate efflux from the cell. Transport to and from the periplasm is a result of fractionation-free diffusion (Mariotti et al. 1988), and, as such, the isotope effect of NAP should be fully expressed to the surrounding media. In contrast, a variable ε_{denit} of up to 30‰, with a consistent $\Delta\delta^{18}O$:$\Delta\delta^{15}N$ ratio of 1:1, is expected for NAR by analogy to the eukaryotic assimilatory nitrate reductase and repeated measurements among several denitrifying species (Granger et al. 2008; Kritee et al. 2012; Karsh et al. 2012; Wunderlich et al.

2012). Therefore, in denitrifier cultures, ε_{denit} values below 30‰ with $\Delta\delta^{18}O{:}\Delta\delta^{15}N$ ratios below 1:1 may be indicative of NAP activity.

In this study, $\Delta\delta^{18}O{:}\Delta\delta^{15}N$ was seen to range from 0.87 ± 0.02 to 1.04 ± 0.12, with measurements for all but *succinate 1* (0.87 ± 0.02) and citrate (1.04 ± 0.12) cultures lying between 0.92 and 0.96 (Figure 10). The relatively low $^{15}\varepsilon_{denit}$ of 17.0 ± 0.7 and $\Delta\delta^{18}O{:}\Delta\delta^{15}N$ of 0.87 ± 0.2 make *succinate 1* cultures the best candidate for NAP influence within this study. Unexpectedly, *succinate 1* had a $\Delta\delta^{18}O{:}\Delta\delta^{15}N$ and a $^{15}\varepsilon_{denit}$ below that of *succinate 2*. While NAP is a possible explanation for this difference, *succinate 1* and *succinate 2* cultures were intended to be grown under identical conditions, so it is not clear what would cause its disproportionate expression. Succinate's moderate oxidation state of +0.5 does not invoke much need for NAP in redox balancing. Nonetheless, growth with succinate has been seen to induce some NAP activity, with aerobic conditions inducing roughly twice as much activity as anaerobic conditions in *Paracoccus pantrotrophus* cultures (Ellington et al. 2002). With an oxidation state of -2 the ethanol grown culture would seem to be the most likely to induce high NAP activity from a redox perspective. Its $^{15}\varepsilon$ was indeed below the maximum allowable by NAR, but its $\Delta\delta^{18}O{:}\Delta\delta^{15}N$ ratio was approximately the same as glucose and pyruvate cultures - which exhibited greater isotope effects. Similarly, *acetate 1* and *acetate 2* cultures had relatively low $^{15}\varepsilon$ values, but $\Delta\delta^{18}O{:}\Delta\delta^{15}N$ ratios equivalent to or greater than those of glucose and pyruvate (Table 4). A major contribution to nitrate reduction by NAP in the ethanol and acetate cultures is thus not likely.

There are three caveats to the use of ε and $\Delta\delta^{18}O{:}\Delta\delta^{15}N$ ratios to determine NAP activity. The first being that the fractionation of N and O isotopes of nitrate by NAP has only been measured in one species, *R. sphaeroides* (Granger et al. 2008). It is unknown whether other

species would exhibit the same $^{15}\varepsilon$ and $^{18}\varepsilon$ for NAP, as its genetic expression differs significantly between organisms (Moreno-Vivián et al. 1999). The second caveat is that the isotope effect of NAR has not been studied in isolation from NAP. A $\Delta\delta^{18}O{:}\Delta\delta^{15}N$ ratio of 1:1 is supported for NAR by analogy to the eukaryotic assimilatory nitrate reductase and repeated measurements near 1:1 among several denitrifying species (Granger et al. 2008; Kritee et al. 2012; Karsh et al. 2012, Wunderlich et al. 2012). Variability in these measurements is considerable, however, with $\Delta\delta^{18}O{:}\Delta\delta^{15}N$ ranging from about 0.79 to 1.02, and this variability may itself be a result of NAP. Lastly, the isotope effect of transport is thought to have a $\Delta\delta^{18}O{:}\Delta\delta^{15}N$ greater than 1:1, counteracting NAP. The transport isotope effect is small, purportedly only becoming significant if the overall ε observed in a culture is ~5‰ or less (Karsh et al. 2014). Ambiguity introduced by the first two issues may be the reason the ε and $\Delta\delta^{18}O{:}\Delta\delta^{15}N$ values of cultures in this study did not reveal clear NAP activity.

Isotope effect of water-column denitrification

Despite the wide range of values measured for $^{15}\varepsilon_{denit}$ in laboratory cultures and in the field (Table 3), the water-column denitrification isotope effect on N isotopes of nitrate ($^{15}\varepsilon_{WC}$) is frequently considered to be 20-30‰ (e.g. Brandes et al. 2002; Sigman et al. 2003; Deutsch et al. 2004; Alkhatib et al. 2012; Eugster et al. 2012). This predicted $^{15}\varepsilon_{WC}$ is high relative to some measurements in laboratory and field studies, and has led to the calculation of a massive imbalance in the N budget of the contemporary ocean using an estimated average $^{15}\varepsilon_{WC}$ of 25‰ (Brandes and Devol 2002; see *Introduction*). The mean $^{15}\varepsilon_{denit}$ measured among all cultures in this study cultures was 23.2 ± 5.3‰. While this value approximates the 25‰ $^{15}\varepsilon_{WC}$ used to generate the N budget of Brandes et al. (2002), the variability among cultures is considerable and

it is unclear which cultures would best represent the average $^{15}\varepsilon_{WC}$ of the world ocean. For example, use of the 17.0‰ $^{15}\varepsilon_{denit}$ measured for *succinate 1* cultures would lower the total outputs estimated in the Brandes et al. (2002) N budget by almost 40%, bringing it much closer to balance. Large imbalances predicted by some modern N budgets (Table 1) have been used in support of the N cycle's role in controlling global climate on geologic time scales (e.g., Codispoti et al. 2001; Karl et al. 2002; Galbraith et al. 2004; Galloway et al. 2004). For further discussion of the role of nitrogen and other limiting nutrients in controlling global climate see *Appendix 1*.

As long as the global mean value of $^{15}\varepsilon_{WC}$ remains ambiguous, its use will be a large source of error in the calculation of marine nitrogen budgets. In order to better elucidate environmental controls on $^{15}\varepsilon_{denit}$ we examined the response of $^{15}\varepsilon_{denit}$ to growth using a variety of carbon substrates. Cultures grown using different carbon sources exhibited distinct $^{15}\varepsilon_{denit}$ values, which were positively correlated with the culture's specific nitrate respiration rate in cultures undergoing exponential growth (Figure 7). We interpret correlation between $^{15}\varepsilon_{denit}$ and specific nitrate respiration rate to indicate a direct causal relationship, in which high growth rates elevate $^{15}\varepsilon_{denit}$ by reducing the ETC (see *Redox and nitrate uptake - growth)*. To understand how the relationship between $^{15}\varepsilon_{denit}$ and growth may alter $^{15}\varepsilon_{WC}$, we must consider denitrification in the context of the oxygen minimum zones (OMZs) in which water-column denitrification occurs.

The vast majority of water-column denitrification in the world ocean occurs in three OMZs, the Eastern Tropical North Pacific (ETNP), Eastern Tropical South Pacific (ETSP), and the Arabian Sea (Kamykowski and Zentara 1990; Paulmier et al. 2009). OMZs manifest as a result of oxygen respiration during heterotrophic metabolism of organic matter descending through the water-column. Once oxygen has reached a sufficiently low concentration

denitrification occurs. Since OMZs are often carbon limited (Voss et al. 2001; Ward et al. 2008; Chang et al. 2014) and hypoxia is reliant upon heterotrophic metabolism, denitrification rates in OMZ's are linked to carbon input from the overlying euphotic zone (Liu and Kaplan 1984). An oxygen gradient exists across OMZs, allowing for a mixture of oxygen and nitrate respiration, while the OMZ core approaches anoxia (Paulmier and Ruiz-Pino 2009). As, at most, 0.1% of the global ocean can be defined as an OMZ (Codispoti et al. 2001), the conditions required to produce and maintain an OMZ are not common. More specifically, the three major OMZs develop in stratified waters that receive exceptionally elevated organic matter input due to high productivity in euphotic zones fed nutrient rich water from proximal upwelling zones. Being reliant on euphotic zone productivity, OMZs are subject to the influence of intra and inter-seasonal productivity changes. Seasonality is evident in the intensity of the ETNP and ETSP OMZs, though the Arabian Sea exhibits by far the greatest temporal variation, as seen through seasonal changes in the spatial extent and oxygen concentrations within the respective OMZs (Paulmier and Ruiz-Pino 2009). Enhanced upwelling during the summer in the Arabian Sea (Naqvi et al. 2000) and during the northern hemisphere winter in the ETNP (Thunell 1998, Altabet et al. 1999) and ETSP (Echevin et al. 2008) leads to phytoplankton blooms, which then feed the OMZ with pulses of organic matter. Pulses of organic matter input lead to successional changes in the microbial composition of the OMZ (Jayakumar et al. 2009), and are capable of releasing carbon limitation (Ward et al. 2008).

Spatial and temporal shifts in the value of $^{15}\varepsilon_{denit}$ may be associated with carbon availability in OMZs. With $^{15}\varepsilon_{denit}$ increasing as a direct result of elevated growth rates, the average $^{15}\varepsilon_{WC}$ in an OMZ may increase during intensified denitrification immediately following high organic carbon input. The connection between growth rate and $^{15}\varepsilon_{denit}$ further implies that

$^{15}\varepsilon_{WC}$ may decrease with depth. Unlike the culture incubations performed here, carbon substrates in OMZs are a mixture of decaying organic matter and breakdown products resulting from the remineralization of this organic matter. As such, available carbon substrates should become more refractory as the organic matter descends through the water-column and favorable compounds are consumed. Additionally, overall availability of carbon decreases with depth, as is seen in the Arabian Sea (Roullier et al. 2014), increasing the likelihood of carbon limitation in deeper portions of the OMZ. With more refractory carbon available at relatively low concentrations, growth slows, and $^{15}\varepsilon_{WC}$ may thus decrease. Analogously, in cultures grown using a complex organic carbon source (bactopeptone and casein extracts) $^{15}\varepsilon_{denit}$ was high during initial nitrate respiration, but declined after nitrate was completely respired and then re-amended (Kritee et al. 2012). The reduced $^{15}\varepsilon_{denit}$ may have resulted from a reduction in the lability of the organic carbon source after initial growth.

Large pulsed inputs of carbon and intermittent periods of carbon limitation within OMZs could cause $^{15}\varepsilon_{WC}$ to change in response to the growth phase of denitrifying microorganisms. As the carbon supply subsides and it becomes limiting following a large input event, cells will not be able to maintain growth. As carbon limitation persists following the cessation of growth and the microbial population stabilizes in response to the lower carbon input, cells may persist in stationary phase. Though little is known in regard to the relationship between growth phase and $^{15}\varepsilon_{denit}$, the ethanol and citrate cultures grown in this study may provide some clues (see *Redox and $^{15}\varepsilon_{denit}$ – growth*). The period following a decline in carbon input may be analogous to citrate grown cultures. Citrate cultures had entered stationary phase, and eventually the cell count declined, following the switch from aerobic to anaerobic conditions. This resulted in the lowest measured $^{15}\varepsilon_{denit}$ in this study, at 12.9 ± 1.4‰, presumably due to the inhibited ability of the cells

to provide electrons to the ETC via citrate catabolism. Extreme carbon limitation in the water-column may thus similarly exhibit a low $^{15}\varepsilon_{denit}$. Cells in stationary phase, but with an available carbon source (ethanol), exhibited a much higher $^{15}\varepsilon_{denit}$ of 26.5 ± 0.8‰. Whether this indicates that stationary phase cells in the water-column will denitrify with a high $^{15}\varepsilon_{WC}$ is unclear due to our sample size of a single culture with a single carbon source. Stationary phase denitrification resulting in both a high $^{15}\varepsilon_{denit}$, as seen in the ethanol culture, or a low $^{15}\varepsilon_{denit}$, as a result of the metabolism of more oxidized or recalcitrant carbon sources, is consistent with the notion that $^{15}\varepsilon_{denit}$ is controlled by the oxidation state of the ETC (discussed above). The relationship between growth phase and $^{15}\varepsilon_{denit}$ may be an important consideration in understanding $^{15}\varepsilon_{WC}$ under nutrient limited conditions, and thus requires further investigation.

The 25‰ $^{15}\varepsilon_{WC}$ used in the N budget of Brandes and Devol (2002) is rationalized by the fact that it is based on field measurements in the studies of Liu (1979), Brandes et al. (1998), Altabet et al. (1999), and Voss et al. (2001), which encompass each of the three major global OMZs (the ETSP, ETNP, and Arabian Sea). Variability related to carbon availability may explain their high $^{15}\varepsilon_{WC}$ values. Of these studies, temporal variation in particulate carbon flux was only reported in Altabet et al. (1999). Consistent with the expectation that high carbon flux will lead to a greater $^{15}\varepsilon_{WC}$, a spike in carbon flux from late May to early June occurred, while the $^{15}\varepsilon_{denit}$ of 22.7‰ was estimated during June (Altabet et al. 1999). Furthermore, $^{15}\varepsilon_{WC}$ values substantially lower than 25‰ have been measured in the field. For example, the studies of Sigman et al. (2003) and Ryabenko et al. (2012) contained $^{15}\varepsilon_{WC}$ estimates of ≤7‰ and 7.6 to 16.0‰, respectively. In both cases, an actual $^{15}\varepsilon_{WC}$ of 25‰ was assumed and the measured isotope effects were hypothesized to have been skewed by the influence of sedimentary denitrification, due to its much lower isotope effect of ~0-4‰ (Brandes and Devol 2002,

Lehmann et al. 2007). The influence of sedimentary denitrification was supported in the study of Ryabenko (2012) by the observation that the measured $^{15}\varepsilon$ value increased with distance from the shore. In light of the wide range of $^{15}\varepsilon_{denit}$ values measured in this study and in other culture studies, however, $^{15}\varepsilon_{WC}$ values measured below 25‰ cannot be assumed to stem solely from the influence of sedimentary denitrification, as the $^{15}\varepsilon_{WC}$ end-member may itself be below 25‰.

The association between high growth rates and high $^{15}\varepsilon_{denit}$ values allows for the prediction of general trends in $^{15}\varepsilon_{denit}$ in response to carbon input, but it does not allow for the calculation of a precise $^{15}\varepsilon_{WC}$ due to the potential significance of other poorly understood factors, such as the following: (1) Since pulsed carbon inputs and carbon limitation are common in OMZs (Thunnel et al. 1999; Voss et al. 2001; Ward et al. 2008; Chang et al. 2014) it is important to understand how the resulting changes in bacterial growth phase may affect their expressed $^{15}\varepsilon_{denit}$. To the best of my knowledge, laboratory measurements of $^{15}\varepsilon_{denit}$ have not been reported during the stationary phase of bacterial growth, aside from three cultures in this study. (2) The existence of significant interspecific responses to environmental conditions would complicate the expression of $^{15}\varepsilon_{denit}$, as OMZ bacterial populations are diverse and exhibit successional changes in their composition following large organic carbon inputs (Jayakumar et al. 2009). It is clear that $^{15}\varepsilon_{denit}$ exhibits intraspecific variation in response to environmental conditions (Granger et al. 2008; Kritee et al. 2012), however, the dearth of knowledge with respect to the control of $^{15}\varepsilon_{denit}$ by environmental conditions has prevented the detailed investigation of how species respond differentially to environmental changes. (3) Denitrification occurs in the presence of oxygen if oxygen concentrations are sufficiently low, and under such conditions oxygen may affect $^{15}\varepsilon_{denit}$ by partially inhibiting nitrate uptake or by competing with nitrate for electrons. The $^{15}\varepsilon_{denit}$ of *P. denitrificans* cultures in the study of Barford et al. (1999) did not change in response to oxygen

concentrations ranging from 0.0 to 0.3 µM. However, given a larger range of oxygen concentrations a relationship may be observed, as denitrification can occur in the presence of 10 µM oxygen or more (Lloyd et al. 1987; Yakusev and Neretin 1997). Growth of denitrifying organisms in the presence of 4 µM oxygen has yielded a reduced average $^{15}\varepsilon_{denit}$ relative to anaerobic cultures, though in some cases oxygen had no noticeable effect (Kritee et al. 2012). Oxygen gradients in OMZs may thus cause $^{15}\varepsilon_{WC}$ to decrease away from the OMZ core, as the oxygen concentration increases. (4) Temperature may affect $^{15}\varepsilon_{denit}$ in the water-column. Soil samples had observed values of 29.4 ± 2.4‰ at 20° C and 24.6 ± 0.9‰ at 30° C (Mariotti et al. 1981). A comparable effect during marine denitrification is another potential cause of variation in $^{15}\varepsilon_{WC}$.

The combined complexity of the environmental controls on $^{15}\varepsilon_{denit}$ and the spatial and temporal variability of the oxygen minimum zone environment does not allow for the confident assignment of a $^{15}\varepsilon_{WC}$ value without extensive further study. The most effective way to resolve this complexity is through combined study of denitrification *in situ* and in the laboratory. Investigations in the laboratory give clues as to what environmental conditions affect $^{15}\varepsilon_{denit}$ and the sign and magnitude of their effect. This knowledge can be used in *in situ* studies to determine what conditions must be monitored during $^{15}\varepsilon_{WC}$ measurement in order to accurately extrapolate its value to the global ocean. Field measurements of $^{15}\varepsilon_{WC}$ could be the temporary result of ephemeral conditions, rather than a representative average of $^{15}\varepsilon_{WC}$ in the marine environment. Due to the connection between growth rate and $^{15}\varepsilon_{denit}$ observed in this study, and the potential connection between $^{15}\varepsilon_{denit}$ and growth phase, it is important for future *in situ* $^{15}\varepsilon_{WC}$ measurements to be made in the context of changes in carbon flux and limitation. If minimal variation is seen in $^{15}\varepsilon_{WC}$ in response to changes in carbon limitation and availability, these

factors could be ruled out as important controls of $^{15}\varepsilon_W$. Significant variation in $^{15}\varepsilon_{WC}$ that is consistent with respect to changes in carbon limitation and availability may allow for the prediction of an average marine $^{15}\varepsilon_{WC}$ when combined with detailed knowledge of conditions within OMZs and a better understanding of the influence of temperature and oxygen. Significant variation in $^{15}\varepsilon_{WC}$ that is inconsistent with respect to changes in carbon limitation and availability would indicate the importance other determining factors, such as oxygen concentration, temperature, and interspecies variability.

Appendix 1 – A brief overview of nutrient limitation and climate change

In the past few decades much work has been done in the attempt to elucidate the relationship between nutrient limitation in the ocean and global climate. Life within the ocean is connected to climate via carbon dioxide (CO_2). Phytoplankton fix carbon from CO_2 into organic matter, partitioning carbon between the atmosphere and the marine organic pool. The resulting export of organic matter to the deep sea sequesters carbon within the ocean before the carbon in organic matter is respired back to CO_2, subsequently upwelled, and allowed to re-equilibrate with the atmosphere (Prentice et al. 2001). Carbon sequestration in the ocean as a result of biological activity is dubbed the "biological pump". The magnitude of carbon sequestered in this manner is a function of the productive capacity of the ocean, as controlled by the availability of nutrients, and the physical dynamics of the ocean. The roles of three limiting nutrients in regulating the strength of the biological pump, nitrogen, phosphorous, and iron, have been heavily debated.

In the attempt to understand how nutrient limitation affects primary production, the initial point of contention was whether nitrogen or phosphorous (P) acts as the dominant limiting

nutrient in the ocean (Broecker 1982; McElroy 1983). Phosphorous limitation would lend great importance to terrestrial weathering and sedimentary burial as drivers of marine productivity, as these processes are the dominant input and output of P in the ocean, respectively (Delaney 1998). On the other hand, nitrogen limitation would shift importance to the N budget of the ocean (Gruber 2008). In this case, the question of balance in the N budget arises, as disproportionate N inputs and outputs over long time scales would lead to large fluctuations in marine primary production. Importance then shifts from drivers of the marine P inventory to the primary controls of balance in the N budget, N input from N_2-fixation and N loss from denitrification (Brandes et al. 2002). Iron's influence further complicates the issue. Iron has the potential to both limit growth directly, as it stimulates growth in high nutrient low chlorophyll zones in high latitude regions (Martin 1990; Boyd et al. 2007), and indirectly, as iron availability has been proposed to limit N_2-fixation in mid and low latitudes (Falkowski 1997).

The argument for P as the limiting nutrient of marine productivity is attractive at face level. The marine phosphorous cycle operates over a greater span of time than the N cycle, as P has a residence time of ≥30,000 years (Delaney 1998) while fixed N has a residence time of 1,500 (Codispoti et al. 2001) to 3,500 years (Gruber and Sarmiento 1997). The input of P to the marine ecosystem is not directly controlled by biology, as it is dominated by riverine transport (Delaney 1998). In contrast, the primary input process (N_2-fixation) for oceanic N is microbial. The abundance of dissolved N_2 in seawater grants N_2-fixing organisms (diazotrophs) practically unlimited access to N, which potentially allows them to add fixed N to the marine environment until phosphorous limitation occurs. The notion that fixed N can be readily added to the marine ecosystem according to the needs of biology, while P cannot, has led many to believe that P is the ultimate limiting nutrient in the ocean on geological timescales (Redfield 1958; Broecker et

al. 1982; Tyrrell 1999). However, P may act merely as an upper limit to primary productivity – becoming important only in the special case that N and Fe are not.

Evidence for the role of iron in regulating climate through its deposition in HNLC zones is growing. Iron deposition at high latitudes allows organisms to grow using N and P that is already abundant in HNLC zones (Martin 1990). Stimulation of growth by iron addition to HNLC regions has been clearly demonstrated, as summarized in Boyd et al. (2007). Additionally, isotopic evidence from sedimentary cores in HNLC regions correlates increased iron flux with increased growth, decreased surface ocean nutrient concentrations, decreased atmospheric CO_2, and decreased temperature over the course of multiple glacial-interglacial cycles (Martinez-Garcia et al. 2014; Sigman et al. 2014).

Substantial support exists for N as the major limiting nutrient in contemporary oligotrophic expanses of the modern ocean. This is implied by the fact that the global average inorganic N:P ratio in the ocean falls below the average N:P seen in organic matter (Fanning 1992; Anderson and Sarmiento 1994; Gruber and Sarmiento 1997) and is indicated directly by the existence of vast expanses of the ocean in which N, but not P, is completely depleted (Moore et al. 2013). With N as the limiting nutrient, sufficient imbalances in the N budget of the ocean could lead to alterations in primary production large enough to modulate the concentration of CO_2 in the atmosphere on the scale of glacial-interglacial cycles. For instance, assuming that the C:N:P ratio of organic matter is constant (106:16:1, Redfield 1958), there is a N deficit of 2.7 $\mu mol\ kg^{-1}$ in the modern ocean (Anderson and Sarmiento 1994), and P is the ultimate limiting nutrient, Falkowski (1997) estimated that adding enough N to the ocean to bring the total marine N:P to 16:1 could sequester 600 Pg C. For comparison, 800 Pg carbon was lost from the

atmospheric CO_2 pool as CO_2 declined for ~10,000 years during the last glacial maximum (LGM) (Reynaud et al. 1993).

The induction or amplification of a glacial event based upon the stimulation of productivity by changes in the N cycle requires an increase in N_2-fixation and/or a decrease in denitrification. A greater Fe flux to oligotrophic regions of the ocean has been hypothesized to stimulate N_2-fixation (Falkowski et al. 1997; Broecker and Henderson 1998). However, iron additions to such waters have, thus far, failed to stimulate growth without the simultaneous addition of N or P (Graziano et al. 1996; Mills 2004; Moore et al. 2008; Moutin et al. 2008). Furthermore, recent studies suggest that N_2-fixation in the Pacific and the Atlantic was actually reduced during the LGM (Ren et al. 2009; Ren et al. 2012). A decrease in denitrification during glaciation is better supported. Reduced water-column denitrification during the LGM is implied by isotopic evidence from several studies (e.g. Altabet et al. 1995; Ganeshram et al. 1995; Pride et al. 1999; Robinson et al. 2007). Additionally, sedimentary denitrification is expected to be diminished during glaciation. Sedimentary denitrification predominantly occurs in the continental shelf benthos, the area of which would decrease during glaciation as a result of fallen sea levels (Christensen 1994).

Evidence for the occurrence of reduced denitrification during the LGM grants some weight to the notion that the N cycle influences glacial-interglacial cycles. To play such a role, however, the reduction in denitrification would have to overcome its coupling to N_2-fixation, a self-induced negative feedback loop (Gruber 2008), and the release of CO_2 from the ocean resulting from any increased burial of $CaCO_3$ associated with greater productivity (Sigman and Boyle 2000). Two mechanisms of N cycle stabilization have been proposed: (1) Increased denitrification would lower the N:P of upwelled water, lowering export production from the

surface ocean. Lower export production would then reduce the size of oxygen minimum zones, in which the majority of water-column denitrification occurs. Sedimentary denitrification would also decrease as its organic N supply is depleted (Broecker and Peng 1982; Codispoti et al. 1989). (2) If N-limitation becomes severe as a result of increased denitrification, nitrogen fixing phytoplankton would become more competitive, elevating overall N_2 fixation rates. While denitrification self-regulates by reducing overall surface export, N_2-fixation would act to increase the surface export. Eventually, N_2-fixation would cause the ocean to approach P limitation, and the associated high export production would stimulate denitrification (Michaels et al. 2001). Whether a reduction in denitrification is capable of overcoming these feedbacks and producing a large scale decline in atmospheric CO_2 is not known.

While studies on past changes in the magnitude of N_2 fixation and denitrification demonstrate that the N cycle is subject to climate correlated variability, the data is too sparse and imprecise to indicate whether N_2-fixation and denitrification have ever been sufficiently decoupled to induce or exacerbate climate change (e.g., Altabet et al. 1995; Ganeshram et al. 1995; Pride et al. 1999; Robinson et al. 2007 Ren et al. 2009; Ren et al. 2012).

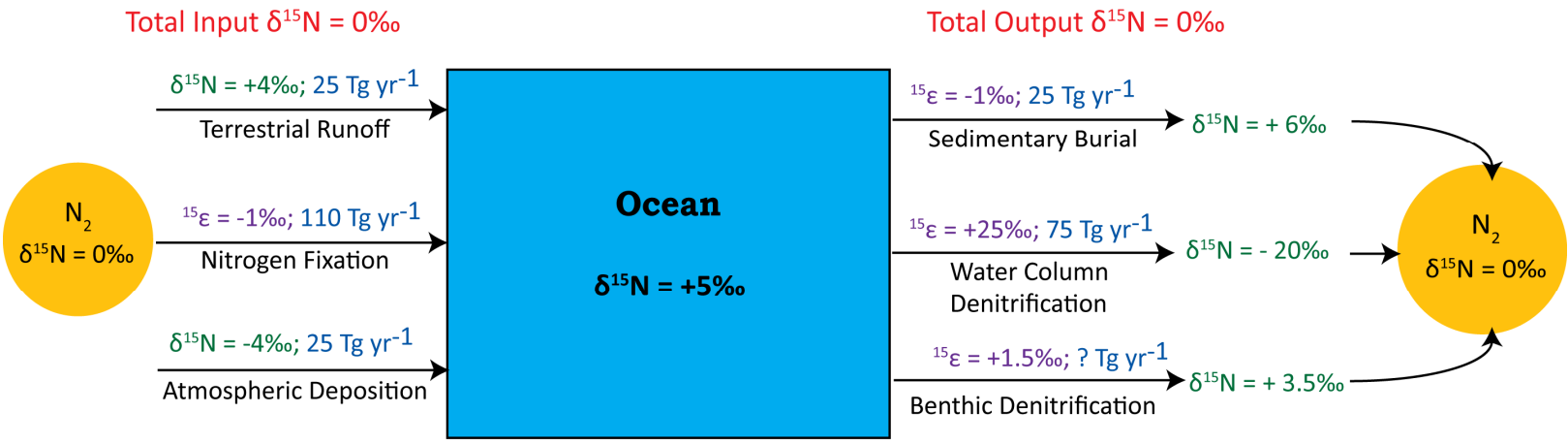

Figure 1. An oceanic nitrogen isotope budget using isotope enrichment and mass flux values compiled in Brandes et al. (2002). The $\delta^{15}N$ of oceanic fixed nitrogen is constant throughout the Holocene at 5‰. Thus, at steady state, the net $\delta^{15}N$ of nitrogen inputs and outputs must be equivalent. Nitrogen inputs were estimated from past studies, and have a net $\delta^{15}N$ of ~0‰, meaning that outputs must have a net $\delta^{15}N$ of ~0‰. The benthic denitrification rate was the sole unknown in the model, and was estimated at 250-300 Tg N yr-1 by a mass balance calculation. However, a smaller $^{15}\varepsilon$ for water-column denitrification would lower the calculated benthic denitrification output rate, bringing the nitrogen isotope budget closer to a balance.

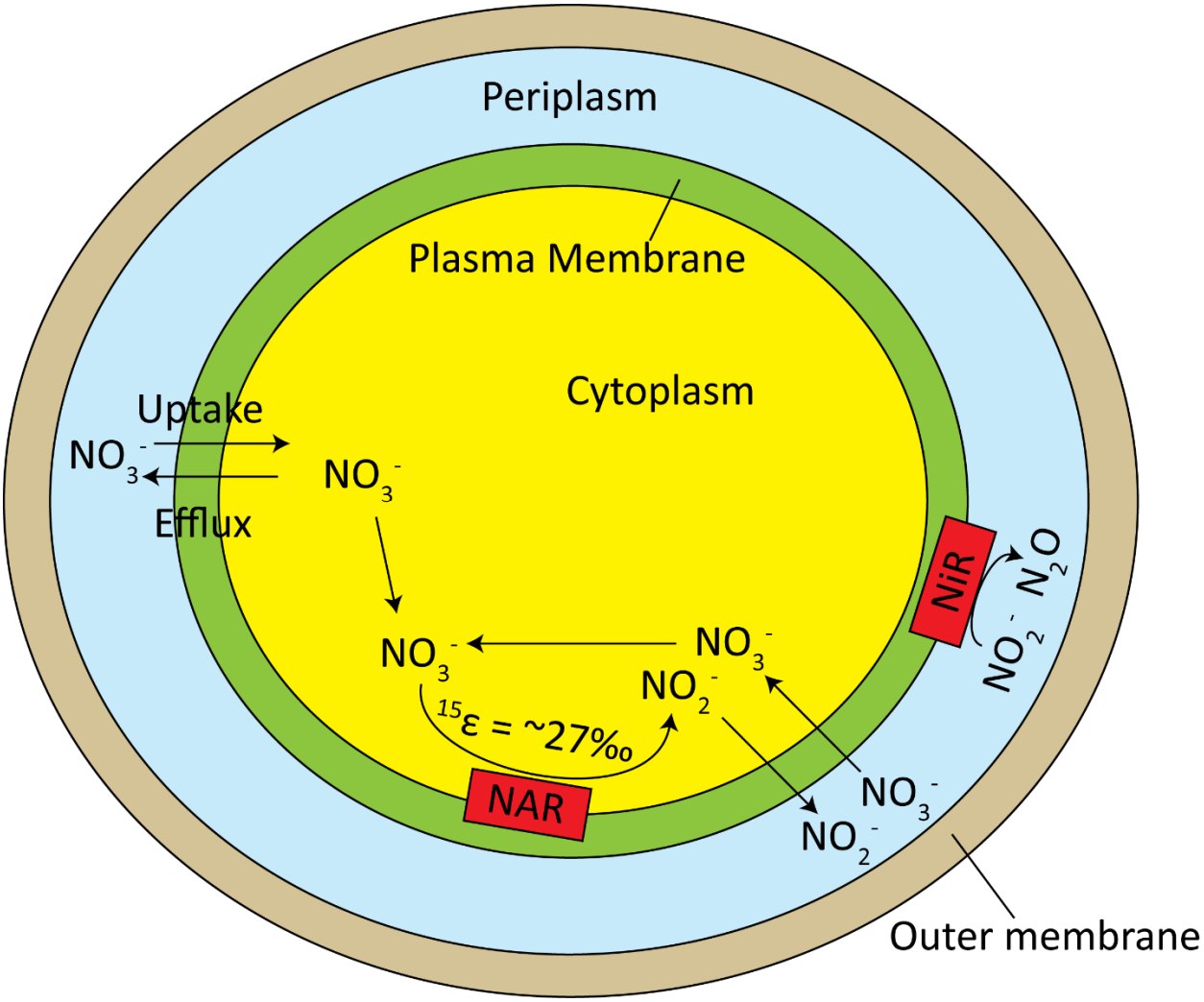

Figure 2. Nitrate isotope fractionation in a gram negative bacterium. NO_3^- is actively transported into the cell against an electrochemical gradient. It is then reduced by respiratory nitrate reductase (NAR) to nitrite. During NO_3^- reduction, NO_3^- bond breakage by NAR enriches the intracellular NO_3^- pool in ^{15}N, with an isotope effect of approximately 27‰. The subsequent diffusion of NO_3^- to the outside of the cell enriches the medium with an elevated $\delta^{15}N_{NO3}$. A NO_3^-/NO_2^- antiporter takes up nitrate while exporting nitrite to the periplasm. The exported NO_2^- may then be reduced to N_2O by respiratory nitrite reductase (NiR), which is embedded on the periplasmic face of the plasma membrane.

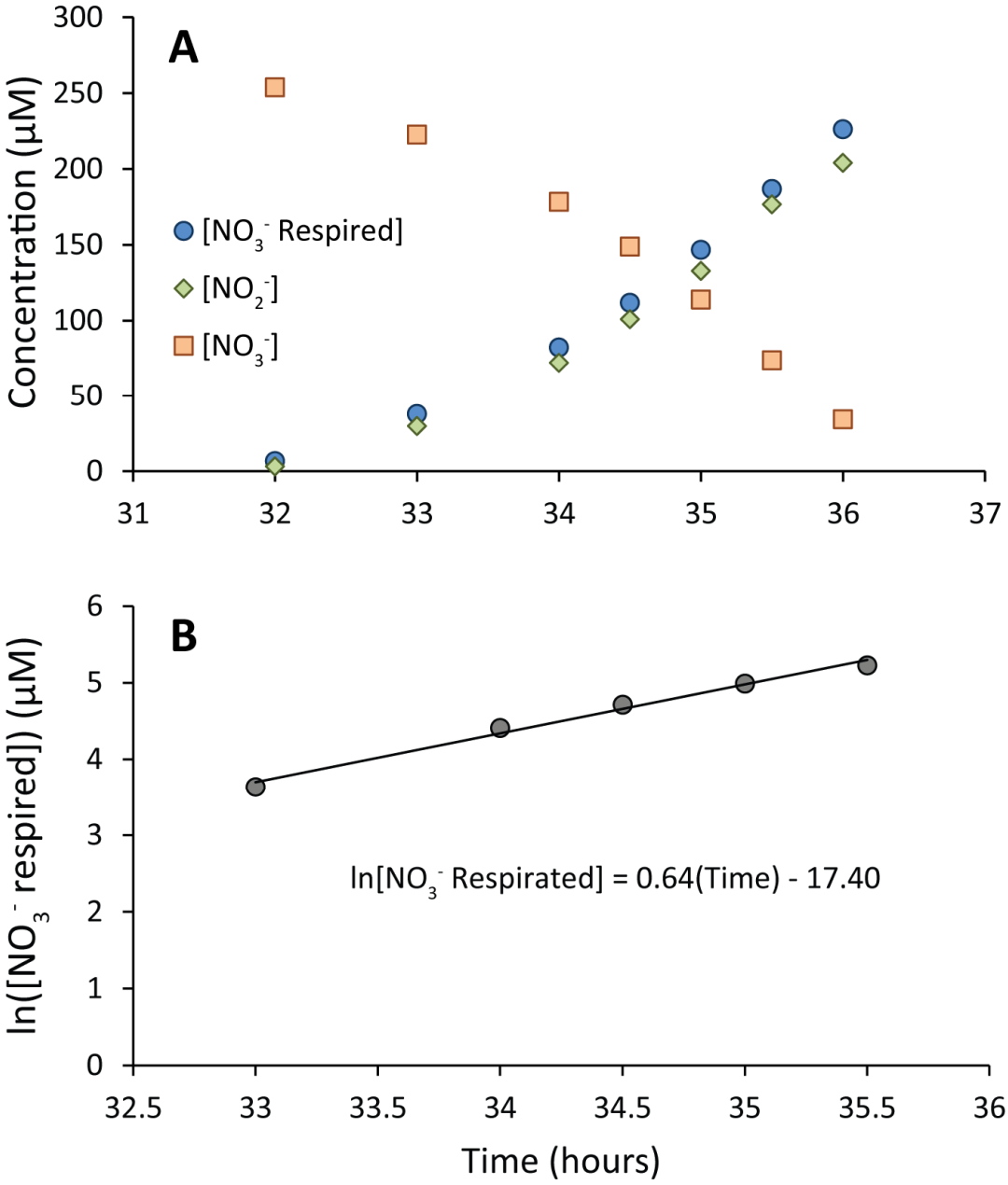

Figure 3. An example of NO_3^- respiration measured within a culture using malate as the carbon substrate. (A) The concentration of NO_3^- respired, NO_2^-, and NO_3^- vs. time. The difference between the concentration of nitrate respired and the nitrite concentration indicates nitrite reduction. (B) The natural logarithm of nitrate respired vs. time. The slope of the linear regression of this data series, seen here to be 0.64 hr^{-1}, equates to the specific respiration rate of the culture.

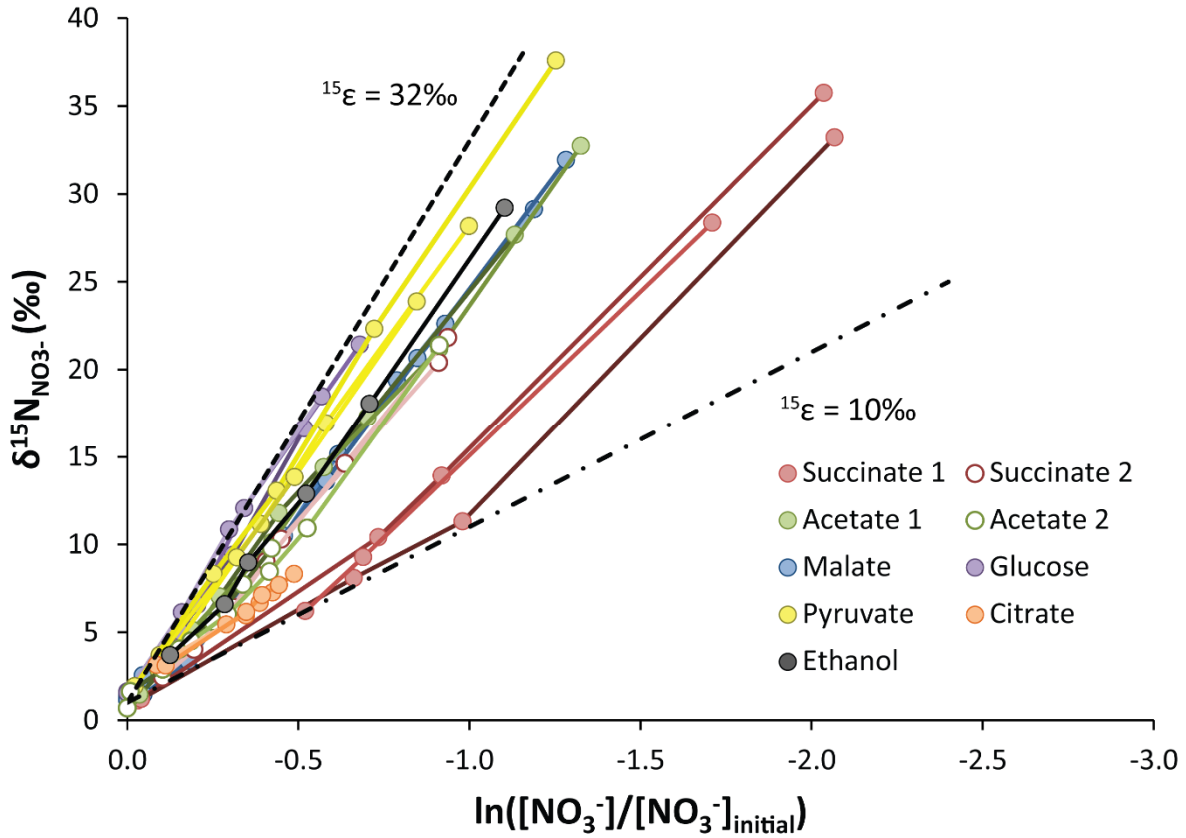

Figure 4. The isotopic enrichment of nitrate nitrogen ($\delta^{15}N_{NO3-}$) in cultures of *P. denitrificans* vs. the natural logarithm of the fraction of nitrate remaining within each individual culture. The slope resulting from the linear regression of each data series equates to a measurement of $^{15}\varepsilon$. The dashed black line represents a $^{15}\varepsilon$ of 32‰, while the dash-dot black line represents a $^{15}\varepsilon$ of 10‰.

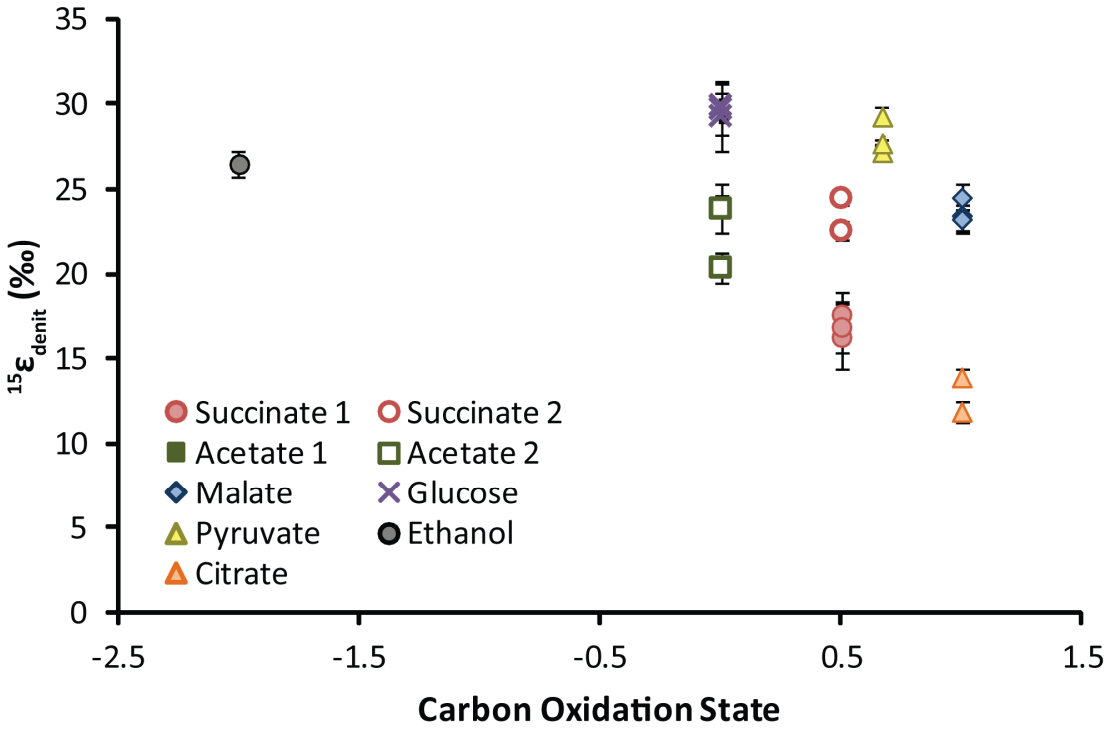

Figure 5. The $^{15}\varepsilon_{denit}$ of individual cultures vs. the culture's carbon substrate oxidation state.

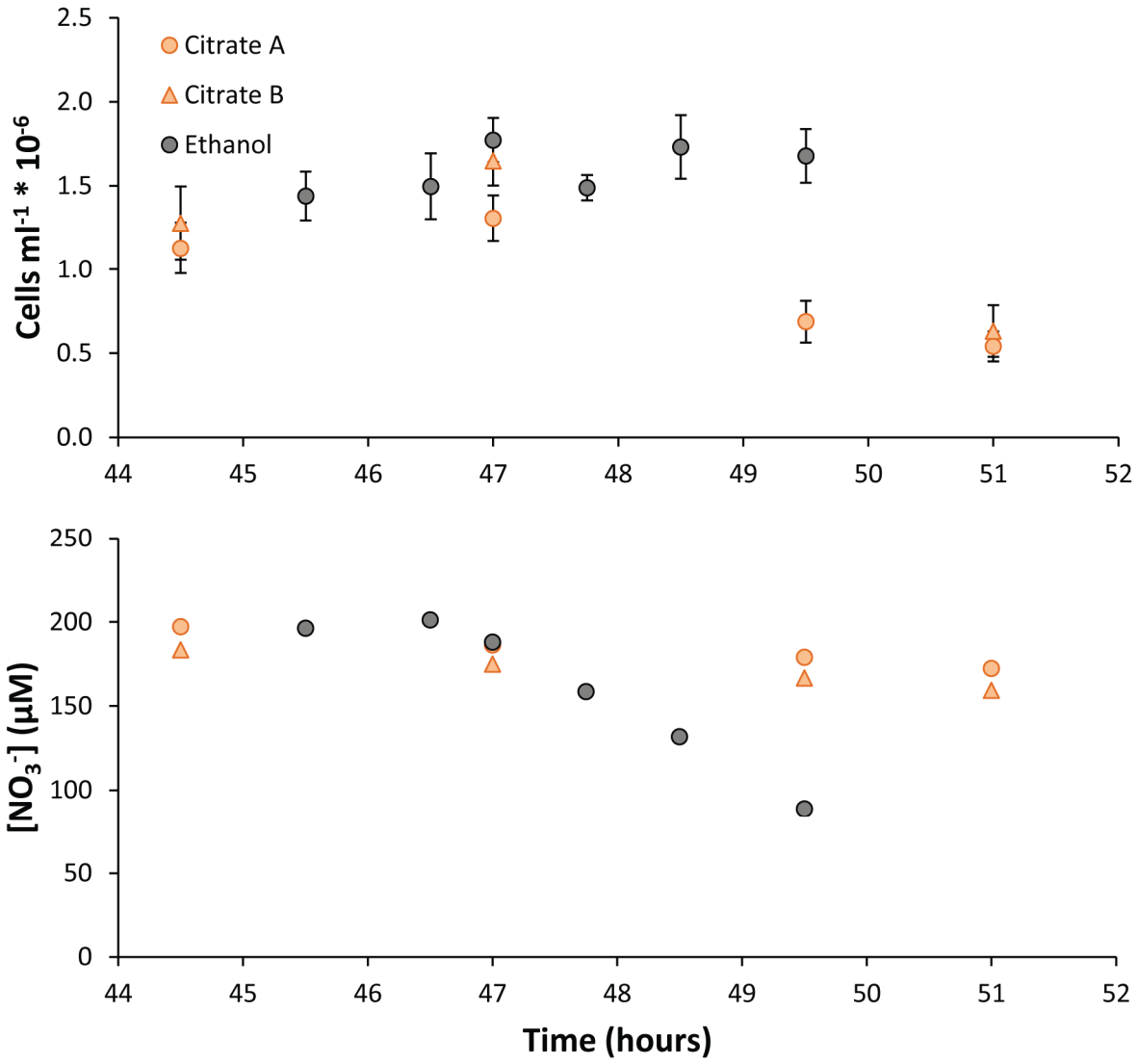

Figure 6. (A) Direct cell counts of the concentration of *P. denitrificans* cells per ml in citrate and ethanol cultures during active denitrification. Ethanol cellular concentrations remain nearly constant, at 1.60E6 ± 0.15E6. However, cells grown on citrate begin to die off after about 47 hours. (B) The concentration of nitrate remaining within citrate and ethanol cultures over the course of denitrification.

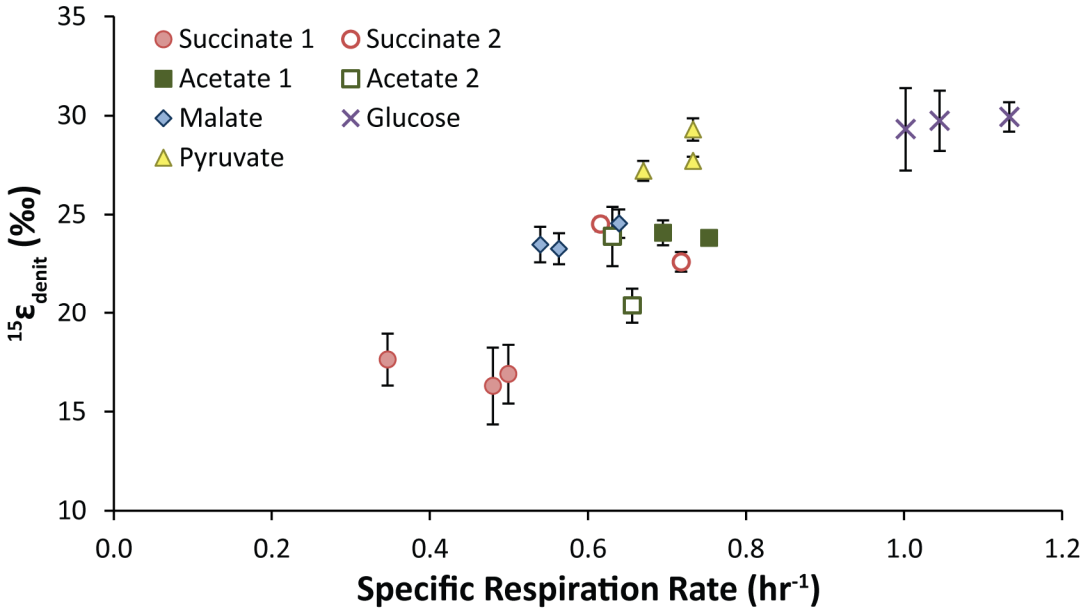

Figure 7. The $^{15}\varepsilon_{denit}$ of individual cultures vs. their specific respiration rate, where the specific respiration rate is the slope of the linear regression of the natural logarithm of the concentration of respired nitrate vs. time. $^{15}\varepsilon_{denit}$ displays a positive relationship with the specific respiration rate.

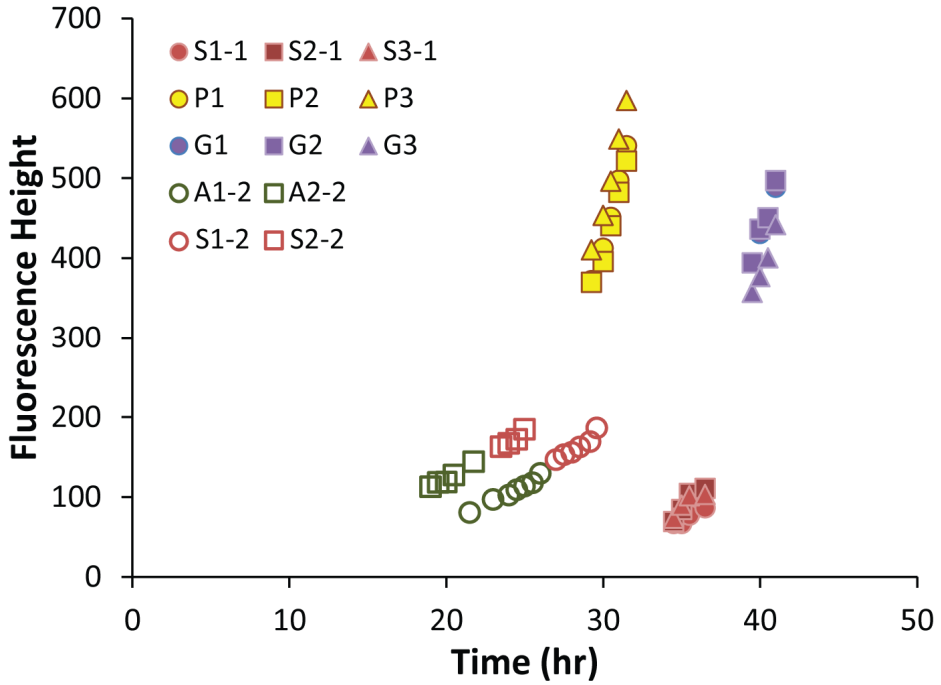

Figure 8. The height of fluorescence emitted by the picogreen DNA probe during spectrofluorometric analysis vs. time. The reported measurements were taken during active denitrification. (A) Repeated measurement of identical samples from malate grown cultures, analyzed in August 2013 or January 2014. (B) Measurements made for succinate, acetate, pyruvate, and glucose grown cultures.

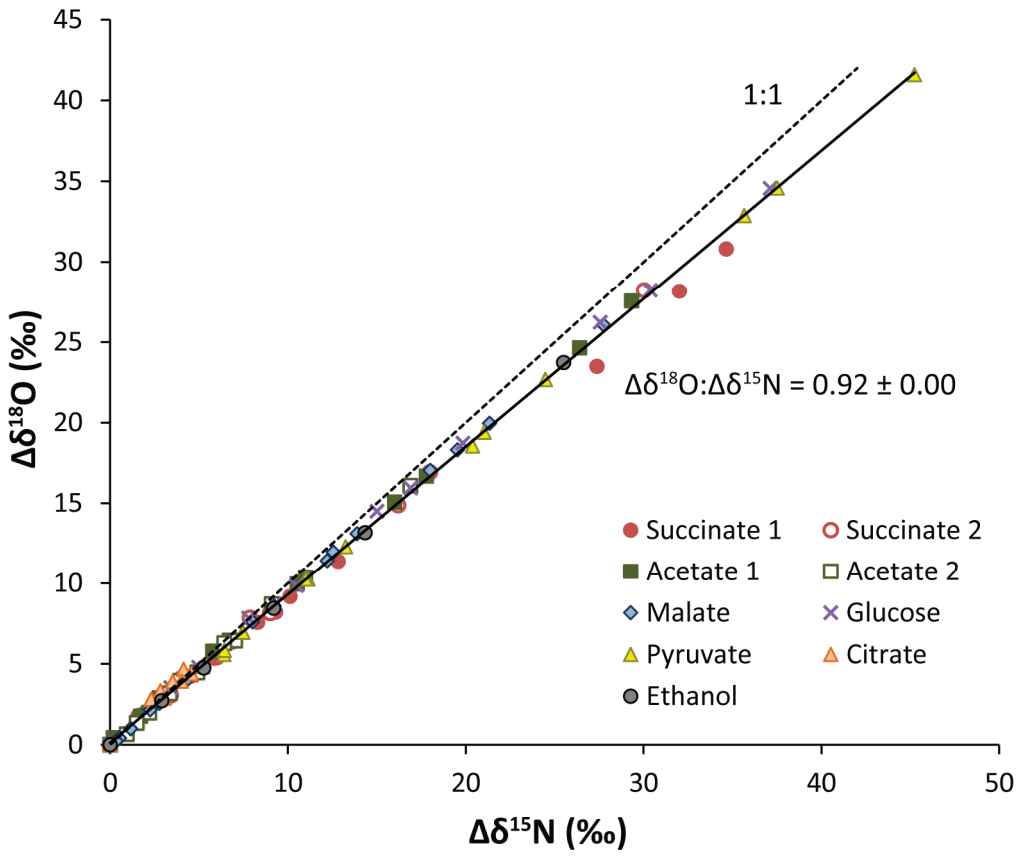

Figure 9. The change in $\delta^{18}O$ vs. the change in $\delta^{15}N$ ($\Delta\delta^{18}O$:$\Delta\delta^{15}N$) of nitrate in the culture medium as it is reduced during denitrification. Among all cultures a pooled $\Delta\delta^{18}O$:$\Delta\delta^{15}N$ of 0.92 ± 0.00 is observed, as represented by the solid line. The dashed line indicates the slope of a 1:1 $\Delta\delta^{18}O$:$\Delta\delta^{15}N$ relationship.

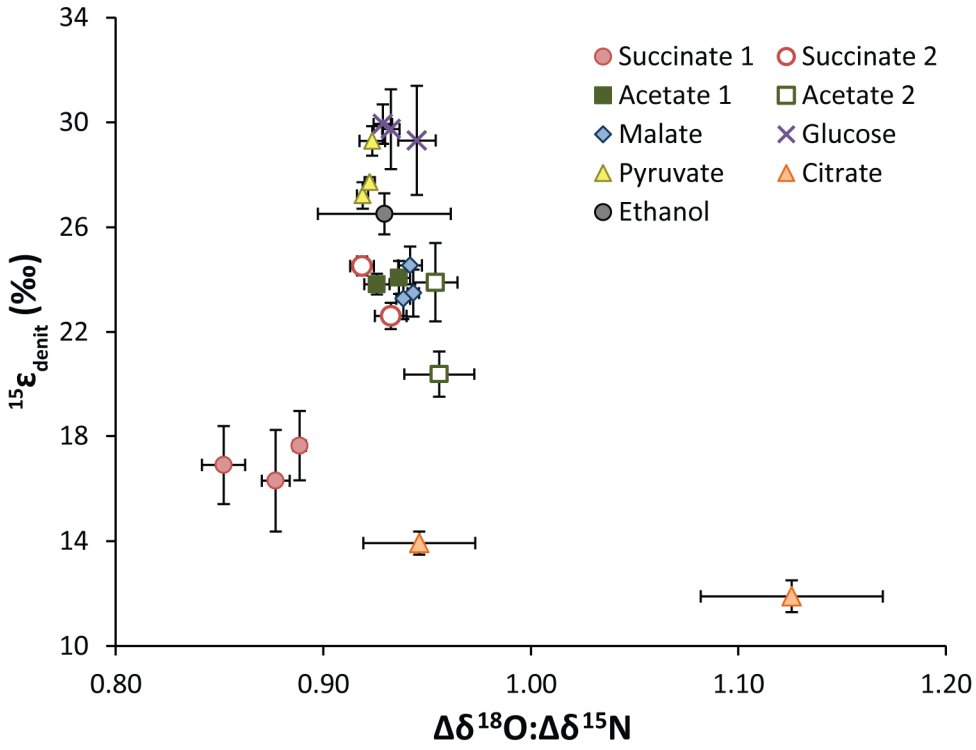

Figure 10. The $^{15}\varepsilon_{denit}$ of individual cultures vs. the ratio of the change in $\delta^{18}O$ to the change in $\delta^{15}N$ ($\Delta\delta^{18}O:\Delta\delta^{15}N$) during nitrate respiration. A remarkably high $\Delta\delta^{18}O:\Delta\delta^{15}N$ is observed in a single citrate culture, and low values are observed for the first set of succinate cultures. Otherwise, $\Delta\delta^{18}O:\Delta\delta^{15}N$ remains nearly constant with respect to $^{15}\varepsilon$.

Table 1. Past Nitrogen Budget Estimates

Reference	Sources (Tg N/yr)	Sinks (Tg N/yr)	Net (Tg N/yr)
Codispoti and Christensen, 1985	90	158	-68
Middelburg et al. 1996	90 to 293	313 to 418	-328 to -20
Gruber and Sarmiento, 1997	181±44	184±29	~Balanced
Codispoti et al. 2001	287	482	-195
Brandes and Devol 2002	160-380*	350 to 400	-240 to +30
Gruber and Sarmiento 2002	238 ± 44	204 ± 29	
Galloway et al. 2004	202	342	-140
Gruber 2004	265 ± 55	275 ± 55	~Balanced

*****The high source magnitude listed here is not robust. This nitrogen budget was developed using N isotopic constraints, and the N_2 fixation rate was thus allowed to vary over an extreme range of 110 to 330 Tg N yr^{-1} due to its minimal effect on the $\delta^{15}N$ of the ocean.

Table 2. Nitrogen fixation vs. denitrification rates estimated in past N budgets

Reference	Nitrogen Fixation (Tg N/yr)	Denitrification (Tg N/yr)
Gruber and Sarmiento, 1997	110 ± 50	165 ± 40
Codispoti et al. 2001	117	450
Karl et al. 2002	100 to 200	-
Brandes and Devol 2002	110 to 330*	275 to 355
Gruber 2004	120 ± 50	245 ± 70
Galloway et al. 2004	106	312

*****The high source magnitude listed here is not robust. This nitrogen budget was developed using N isotopic constraints, and the N_2 fixation rate was thus allowed to vary over an extreme range of 110 to 330 Tg N yr^{-1} due to its minimal effect on the $\delta^{15}N$ of the ocea

Table 3. N isotope effects of denitrification observed in monoculture and measured in the field.

Reference	$^{15}\varepsilon_{denit}$ (‰)	Conditions
Wellman et al. 1968	20-30	Laboratory culture of *Pseudomonas stutzeri*
Delwiche and Stein 1970	13 to 20	Laboratory culture of *Paracoccus denitrificans*
Brandes et al. 1998	22 to 25	Arabian Sea
Brandes et al. 1998	25 to 30	Eastern Tropical North Pacific
Altabet et al. 1999	22.7	Eastern Tropical North Pacific
Barford et al. 1999	28.6	Laboratory culture of *Paracoccus denitrificans*
Voss et al. 2001	22 to 30	Eastern Tropical North Pacific
Sigman et al. 2003*	7*	Eastern Tropical North Pacific
Granger et al. 2008	16.9 to 23	Laboratory culture of *Pseudomonas aureofaciens*
Granger et al. 2008	5.4 to 19.7	Laboratory culture of *Pseudomonas stutzeri*
Granger et al. 2008	17.6 to 24.8	Laboratory culture of *Paracoccus denitrificans*
Kritee et al. 2012	9.3 to 22.3	Laboratory culture of *Paracoccus denitrificans*
Kritee et al. 2012	11 to 29.5	Laboratory culture of *Pseudomonas stutzeri*
Ryabenko et al. 2012	7.6 to 16.0*	Eastern Tropical South Pacific OMZ

***These low water-column $^{15}\varepsilon_{denit}$ values were hypothesized to result from the influence of sedimentary denitrification.**

Table 4. The nitrate nitrogen isotope effect ($^{15}\varepsilon$), specific respiration rate, ratio of the change in $\delta^{18}O$ vs. the change in $\delta^{15}N$ ($\Delta\delta^{18}O$:$\Delta\delta^{15}N$), and carbon oxidation state for cultures of *P. denitrificans*. The reported values correspond with simultaneously grown replicate cultures containing the given carbon substrate, and are stated ±1 standard deviation. Since only a single ethanol cultures was measured, the standard deviation of ethanol data points corresponds with the linear regression analyses associated with their calculation.

Carbon Source	# Replicate Cultures	$^{15}\varepsilon$ (‰)	Respiration Rate (hr^{-1})	Δδ18O:Δδ15N	Carbon Oxidation State
Acetate 1	2	24.0 ± 0.2	0.72 ± 0.04	0.93 ± 0.01	0
Acetate 2	2	22.1 ± 2.5	0.64 ± 0.02	0.96 ± 0.00	0
Citrate	2	12.9 ± 1.4	-	1.04 ± 0.13	1.0
Ethanol	1	26.5 ± 0.8	-	0.93 ± 0.01	-2
Glucose	3	29.7 ± 0.3	1.06 ± 0.07	0.94 ± 0.01	0
Malate	3	23.8 ± 0.7	0.58 ± 0.05	0.94 ± 0.00	1
Pyruvate	3	28.4 ± 1.1	0.71 ± 0.04	0.92 ± 0.00	0.67
Succinate 1	3	17.0 ± 0.7	0.44 ± 0.08	0.87 ± 0.02	0.5
Succinate 2	2	23.6 ± 1.4	0.67 ± 0.07	0.93 ± 0.01	0.5

References:

Addison SL, McDonald IR, Lloyd-Jones G. 2010. Identifying diazotrophs by incorporation of nitrogen from N-15(2) into RNA. Appl Microbiol Biotechnol 87(6):2313-22.

Alefounder, PR & Ferguson, SJ. 1980. The location of dissimilatory nitrite reductase and the control of dissimilatory nitrate reductase by oxygen in *Paracoccus denitrificans*. Biochemical Journal, 192:231-240.

Alefounder, PR, McCarthy, J.E.G. & Ferguson, SJ. 1981. The basis of the control of nitrate reduction by oxygen in *Paracoccus denitrificans*. Fems Microbiology Letters, 12:321-326.

Alefounder PR, Greenfield AJ, McCarthy JEG, Ferguson SJ. 1983. Selection and organisation of denitrifying electron-transfer pathways in *Paracoccus denitrificans*. BBA - Bioenergetics 724(1):20-39.

Alkhatib MA, Lehmann MF, Del Giorgio PA. 2012. The nitrogen isotope effect of benthic remineralization-nitrification-denitrification coupling in an estuarine environment. Biogeosciences 9(5):1633-46.

Altabet MA, Francois R, Murray DW, Prell WL. 1995. Climate-related variations in denitrification in the Arabian Sea from sediment $^{15}N/^{14}N$ ratios. Nature 373(6514):506-9.

Altabet MA, Pilskaln C, Thunell R, Pride C, Sigman D, Chavez F, Francois R. 1999. The nitrogen isotope biogeochemistry of sinking particles from the margin of the Eastern North Pacific. Deep-Sea Research Part I: Oceanographic Research Papers 46(4):655-79.

Anderson LA and Sarmiento JL. 1994. Redfield ratios of remineralization determined by nutrient data analysis. Global Biogeochem Cycles 8(1):65-80.

Barford, CC, Montoya, JP, Altabet, MA, Mitchell R. 1999. Steady-state nitrogen isotope effects of N_2 and N_2O production in *Paracoccus denitrificans*. Applied and Environmental Microbiology, 65, 989-994.

Barnola, JM, Anklin M, Porchcron J, Rayhand D, Schwander J, and Stauffer B. 1995. CO_2 evolution during the last millennium as recorded by Antarctic and Greenland ice, Tellus, Ser. B., d7, 264-272

Baumann B, Van Der Meer JR, Snozzi M, Zehnder AJB. 1997. Inhibition of denitrification activity but not of mRNA induction in *Paracoccus dentrificans* by nitrite at a suboptimal pH. Antonie Van Leeuwenhoek, International Journal of General and Molecular Microbiology 72(3):183-9.

Blumle S and Zumft WG. 1991. Respiratory nitrate reductase from denitrifying *Pseudomonas stutzeri*, purification, properties and target of proteolysis. Biochimica Et Biophysica Acta - Bioenergetics 1057(1):102-8.

Böhlke JK, Mroczkowski SJ, Coplen TB. 2003. Oxygen isotopes in nitrate: new reference materials for $^{18}O:^{17}O:^{16}O$ measurements and observations on nitrate water equilibration. Rapid Communications in Mass Spectrometry, 17:1835-1846.

Boogerd FC, Van Verseveld HW, Stouthamer AH. 1983. Dissimilatory nitrate uptake in *Paracoccus denitrificans* via a gmH+-dependent system and a nitrate-nitrite antiport system. BBA - Bioenergetics 723(3):415-27.

Boyd PW, Jickells T, Law CS, Blain S, Boyle EA, Buesseler KO, Coale KH, Cullen JJ, De Baar HJW, Follows M, et al. 2007. Mesoscale iron enrichment experiments 1993-2005: Synthesis and future directions. Science 315(5812):612-7.

Braman RS and Hendrix SA. 1989. Nanogram nitrite and nitrate determination in environmental and biological materials by V(III) reduction with chemiluminescence detection. Anal. Chem. 61:2715–2718.
Brandes JA, Devol AH, Yoshinari T, Jayakumar DA, Naqvi SWA. 1998. Isotopic composition of nitrate in the central Arabian Sea and eastern tropical North Pacific: A tracer for mixing and nitrogen cycles. Limnology and Oceanography, 43:1680-1689.
Brandes JA and Devol AH. 2002. A global marine-fixed nitrogen isotopic budget: Implications for Holocene nitrogen cycling. Global Biogeochemical Cycles, 16
Broecker WS and Peng TH. 1982. Tracers in the Sea. Palisades, NY: Lamont-Doherty Geological Observatory. 705
Broecker WS. 1982. Ocean chemistry during glacial time. Geochim Cosmochim Acta 46(10):1689-705.
Broecker WS and Henderson GM. 1998. The sequence of events surrounding termination II and their implications for the cause of glacial-interglacial CO_2 changes. Paleoceanography 13(4):352-64.
Button DK. 1985. Kinetics of nutrient-limited transport and microbial growth. Microbiol Rev 49(3):270-97.
Chang BX, Rich JR, Jayakumar A, Naik H, Pratihary AK, Keil RG, Ward BB, Devol AH. 2014. The effect of organic carbon on fixed nitrogen loss in the eastern tropical South Pacific and Arabian Sea oxygen deficient zones. Limnol Oceanogr 59(4):1267-74.
Christensen JP. 1994. Carbon export from continental shelves, denitrification and atmospheric carbon dioxide. Cont Shelf Res 14(5):547-76.
Codispoti, LA, and Christensen JP. 1985. Nitrification, denitrification and nitrous oxide cycling in the eastern tropical South Pacific Ocean, Mar. Chem., 16:277-300.
Codispoti, LA, Brandes, J, Christensen J, Devol A, Naqvi S, Paerl H, and Yoshinari T. 2001. The oceanic fixed nitrogen and nitrous oxide budgets: Moving targets as we enter the anthropocene?, Sci. Mar., 65:85–105.
Constantin H and Fick M. 1997. Influence of C-sources on the denitrification rate of a high-nitrate concentrated industrial wastewater. Water Res 31(3):583-9.
Craske AL and Ferguson SJ. 1986. The nitrate reductase of *Paracoccus denitrificans*. Biochem Soc Trans 14(6):1204.
Dalsgaard T, Canfield DE, Petersen J, Thamdrup B, Acuña-González J. 2003. N_2 production by the anammox reaction in the anoxic water column of Golfo Dulce, Costa Rica. Nature 422(6932):606-8.
Dalsgaard T, Thamdrup B, Farías L, Revsbech NP. 2012. Anammox and denitrification in the oxygen minimum zone of the eastern South Pacific. Limnol Oceanogr 57(5):1331-46.
Delaney ML. 1998. Phosphorus accumulation in marine sediments and the oceanic phosphorus cycle. Global Biogeochem Cycles 12(4):563-72.
Delwiche CC, and Steyn, PL. 1970. Nitrogen isotope fractionation in soils and microbial reactions. Environmental Science & Technology, 4, 929-&.
Deutsch C, Sigman DM, Thunell RC, Meckler AN, Haug GH. 2004. Isotopic constraints on glacial/interglacial changes in the oceanic nitrogen budget. Global Biogeochem Cycles 18(4):1-22.
Deutsch, CA, Kritee K, Sigman DM, Khatiwala S, Granger J. 2010. The isotopic signature of denitrification and the global marine nitrogen balance. In: Ocean Sciences Meeting, Portland.

Deutsch C and Weber T. 2012. Nutrient ratios as a tracer and driver of ocean biogeochemistry. Annual Review of Marine Science 4:113-41.
Dimmer EC, Huntley RP, Alam-Faruque Y, Sawford T, O'Donovan C, Martin MJ et al. 2012. The UniProt-GO Annotation database in 2011. Nucleic Acids Research 2012 40: D565-D570.
Echevin V, Aumont O, Ledesma J, Flores G. 2008. The seasonal cycle of surface chlorophyll in the Peruvian upwelling system: A modelling study. Prog Oceanogr 79(2-4):167-76.
Ellington MJK, Bhakoo KK, Sawers G, Richardson DJ, Ferguson SJ. 2002. Hierarchy of carbon source selection in *Paracoccus pantotrophus*: Strict correlation between reduction state of the carbon substrate and aerobic expression of the nap operon. J Bacteriol 184(17):4767-74.
Eugster O and Gruber N. 2012. A probabilistic estimate of global marine N-fixation and denitrification. Global Biogeochem Cycles 26(4).
Falkowski PG. 1997. Evolution of the nitrogen cycle and its influence on the biological sequestration of CO2 in the ocean. Nature 387(6630):272-5.
Fanning KA. 1992. Nutrient provinces in the sea: concentration ratios, reaction rate ratios and ideal covariation. J. Geophys. Res., 97, 5693-5712.
Galbraith ED, Kienast M, Pedersen TF, Calvert SE. 2004. Glacial-interglacial modulation of the marine nitrogen cycle by high-latitude O2 supply to the global thermocline. Paleoceanography 19(4):1-12.
Galloway JN, Dentener FJ, Capone DG, Boyer EW, Howarth RW, Seitzinger SP, Asner GP, Cleveland CC, Green PA, Holland EA, et al. 2004. Nitrogen cycles: Past, present, and future. Biogeochemistry 70(2):153-226.
Ganeshram RS, Pedersen TF, Calvert SE, Murray JW. 1995. Large changes in oceanic nutrient inventories from glacial to interglacial periods. Nature 376(6543):755-8.
Ghose TK. and Bhadra A. 1985. Acetic acid. In Comprehensive Biotechnology, The Practice of Biotechnology: Current Commodity Products. Pergamon Press, London, U.K. 3, 701-729.
Goddard AD, Moir JWB, Richardson DJ, Ferguson SJ. 2008. Interdependence of two NarK domains in a fused nitrate/nitrite transporter. Mol Microbiol 70(3):667-81.
Gonfiantini, R., W. Stichler, AND K. Rosanski. 1995. Standards and intercomparison materials distributed by the IAEA for stable isotope measurements. p. 13–29. In Reference and intercomparison materials for stable isotopes of light elements. International Atomic Energy Agency. IAEA-TECDOC-825.
Graziano LM, Geider RJ, Li WKW, Olaizola M. 1996. Nitrogen limitation of north Atlantic phytoplankton: Analysis of physiological condition in nutrient enrichment experiments. Aquat Microb Ecol 11(1):53-64.
Granger J, Sigman DM, Needoba JA. & Harrison PJ. 2004. Coupled nitrogen and oxygen isotope fractionation of nitrate during assimilation by cultures of marine phytoplankton. Limnology and Oceanography, 49, 1763-1773.
Granger J, Sigman DM, Prokopenko MG, Lehmann MF, Tortell PD. 2006. A method for nitrite removal in nitrate N and O isotope analyses. Limnology and Oceanography: Methods 4: 205–212.
Granger J, Sigman DM, Lehmann MF, Tortell PD. 2008. Nitrogen and oxygen isotope fractionation of during dissimilatory nitrate reduction by denitrifying bacteria. Limnology and Oceanography, 53, 2533-2545.

Granger J. and Sigman D. 2009. Removal of nitrite with sulfamic acid for nitrate N and O isotope analysis with the denitrifier method. Rapid Commun. Mass Spectrom. 23, 3753–3762.
Gruber N and Sarmiento JL. 1997. Global patterns of marine nitrogen fixation and denitrification. Global Biogeochem Cycles 11(2):235-66.
Gruber N. 2004. The dynamics of the marine nitrogen cycle and its influence on the atmospheric CO_2 variations. In: *The ocean carbon cycle and climate*, Eds, Follows M and Oguz T, NATO ASI Series, Kluwer Academic, Dordrecht, 97-148, 2004.
Gruber N and Galloway JN. 2008. An earth-system perspective of the global nitrogen cycle. Nature 451(7176):293-6.
Gruber N. 2008. The marine nitrogen cycle: Overview and challenges. Nitrogen in the Marine Environment :1-50.
Hernandez D and Rowe JJ. 1988. Oxygen inhibition of nitrate uptake is a general regulatory mechanism in nitrate respiration. J Biol Chem 263(17):7937-9.
Hobbie JE, Daley RJ, Jasper S. 1977. Use of nuclepore filters for counting bacteria by fluorescence microscopy. Appl Environ Microbiol 33(5):1225-8.
Indermühle A, Stocker TF, Joos F, Fischer H, Smith HJ, Wahlen M, Deck B, Mastroianni D, Tschumi J, Blunier T, et al. 1999. Holocene carbon-cycle dynamics based on CO_2 trapped in ice at Taylor Dome, Antarctica. Nature 398(6723):121-6.
Jayakumar A, O'Mullan GD, Naqvi SWA, Ward BB. 2009. Denitrifying bacterial community composition changes associated with stages of denitrification in oxygen minimum zones. Microb Ecol 58(2):350-62.
John P. 1977. Aerobic and anaerobic bacterial respiration monitored by electrodes. J Gen Microbiol 98(JAN):231-8.
Kanehisa, M., Goto, S., Sato, Y., Kawashima, M., Furumichi, M., and Tanabe, M.; Data, information, knowledge and principle: back to metabolism in KEGG. Nucleic Acids Res. 42, D199–D205 (2014).
Kanehisa, M. and Goto, S.; KEGG: Kyoto Encyclopedia of Genes and Genomes. Nucleic Acids Res. 28, 27-30 (2000).
Karl D, Michaels A, Bergman B, Capone D, Carpenter E, Letelier R, Lipschultz F, Paerl H, Sigman D, Stal L. 2002. Dinitrogen fixation in the world's oceans. Biogeochemistry 57-58:47-98.
Karsh KL, Granger J, Kritee K, Sigman DM. 2012. Eukaryotic assimilatory nitrate reductase fractionates N and O isotopes with a ratio near unity. Environmental Science and Technology
Karsh KL, Trull TW, Sigman DM, Thompson PA, Granger J. 2014. The contributions of nitrate uptake and efflux to isotope fractionation during algal nitrate assimilation. Geochim Cosmochim Acta 132:391-412.
Kienast M. 2000. Unchanged nitrogen isotopic composition of organic matter in the South China Sea during the last climatic cycle: Global implications, Paleoceanography, 15(2):244–253.
Kamykowski D and Zentara S. 1990. Hypoxia in the world ocean as recorded in the historical data set. Deep Sea Research Part A, Oceanographic Research Papers 37(12):1861-74.
Kritee K, Sigman DM, Granger J, Ward BB, Jayakumar A, Deutsch C. 2012. Reduced isotope fractionation by denitrification under conditions relevant to the ocean. Geochim Cosmochim Acta 92:243-59.
Kucera I, Karlovský P, Dadák V. 1981. Control of nitrate respiration in *Paracoccus denitrificans* by oxygen. FEMS Microbiol Lett 12(4):391-4.

Kucera I, Dadak V, Dobry R. 1983. The distribution of redox equivalents in the anaerobic respiratory chain of *Paracoccus denitrificans*. European Journal of Biochemistry 130(2):359-64.

Kucera I. 2003. Inhibition by phenylglyoxal of nitrate transport in *Paracoccus denitrificans*: A comparison with the effect of a protonophorous uncoupler. Arch Biochem Biophys 409(2):327-34.

Lam P, Lavik G, Jensen MM, Van Vossenberg JD, Schmid M, Woebken D, Gutiérrez D, Amann R, Jetten MSM, Kuypers MMM. 2009. Revising the nitrogen cycle in the Peruvian oxygen minimum zone. Proc Natl Acad Sci U S A 106(12):4752-7.

Lehmann MF, Sigman DM, McCorkle DC, Granger J, Hoffmann S, Cane G, Brunelle BG. 2007. The distribution of nitrate $^{15}N/^{14}N$ in marine sediments and the impact of benthic nitrogen loss on the isotopic composition of oceanic nitrate. Geochim Cosmochim Acta 71(22):5384-404.

Liu KK. 1979. Geochemistry of Inorganic Nitrogen Compounds in Two Marine Environments: The Santa Barbara Basin and the Ocean off Peru, PhD in Geochemistry, University of California, Los Angeles.

Liu K and Kaplan IR. 1984. Denitrification rates and availability of organic matter in marine environments. Earth Planet Sci Lett 68(1):88-100.

Lloyd D, Boddy L, Davies KJP. 1987. Persistence of bacterial denitrification capacity under aerobic conditions: The rule rather than the exception. FEMS Microbiol Lett 45(3):185-90.

Mariotti, A., J. C. Germon, P. Hubert, P. Kaiser, R. Letolle, A. Tardieux, and P. Tardieux. 1981. Experimental determination of nitrogen kinetic isotope fractionation: Some principles; Illustration for the denitrification and nitrification processes. Plant Soil 62: 413–430.

Mariotti A, Landreau A, Simon B. 1988. ^{15}N isotope biogeochemistry and natural denitrification process in groundwater: Application to the chalk aquifer of northern France. Geochim Cosmochim Acta 52(7):1869-78.

Martin JH. 1990. Glacial-interglacial CO_2 change: The iron hypothesis. Paleoceanography 5(1):1-13.

Martínez-García A, Sigman DM, Ren H, Anderson RF, Straub M, Hodell DA, Jaccard SL, Eglinton TI, Haug GH. 2014. Iron fertilization of the sub-Antarctic ocean during the last ice age. Science 343(6177):1347-50.

McElroy MB. 1983. Marine biological controls on atmospheric CO2 and climate. Nature 302(5906):328-9.

Melander L and Saunders WH. 1980. Reaction rates of isotopic molecules. New York (NY): Wiley.

Michaels AF, Karl DM, Capone DG. 2001. Element stoichiometry, new production and nitrogen fixation. Oceanography 14(SPL.ISS. 4):68-77.

Middelburg JJ., Soetaert K, Herman PMJ, Heip CHR. 1996. Denitrification in marine sediments: A model study. Global Biogeochem. Cycles, 10, 661-673.

Mills MM, Ridame C, Davey M, La Roche J, Geider RJ. 2004. Iron and phosphorus co-limit nitrogen fixation in the eastern tropical north Atlantic. Nature 429(6989):292-4.

Moore CM, Mills MM, Langlois R, Milne A, Achterberg EP, La Roche J, Geider RJ. 2008. Relative influence of nitrogen and phosphorus availability on phytoplankton physiology and productivity in the oligotrophic sub-tropical north Atlantic ocean. Limnol Oceanogr 53(1):291-305.

Moore CM, Mills MM, Arrigo KR, Berman-Frank I, Bopp L, Boyd PW, Galbraith ED, Geider RJ, Guieu C, Jaccard SL, et al. 2013. Processes and patterns of oceanic nutrient limitation. Nature Geoscience 6(9):701-10.

Moreno-Vivián C, Cabello P, Martínez-Luque M, Blasco R, Castillo F. 1999. Prokaryotic nitrate reduction: Molecular properties and functional distinction among bacterial nitrate reductases. J Bacteriol 181(21):6573-84.

Moutin T, Karl DM, Duhamel S, Rimmelin P, Raimbault P, Van Mooy BAS, Claustre H. 2008. Phosphate availability and the ultimate control of new nitrogen input by nitrogen fixation in the tropical pacific ocean. Biogeosciences 5(1):95-109.

Naqvi SWA, Jayakumar DA, Narvekar PV, Naik H, Sarma VVSS, D'Souza W, Joseph S, George MD. 2000. Increased marine production of N2O due to intensifying anoxia on the Indian continental shelf. Nature 408(6810):346-9.

Needoba, J. A., Waser, N. A., Harrison, P. J. & Calvert, S. E. 2003. Nitrogen isotope fractionation in 12 species of marine phytoplankton during growth on nitrate. Mar. Ecol. Prog. Ser. 255:81–91.

Needoba JA, Sigman DM, Harrison PJ. 2004. The mechanism of isotope fractionation during algal nitrate assimilation as illuminated by the $^{15}N/^{14}N$ of intracellular nitrate. J. Phycol. 40:517–522.

Needoba JA, Joseph A, et al. "Nitrogen fixation by unicellular diazotrophic cyanobacteria in the temperate oligotrophic North Pacific Ocean." American Society of Limnology and Oceanography (2007): 1317-28.

Parsonage D, Greenfield AJ, Ferguson SJ. 1985. The high affinity of *Paracoccus denitrificans* cells for nitrate as an electron acceptor. analysis of possible mechanisms of nitrate and nitrite movement across the plasma membrane and the basis for inhibition by added nitrite of oxidase activity in permeabilised cells. Biochimica Et Biophysica Acta - Bioenergetics 807(1):81-95.

Parsons TR, Maita Y, and Lalli CM. 1984. A manual of biological and chemical methods for seawater analysis. Pergamon Press.

Paulmier A and Ruiz-Pino D. 2009. Oxygen minimum zones (OMZs) in the modern ocean. Prog Oceanogr 80(3-4):113-28.

Pride C, Thunell R, Sigman D, Keigwin L, Altabet M, Tappa E. 1999. Nitrogen isotopic variations in the Gulf of California since the last deglaciation: Response to global climate change.

Raynaud D, Jouzel J, Barnola JM, Chappellaz J, Delmas RJ, Lorius C. 1993. Erratum: The ice record of greenhouse gases (science (926-927)). Science 260(5113):1411.

Redfield AC. 1958. The biological control of chemical factors in the environment. Am Sci 46(3):205-221

Ren H, Sigman DM, Chen M, Kao S. 2012. Elevated foraminifera-bound nitrogen isotopic composition during the last ice age in the south china sea and its global and regional implications. Global Biogeochem Cycles 26(1).

Ren H, Sigman DM, Meckler AN, Plessen B, Robinson RS, Rosenthal Y, Haug GH. 2009. Foraminiferal isotope evidence of reduced nitrogen fixation in the ice age Atlantic ocean. Science 323(5911):244-8.

Richardson DJ and Ferguson SJ. 1992. The influence of carbon substrate on the activity of the periplasmic nitrate reductase in aerobically grown *Thiosphaera pantotropha*. Arch Microbiol 157(6):535-7.

Robertson LA, Kuenen JG. 1983. *Thiosphaera pantotropha* gen. nov. sp. nov., a facultatively anaerobic, facultatively autotrophic sulphur bacterium. J. Gen. Microbiol. 129, 2847-2855.
Robertson LA and Kuenen JG. 1985. Further evidence for aerobic denitrification by *Thiosphaera pantotropha*. Antonie Van Leeuwenhoek 51(5-6):561.
Roullier F, Berline L, Guidi L, Durrieu De Madron X, Picheral M, Sciandra A, Pesant S, Stemmann L. 2014. Particle size distribution and estimated carbon flux across the Arabian Sea oxygen minimum zone. Biogeosciences 11(16):4541-57.
Rowe JJ, Ubbink-Kok T, Molenaar D, Konings WN, Driessen AJM. 1994. NarK is a nitrite-extrusion system involved in anaerobic nitrate respiration by *Escherichia coli*. Mol Microbiol 12(4):579-86.
Roy SO and Packard TT. 1998. NADP-isocitrate dehydrogenase from pseudomonas nautica: Kinetic constant determination and carbon limitation effects on the pool of intracellular substrates. Appl Environ Microbiol 64(12):4958-64.
Ryabenko E, Kock A, Bange HW, Altabet MA, Wallace DWR. 2012. Contrasting biogeochemistry of nitrogen in the Atlantic and Pacific oxygen minimum zones. Biogeosciences 9(1):203-15.
Schmidt HL. and Medina R. 1991. Possibilities and scope of the double isotope effect method in the elucidation of mechanisms of enzyme catalyzed reactions. Isotopenpraxis, 27:1-4.
Sears HJ, Spiro S, Richardson DJ. 1997. Effect of carbon substrate and aeration on nitrate reduction and expression of the periplasmic and membrane-bound nitrate reductases in carbon-limited continuous cultures of *Paracoccus denitrificans* Pd1222. Microbiology 143(12):3767-74.
Sigman DM and Boyle EA. 2000. Glacial/interglacial variations in atmospheric carbon dioxide. Nature 407(6806):859-69.
Sigman DM, Robinson R, Knapp AN, Van Geen A, McCorkle DC, Brandes JA, Thunell RC. 2003. Distinguishing between water-column and sedimentary denitrification in the Santa Barbara Basin using the stable isotopes of nitrate. Geochem Geophys Geosyst 4(5).
Sigman DM, Casciotti KL, Andreani M, Barford C, Galanter M, Bohlke JK. 2001. A bacterial method for the nitrogen isotopic analysis of nitrate in seawater and freshwater. Anal. Chem. 73:4145–4153.
Sigman DM, Haug GH. 2014. The biological pump in the past. Elsevier 6:491-528
Shearer G., Schneider JD, Kohl DH. 1991. Separating the efflux and influx components of net nitrate uptake by Synechococcus-R2 under steady-state conditions. Journal of General Microbiology, 137:1179-1184.
Stouthamer AH, Boogerd FC, Van Verseveld HW. 1982. The bioenergetics of denitrification. Antonie Van Leeuwenhoek, International Journal of General and Molecular Microbiology 48(6):545-53.
Stouthamer, AH. 1991 "Metabolic regulation including anaerobic metabolism in *Paracoccus denitrificans*." Journal of Bioenergetics and Biomembranes 23.2:163-85.
Tranvik, Lars. 1997. Rapid fluorometric assay of bacterial density in lake water and seawater. American Society of Limnology and Oceanography 42(7):1629-34.
Thunell C R. 1998. Seasonal and annual variability in particle fluxes in the Gulf of California: A response to climate forcing. Deep-Sea Research Part I: Oceanographic Research Papers 45(12):2059-83.
Tyrrell T. 1999. The relative influences of nitrogen and phosphorus on oceanic primary production. Nature 400(6744):525-31.

Van De Graaf AA, De Bruijn P, Robertson LA, Jetten MSM, Kuenen JG. 1996. Autotrophic growth of anaerobic ammonium-oxidizing micro-organisms in a fluidized bed reactor. Microbiology 142(8):2187-96.

Voss M, Dippner JW, Montoya, JP. 2001. Nitrogen isotope patterns in the oxygen deficient waters of the Eastern Tropical North Pacific Ocean. Deep-Sea Research Part I Oceanographic Research Papers, 48:1905-1921.

Vitousek PM and Howarth RW. 1991. Nitrogen limitation on land and in the sea: How can it occur? Biogeochemistry 13(2):87-115.

Ward BB, Tuit CB, Jayakumar A, Rich JJ, Moffett J, Naqvi SWA. 2008. Organic carbon, and not copper, controls denitrification in oxygen minimum zones of the ocean. Deep-Sea Research Part I: Oceanographic Research Papers 55(12):1672-83.

Warnecke-Eberz U and Friedrich B. 1993. Three nitrate reductase activities in *Alcaligenes eutrophus*. Arch Microbiol 159(5):405-9.

Wellman, RP, Cook FD, Krouse HR. 1968. Nitrogen-15: microbiological alteration of abundance. Science, 161:269-270.

Wunderlich, Anja, Rainer Meckenstock, and Florian Einsiedl. 2012 "Effect of different Carbon substrates on nitrate stable isotope fractionation during microbial denitrification." American Chemical Society 4861-68.

Yakushev EV and Neretin LN. 1997. One-dimensional modeling of nitrogen and sulfur cycles in the aphotic zones of the Black and Arabian seas. Global Biogeochem Cycles 11(3):401-14.

Chapter 2

The contamination of commercial ^{15}N-labeled nitrogen gas with ^{15}N-labeled bioavailable compounds and consequences for nitrogen fixation measurements

Richard Dabundo, Moritz F. Lehmann, Lija Treibergs, Craig R. Tobias, Mark A. Altabet, Pia H. Moisander, Julie Granger

Introduction

Nitrogen (N) is a major nutrient required universally by photosynthetic organisms. Its availability in the environment can directly affect the ecology and productivity of terrestrial and marine ecosystems, with important implications for the regional and global carbon cycles. The natural input of bioavailable N to the biosphere is dominated by nitrogen fixation, the biological reduction of dinitrogen (N_2) gas to ammonium (NH_4^+). Two methods are commonly utilized to measure N_2 fixation rates in the field, the $^{15}N_2$ tracer assay (e.g., Montoya et al. 1996) and the acetylene (C_2H_2) reduction assay (Stewart et al. 1967, Hardy et al. 1968). The $^{15}N_2$ tracer assay was originally developed when artificially ^{15}N-enriched substrate N_2 first became available (Burris and Miller 1941). This approach was then superseded by the acetylene reduction technique, as the cost and availability of high precision isotope ratio measurements proved restrictive (Hardy et al. 1968). The acetylene reduction assay, however, is associated with variations in the factor used to convert C_2H_2 reduction into N_2 equivalents, and with potentially biasing effects of C_2H_2 on the physiology of N_2 fixing organisms, among other issues (Giller 1987, Hardy et al. 1973, Staal et al. 2001). Interest in the $^{15}N_2$ tracer assay later regained momentum, owing to the increased affordability of Isotope Ratio Mass Spectrometry (IRMS) instrumentation and to concurrent developments in ^{15}N tracer techniques. Today, it is generally the preferred method to quantify N_2 fixation rates in both terrestrial and aquatic environments (Montoya et al. 1996), owing to its high sensitivity, and ability to provide qualitative and quantitative constraints on the translocation and the fate of biologically fixed N (Addison et al. 2010, Belay et al. 1988, Scharff et al. 2003).

A salient strength of the $^{15}N_2$ tracer assay is that ^{15}N-enrichment detected in biomass can be ascribed to the biological reduction of N_2 exclusively, as no interfering processes can carry out

the reduction of $^{15}N_2$ gas concurrently. This premise requires that the $^{15}N_2$ stock be devoid of any contaminant ^{15}N-species that could be assimilated into biomass simultaneously. However, during recent research projects on N_2 fixation conducted independently in our laboratories at the University of Connecticut Avery Point and the University of Massachusetts Dartmouth, convergent observations indicated that some commercial $^{15}N_2$ stocks could be contaminated with ^{15}N-enriched N-species other than N_2, including nitrate, nitrite and/or ammonium. These reactive forms of N would be readily assimilated by microorganisms, leading to significantly biased (i.e., overestimated) N_2 fixation rate measurements.

These observations motivated the current study, with the goal of testing whether commercially available $^{15}N_2$ stocks contain ^{15}N-contaminants at levels that would interfere with $^{15}N_2$ tracer N_2 fixation assays, particularly in the open ocean, and to assess if such contaminants are prevalent among $^{15}N_2$ stocks from different suppliers. We thus uncovered substantial contamination of one of three brands of commercial $^{15}N_2$ gas with bioavailable inorganic ^{15}N-species. Our findings raise important concerns regarding the pervasiveness of reactive ^{15}N contamination of the $^{15}N_2$ stocks, and the extent to which these contaminants may have affected the magnitude of the N_2 fixation rate estimates reported in the literature. We outline steps to contend with this issue to ensure the veracity of future N_2 fixation estimates.

Methods

Reagents – Four 33 mL lecture bottles of 98+ at% ^{15}N-labeled N_2 gas were purchased from Sigma-Aldrich (produced by their subsidiary, Isotec Stable Isotopes; St. Louis, MO; Stock Keeping Unit 364584), three from lot # SZ1670V, synthesized in 2010, and one from lot # MBBB0968V, synthesized in 2014. Two 1L lecture bottles of 98+ at% $^{15}N_2$ were purchased from Cambridge Isotopes (Tewksbury, MA, part # NLM-363-1-LB) from respective lot #'s I1-

11785A and I-16727. One 1L lecture bottle of 98+ at% $^{15}N_2$ was purchased from Campro Scientific (Berlin, Germany; catalogue # CS01-185_261) from lot # EB1169V. Ammonium and nitrate solutions were prepared with salts or with solutions obtained from different distributors: sodium nitrate ($NaNO_3$: CAS 7631-99-4), potassium nitrate (KNO_3: CAS 7757-79-1), and ammonium chloride (NH_4Cl: CAS 12125-02-9) from Fisher Scientific (Pittsburgh, PA); analytical-grade potassium nitrate (CAS 7757-79-1) from Fluka Analytical and a gravimetric solution of ammonium chloride (catalogue # AS-NH3N9-2Y) from SPEX CertiPrep (Metuchen, NJ).

Preparation of nitrate and ammonium solutions equilibrated with $^{15}N_2$ gas - In order to determine whether the $^{15}N_2$ gas stocks contained ^{15}N-labeled ammonia (NH_3) or nitrate and/or nitrite (NO_x) contaminants, aqueous solutions of natural abundance (unlabeled) ammonium and nitrate salts were equilibrated overnight with an air headspace supplemented with an injection of $^{15}N_2$ gas. After equilibration, the $^{15}N/^{14}N$ ratio of ammonium and the $^{15}N/^{14}N$ and $^{18}O/^{16}O$ ratios of nitrate/nitrite in solution were measured, as well as the $^{15}N/^{14}N$ ratio of N_2 gas in the headspace, as described below. The isotope ratios of nitrate and ammonium were compared to those in control solutions, which were not supplemented with $^{15}N_2$ gas. Experiments with the Campro Scientific $^{15}N_2$ stock were verified for ^{15}N-nitrate/nitrite contaminants only (and not for ^{15}N-ammonium).

Initial experiments consisted of 40 mL or 100 mL solutions of 10, 50, 100, 200, or 300 µmol L^{-1} nitrate and 5 µmol L^{-1} ammonium chloride in 60 mL or 120 mL serum vials that were sealed with Thermo Scientific gas-impermeant stoppers (part # C4020-30) or with Bellco Glass septum stoppers (catalogue # 2048-11800). The 20 mL of air headspace in each of the treatment vials was supplemented with 0.1 mL of $^{15}N_2$ gas from respective bottles from each of the three

suppliers (three lecture bottles from Sigma-Aldrich lot # SZ1670V and one bottle from lot # MBBB0968V, two bottles from Cambridge Isotopes lot # I1-11785A and lot # I-16727, and one bottle from Campro Scientific lot # EB1169V). The solutions were equilibrated overnight on a shaker, after which the $^{15}N/^{14}N$ and $^{18}O/^{16}O$ isotope ratios of nitrate were analyzed as described below. The $^{15}N/^{14}N$ isotope ratio of ammonium was also analyzed (described below) in experimental solutions treated with the Sigma-Aldrich and Cambridge Isotopes stocks, but not the Campro Scientific stock.

The experimental sensitivity to ^{15}N-contaminants was increased in subsequent experiments involving $^{15}N_2$ stocks that did not show clear evidence of contamination in the experiments described above (see *Results*) by increasing the volume of $^{15}N_2$ gas injections and decreasing solution volumes. Experiments were initiated in which 2 mL $^{15}N_2$ gas was equilibrated overnight in 20 mL serum vials containing 10 mL solutions of 10 μmol L^{-1} sodium nitrate, after which the $^{15}N/^{14}N$ and $^{18}O/^{16}O$ ratios of nitrate were measured as described below. Similarly, 10 mL solutions of 5 μmol L^{-1} ammonium chloride were dispensed in 20 mL serum vials and equilibrated overnight with 2 mL $^{15}N_2$ gas, after which the $^{15}N/^{14}N$ isotope ratios of ammonium were analyzed (described below).

The measured $^{18}O/^{16}O$ ratios of nitrate/nitrite in solutions equilibrated with $^{15}N_2$ gas from some stocks suggested the presence of $^{46}N_2O$ contamination. As our analyte for isotope ratio analysis is N_2O, and $^{46}N_2O$ can be explained by both $^{15}N^{15}N^{16}O$ and $^{14}N^{14}N^{18}O$, N_2O that is doubly labeled with ^{15}N is falsely detected as $\delta^{18}O_{NO3}$ enrichment. The presence of $^{46}N_2O$ contamination in $^{15}N_2$ gas was verified directly for one of the Sigma-Aldrich stocks (Lot # SZ1670V) by adding 0.0125, 0.020, or 0.025 mL of $^{15}N_2$ stock to 20 mL serum vials containing

10 nmoles of reference N_2O in helium. The N and O isotopic composition of the N_2O was analyzed as described below, and compared to unamended N_2O injections.

Dunaliella tertiolecta cultures – The marine green alga *Dunaliella tertiolecta* was cultured in growth media equilibrated with $^{15}N_2$ gas in order to ascertain the susceptibility of ^{15}N-labeled gas contaminants to assimilation by non-N_2-fixing organisms. Culture medium was prepared from filtered Long Island Sound sea water supplemented with 50 µmol L^{-1} $NaNO_3$, 36.3 µmol L^{-1} $NaH_2PO_4*H_2O$, and 107 µmol L^{-1} $Na_2SiO_3*9H_2O$, as well as f/2 trace metals and f/2 vitamins (Guillard and Ryther 1962), added from filter sterilized stock solutions. Medium (200 mL) was dispensed in 250 mL stoppered glass bottles. Experimental treatment bottles were equilibrated overnight with 0.2 mL $^{15}N_2$ gas from either a Cambridge Isotopes (lot #I-16727) or Sigma-Aldrich (lot # SZ1670V) lecture bottle. Following inoculation, cultures were left loosely capped and placed on a windowsill with exposure to natural light. Nitrate concentrations were monitored daily. Upon the complete depletion of nitrate, 8 days after inoculation, the cultures were harvested on pre-combusted GF/F filters. Filters were dried at 60°C for 18 h pending N isotopic analysis of the particulate nitrogen (described below).

Nitrate and ammonium concentrations - Nitrate concentrations in the experimental solutions were verified *via* reduction to nitric oxide in hot vanadium (III) solution followed by detection with a chemiluminescence NO_x analyzer (model T200 Teledyne Advanced Pollution Instrumentation; Braman and Hendrix 1989). Ammonium concentrations were measured by derivatization with orthophthaldialdehyde (OPA) and fluorometric detection on an AJN Scientific f-2500 Fluorescence Spectrophotometer (Holmes et al. 1999).

Nitrate N and O isotope ratio analyses – Nitrate/nitrite nitrogen ($^{15}N/^{14}N$) and oxygen ($^{18}O/^{16}O$) isotope ratios were measured using the denitrifier method (Sigman *et al.* 2001,

Casciotti *et al*. 2002). Nitrate (and nitrite) in experimental samples was converted stoichiometrically to nitrous oxide (N_2O) by a denitrifying bacterial strain (*Pseudomonas chlororaphis* f. sp. *aureofaciens*, ATCC 13985) that lacks nitrous oxide reductase. The N and O isotopic composition of N_2O was then measured on a Delta V Advantage Isotope Ratio Mass Spectrometer (IRMS) interfaced with a modified Gas Bench II gas chromatograph (Thermo Fisher) purge and trap system. The isotope ratio measurements are reported in the conventional delta (δ) notation in per mille (‰) units, defined for N and O by the following equations:

$$\delta^{15}N_{sample} = \left[\frac{{}^{15}N_{sample}/{}^{14}N_{sample}}{{}^{15}N_{reference}/{}^{14}N_{reference}} - 1\right] * 1{,}000$$

$$\delta^{18}O_{sample} = \left[\frac{{}^{18}O_{sample}/{}^{16}O_{sample}}{{}^{18}O_{reference}/{}^{16}O_{reference}} - 1\right] * 1{,}000$$

The $^{15}N/^{14}N$ reference is N_2 in air, and the $^{18}O/^{16}O$ reference is Vienna Standard Mean Ocean water (V-SMOW). Individual analyses on the GC-IRMS were referenced to injections of N_2O from a pure N_2O gas cylinder, and then standardized through comparison to the international nitrate standards USGS-34 ($\delta^{15}N$ of -1.8‰ *vs.* air; $\delta^{18}O$ of -27.9‰ *vs.* V-SMOW), USGS-32 ($\delta^{15}N$ of +180‰ *vs.* air; $\delta^{18}O$ of +25.7‰ *vs.* V-SMOW), and IAEA-NO-3 ($\delta^{15}N$ of +4.7‰ *vs.* air; $\delta^{18}O$ of +25.6‰ *vs.* V-SMOW; see Gonfiantini et al. 1984, Böhlke et al. 1995, Böhlke et al. 2003), using standard bracketing techniques. Nitrate samples from experiments with Campro Scientific $^{15}N_2$ were standardized with USGS-32 and IAEA-NO-3, and an additional internal lab nitrate standard (UBN-1; $\delta^{15}N$ of 14.15‰ *vs.* air; $\delta^{18}O$ of +25.7‰ *vs.* V-SMOW). Precision for analytical replicates was ≤ 0.2‰ for $\delta^{15}N_{NO3}$ and ≤ 0.2‰ for $\delta^{18}O_{NO3}$ for isotope ratio amplitudes encompassed by the standards. Above 200‰, the precision decreased in proportion to $\delta^{15}N_{NO3}$ amplitude, with standard deviations of 7.5‰ for $\delta^{15}N_{NO3}$ at or above 1000‰. Similarly, precision decreased with increasing $\delta^{18}O_{NO3}$, with standard deviations of 1.3‰ to 6.1‰ for

$\delta^{18}O_{NO3}$ values ≥ 80‰. The poor precision of the higher range measurements is likely due to the variable contribution of a trace NO_X contaminant in denitrifier preparations with $\delta^{15}N$ and $\delta^{18}O$ values that are in the range of natural abundance samples (*see* McIlvin and Casciotti, 2011).

Nitrous oxide N and O isotope ratio analyses – N_2O isotope ratios were measured directly on the GC-IRMS, and referenced against the N_2O tank, which was standardized indirectly by comparison to the $\delta^{15}N$ and $\delta^{18}O$ of nitrate standards.

Ammonium N isotope ratio analyses – The ammonium $\delta^{15}N_{NH4}$ was measured using the hypobromite-azide method (Zhang et al. 2007). Ammonium in basic solution was converted to N_2O *via* oxidation to nitrite (NO_2^-) with hypobromite, followed by reduction of nitrite to N_2O with sodium azide in acetic acid. The $\delta^{15}N$ of the N_2O analyte was measured on the GC-IRMS, as outlined above. Measurements were calibrated using solutions made from the international standard ammonium salts, IAEA-N1 and IAEA-N2, with assigned $\delta^{15}N$ values of +0.4‰, +20.3‰ *vs.* air, respectively (Gonfiantini 1984, Kendall 1990, Böhlke et al. 1993, Böhlke et al. 1995). Our standard error for analytical replicates was ≤ 0.6‰ at relatively low ^{15}N-abundances, but increased substantially for $\delta^{15}N_{NH4}$ from 100‰ to 9000‰, varying from 2.9‰ to as high as 59.7‰. As with the nitrate analyses, the low precision of higher range measurements likely stems from the variable contribution of a trace ammonium or nitrite contaminant with a natural abundance $\delta^{15}N$ value, inadvertently introduced during the analyses.

Headspace N_2 isotope ratio analyses - To measure the $\delta^{15}N$ of N_2 gas in the headspace of experimental samples, 75 µL of headspace was injected into 12 mL Exetainer® vials previously flushed with helium, then analyzed on a Gas Bench II GC-IRMS (Delta V Advantage *Plus*) operated in continuous flow mode. N_2 and (O_2 + Ar) were separated on a 5-Å mole-sieve capillary gas chromatography column. The analyses were standardized with parallel analyses of

ambient N_2 gas in air. These direct N_2 gas measurements were carried out for experiments conducted using two of three lecture bottles from Sigma-Aldrich lot # SZ1670V, and for experiments conducted using the lecture bottle from Cambridge Isotopes lot # I1-11785A. The $^{15}N_2$ concentration in the headspace of other experiments was estimated from the tracer injection volume rather than from direct measurements.

Particulate nitrogen isotope ratio analyses – The $\delta^{15}N$ of particulate nitrogen (PN) was analyzed using a Costech Instruments elemental combustion system (model 4010) coupled to a Thermo Scientific Delta V Advantage IRMS. Analyses were standardized using L-glutamic acid reference materials, USGS-40 ($\delta^{15}N$ of -4.52‰ *vs.* air) and USGS-41 ($\delta^{15}N$ of +47.57‰ *vs.* air) (Qi et al. 2003).

Results

Nitrate solutions equilibrated with any of three $^{15}N_2$ gas stocks from Sigma-Aldrich lot # SZ1670V (referred to hereafter as *'Sigma A1, A2 and A3'*) showed a substantial increase in the $\delta^{15}N$ of nitrate (and possibly nitrite) compared to control solutions in the lower sensitivity nitrate dilutions (Fig 11a). Respective ^{15}N enrichments evidenced by the $\delta^{15}N_{NO3+NO2}$ were inversely proportional to the concentration of nitrate in the solutions, from nearly 1000‰ at 10 µmol L^{-1} nitrate to 30‰ at 290 µmol L^{-1} nitrate, compared to a $\delta^{15}N_{NO3}$ of 23.5 ± 0.5‰ in the corresponding potassium nitrate control solutions. The ^{15}N enrichments imparted on the nitrate solutions were comparable among the three lecture bottles from this lot (# SZ1670V). The $\delta^{15}N_{NO3+NO2}$ resulting from equilibration with a single Sigma-Aldrich gas stock from lot # MBBB0968V (*'Sigma B'*) was relatively modest, but still significant, averaging 28.4 ± 0.3‰ at 10 µmol L^{-1} nitrate, compared to 23.5 ± 0.5‰ in the corresponding control solutions (Fig. 1a).

When tested at the more sensitive experimental dilution, equilibrations of nitrate solutions with the *Sigma B* stock resulted in a $\delta^{15}N_{NO3+NO2}$ of 200.2 ± 70.9‰, compared to a $\delta^{15}N_{NO3}$ of 1.3 ± 0.1‰ in control solutions (Fig. 12a). These measurements thus indicate that N_2 gas stocks sourced from lot # SZ1670V contained 410 ± 80 µmoles of ^{15}N-nitrate and/or nitrite per mole of $^{15}N_2$, whereas the bottle from lot # MBBB0968V contributed 1.8 ± 0.6 µmoles of ^{15}N-nitrate and/or nitrite per mole of $^{15}N_2$ (Table 5). The ^{15}N-nitrate additions were determined by a mass balance calculation:

$$^{15}NO_3^- + {}^{15}NO_{2\,\text{added}}^- = \frac{(\delta^{15}N_{NO3+NO2,\text{final}} * NO_{3\,\text{final}}^-) - (\delta^{15}N_{NO3,\text{initial}} * NO_{3\,\text{initial}}^-)}{\delta^{15}N_{NO3+NO2,\text{added}}}$$

where $^{15}NO_3^-$ + $NO_{2\,\text{added}}^-$ is the moles of ^{15}N-labeled nitrate and/or nitrite added by the $^{15}N_2$ gas injection, $\delta^{15}N_{NO3+NO2,added}$ is presumed to be equivalent to the δ^{15}N of $^{15}N_2$ tracer gas (266,540‰), $NO_{3\,\text{initial}}^-$ and $NO_{3\,\text{final}}^-$ refer to the moles of nitrate in solution before and after $^{15}N_2$ equilibration, and $\delta^{15}N_{NO3,initial}$ and $\delta^{15}N_{NO3+NO2,final}$ refer to the $\delta^{15}N_{NO3}$ of nitrate solutions before and after $^{15}N_2$ equilibration. The quantity of $^{15}N_2$ gas added to experimental treatments was measured explicitly in *Sigma A1* and *A2* bottles, and was calculated from the $^{15}N_2$ injection volumes for experiments treated with *Sigma A3* and *B* stocks.

In contrast to the Sigma-Aldrich stocks, $^{15}N_{NO3+NO2}$ contaminants were significantly lower, or possibly absent, in Cambridge Isotopes and Campro Scientific $^{15}N_2$ stocks. The $\delta^{15}N_{NO3+NO2}$ values of solutions treated with Cambridge Isotopes $^{15}N_2$ gas (lots # I1-11785A and I-16727, hereafter referred to as *Cambridge A* and *Cambridge B*, respectively) and with Campro Scientific $^{15}N_2$ gas (lot # EB1169V) were indistinguishable from those of control solutions at all experimental nitrate concentrations in the lower sensitivity tests (Fig. 1a). In the more sensitive experimental treatments, however, solutions treated with *Cambridge B* $^{15}N_2$ gas (lot # I-16727) had a $\delta^{15}N_{NO3+NO2}$ of 4.8 ± 0.8‰, compared to a $\delta^{15}N_{NO3}$ of 1.3 ± 0.1‰ in control solutions (Fig.

12a). This stock thus contributed trace contaminants on the order of 0.024 ± 0.006 µmoles of ^{15}N-nitrate and/or nitrite per mole of $^{15}N_2$ (Table 5). Nitrate isotope ratios in the *Cambridge A* (lot # I1-11785A) and Campro Scientific $^{15}N_2$ gas stocks were not tested at these lower experimental dilutions.

In treatments using several $^{15}N_2$ gas stocks, $\delta^{18}O_{NO3}$ was found to be elevated relative to control solutions. The denitrifier method, employed for $\delta^{18}O_{NO3}$ measurements, involves the bacterial reduction of NO_3^- and NO_2^- to N_2O, and the subsequent analysis of N_2O using an IRMS. However, the elevated $\delta^{18}O_{NO3}$ values detected within experimental treatments are expressly *not* explained by the formation of $^{14}N^{14}N^{18}O$ during bacterial reduction of ^{15}N-enriched nitrate, which could only account for a negligible portion of the observed $\delta^{18}O_{NO3+NO2}$ increase. Instead, the values are best explained by the presence of doubly-labeled ^{15}N-N_2O (i.e., $^{46}N_2O$) in the $^{15}N_2$ gas stocks. The apparent $\delta^{18}O_{NO3+NO2}$ of nitrate solutions equilibrated with all of the Sigma-Aldrich stocks, the Campro Scientific stock, and the *Cambridge B* $^{15}N_2$ stock proved to be greater than that of control solutions in the low sensitivity treatments (Fig. 11b). At 10 µmol L^{-1} nitrate, the apparent $\delta^{18}O_{NO3+NO2}$ of treated solutions was 188.5 ± 83.8 among the *Sigma A1-A3* stocks (lot # SZ1670V), 169.8 ± 17.9‰ for the *Sigma B* stock (lot # MBBB0968V), and 20.1 ± 0.2 for the *Cambridge B* stock, compared to 18.9 ± 0.3‰ in corresponding control solutions. The apparent $\delta^{18}O_{NO3+NO2}$ of the Campro Scientific stock at 10 µmol L^{-1} nitrate was 70.4 ± 1.4‰, compared to 25.7 ± 0.1‰ in corresponding control solutions. The apparent $\delta^{18}O_{NO3+NO2}$ of the samples decreased coherently with increasing nitrate concentrations for respective stocks. The apparent $\delta^{18}O_{NO3+NO2}$ values of solutions equilibrated with the *Cambridge A* stock, at 19.1 ± 0.2‰, were not distinguishable from the control solutions. In the more sensitive equilibrations, nitrate solutions equilibrated with *Sigma B* $^{15}N_2$ gas had a $\delta^{18}O_{NO3+NO2}$ of 13,129 ± 1186‰

compared to 23.9 ± 0.2‰ in control solutions, whereas the $\delta^{18}O_{NO3+NO2}$ of the *Cambridge B* stock was 216.7 ± 78.4‰ (Fig. 2b). Given that the apparent $\delta^{18}O_{NO3}$ enrichments are explained by the presence of $^{46}N_2O$, the inverse relationship between $\delta^{18}O$ values and nitrate concentration stems from the fact that the detected $^{46}N_2O$ derives from $^{46}N_2O$ dissolved in the nitrate solutions, and solutions containing higher nitrate concentrations require lower sample volume injections when using the denitrifier method for IRMS analysis. The observed excess $^{46}N_2O$ levels indicate $^{15}N^{15}N^{16}O$ contaminants (μmole $^{46}N_2O$ per mole of $^{15}N_2$) on the order of 41 ± 21 among the *Sigma A1-A3* bottles, 49 ± 17 in *Sigma B*, 11 ± 3 in Campro Scientific, and 0.81 ± 0.24 in *Cambridge B* (Table 5). The *Cambridge A* bottle was not tested in higher sensitivity dilutions that could have revealed the presence of some N_2O therein. The presence of $^{46}N_2O$ contaminant was verified directly for the *Sigma A2* lecture bottle from analyses of N_2O amended with injections of $^{15}N_2$ gas. Among four experimental samples, 109 ± 5 μmoles of $^{46}N_2O$ were detected per mole of *Sigma A2* $^{15}N_2$ added, more than double the $^{46}N_2O$ that was detected in samples analyzed by the denitrifier method (39 ± 8 μmole $^{46}N_2O$ per mole of $^{15}N_2$). This discrepancy likely resulted because samples analyzed by the denitrifier method were uncapped immediately prior to their injection into *P. aureofaciens* denitrifier cultures, allowing N_2O to escape to the atmosphere. As contaminant N_2O was not the target analyte of the denitrifier measurements, precautions were not taken to prevent N_2O gas loss at this step. The $^{46}N_2O$ concentrations derived from solution equilibrations of respective $^{15}N_2$ stocks thus constitute lower limits (Table 5).

Solutions equilibrated with Sigma-Aldrich $^{15}N_2$ gas showed substantial ^{15}N-enrichments of ammonium compared to control solutions (Fig. 13a): Equilibration with $^{15}N_2$ from the *Sigma A1* lecture bottle (lot # SZ1670V) resulted in a $\delta^{15}N_{NH4}$ of 99 ± 39‰, compared to 0.6 ± 0.5‰

for the control solution (NH_4Cl, SPEX CertiPrep); equilibration with $^{15}N_2$ from the *Sigma A2* bottle (lot # SZ1670V) yielded a $\delta^{15}N_{NH4}$ of 940 ± 60‰, compared to 7.6 ± 0.3‰ for the control solution (NH_4Cl salt, Fisher Scientific); equilibration with $^{15}N_2$ from the *Sigma B* bottle (lot # MBBB0968V) resulted in a $\delta^{15}N_{NH4}$ of 7030 ± 2100‰, compared to 9.0 ± 0.06‰ for the corresponding control solutions (NH_4Cl salt, Fisher Scientific). Mass balance calculations based on these isotope ratio values thus evidence the presence of 34 ± 11, 518 ± 26, and 1890 ± 560 μmoles of ^{15}N-ammonium per mole of $^{15}N_2$ injected from *Sigma A1*, *A2*, and *B* $^{15}N_2$ bottles, respectively (Table 5). Unlike ^{15}N-labelled nitrate/nitrite contaminants, the ^{15}N-ammonium contaminants appeared to be variable among bottles of lot # SZ1670V (Fig. 13a). The *Sigma A3* lecture bottle was not tested for ^{15}N-ammonium.

In contrast to Sigma-Aldrich stocks, ammonium solutions equilibrated with $^{15}N_2$ from the *Cambridge A* bottle had a $\delta^{15}N_{NH4}$ of 8.3 ± 1.0‰, comparable to that of the corresponding control solution of 7.6 ± 0.3‰ (NH_4Cl salt, Fisher Scientific) in the lower sensitivity experiments (Fig. 13a). In the more sensitive dilutions, however, ^{15}N-ammonium contaminants were detected in both of the *Cambridge A* and *B* stocks (Fig. 13b). Solutions equilibrated with *Cambridge A* had a $\delta^{15}N_{NH4}$ of 24.0 ± 5.9‰, compared to 8.7 ± 0.1‰ for the control solutions (NH_4Cl salt, Fisher Scientific) and solutions equilibrated with *Cambridge B* had a $\delta^{15}N_{NH4}$ of 13.1 ± 1.1‰, compared to 9.0 ± 0.1‰ for the control solutions ((NH_4Cl salt, Fisher Scientific). The enrichment relative to control solutions invariably originates from a ^{15}N-ammonium contaminant, and cannot be attributed to a trace N_2O ($^{15}N^{14}N^{16}O$) contaminant, because the samples were purged when conducting ^{15}N-ammonium analyses, following the oxidation of ammonium to nitrite with hypobromite. These more sensitive treatments thus reveal the presence of minuscule ^{15}N-ammonium concentrations in the Cambridge Isotopes stocks, on the order

0.052 ± 0.020 and 0.014 ± 0.004 μmoles of ^{15}N-ammonium per mole of $^{15}N_2$ gas in lots # I1-11785A and I-16727, respectively (Table 5).

The control solutions in the ^{15}N-ammonium experiments prepared from a single Fisher Scientific NH_4Cl salt stock revealed progressively heavier mean $\delta^{15}N_{NH4}$ values among experiments, at 7.6 ± 0.3‰, 8.7 ± 0.1‰, or 9.0 ± 0.06‰. The solutions with a $\delta^{15}N_{NH4}$ estimated at 7.6 ± 0.3‰ and 8.7 ± 0.1‰ were made fresh from the salts for each experiment, such that the ^{15}N-enrichment of ammonium cannot be attributed to the progressive degassing of ammonia in solution during storage. In turn, isotopic standards for NH_4^+ (IAEA-N1 and N2) were stored in acidic solution, and thus were not subject to progressive degassing. Moreover, degassing of the isotopic standards would manifest as progressively lower $\delta^{15}N$ values measured for control solutions. Inter-batch variability intrinsic to the hypobromite-azide method (Zhang et al. 2007) is plausible, as this technique is relatively recent, such that subtle sensitivities may not yet be apparent.

D. tertiolecta cultures grown in medium equilibrated with $^{15}N_2$ gas from the *Sigma A3* bottle expectedly showed substantial ^{15}N enrichment of particulate nitrogen ($\delta^{15}N_{PN}$), averaging 44.3 ± 6.1‰ among triplicate treatment cultures compared to 1.9 ± 0.1‰ in control cultures (Fig. 14). Conversely, the $\delta^{15}N_{PN}$ of cultures equilibrated with *Cambridge B* $^{15}N_2$ gas was 2.1 ± 0.2‰, and thus not detectably different from that of control cultures, at 1.9 ± 0.1‰ (Fig. 14).

Discussion

This study reveals that some commercial $^{15}N_2$ gas stocks contain contaminant ^{15}N-labeled bioavailable nitrogen species, including nitrate/nitrite, ammonium and nitrous oxide. Substantial levels of ^{15}N-labeled nitrate/nitrite, ammonium, and nitrous oxide were detected in Sigma-

Aldrich stocks from lot # SZ1670V. Another Sigma-Aldrich stock from a different lot (# MBBB0968V) contained considerably less, but still significant, ^{15}N-nitrate/nitrite contaminants, similar nitrous oxide concentrations, and a greater concentration of ^{15}N-ammonium. Cambridge Isotopes stocks, in turn, contained relatively low concentrations of ^{15}N-nitrate/nitrite, ^{15}N-ammonium and ^{15}N-nitrous oxide. A $^{15}N_2$ stock from Campro Scientific contained no detected ^{15}N-nitrate/nitrite contaminants in low sensitivity experiments, but measurable ^{15}N-nitrous oxide. Indeed, a certificate of analysis provided by Campro Scientific attests that stocks may contain up to 15 ppm N_2O. ^{15}N-ammonium was not analyzed in Campro Scientific gas, nor was the stock tested at more sensitive $^{15}N_2$ dilutions, which could have revealed trace ^{15}N-nitrate or ammonium contaminants in the stock. In any case, ^{15}N-contamination with nitrous oxide is of no obvious consequence for biological $^{15}N_2$ applications, such as N_2 fixation rate measurements. However, the presence of ^{15}N-nitrate, nitrite and ammonium has serious implications for measurements of N_2 fixation, as these contaminants could lead to the detection of false positives or inflated rates.

The propensity of the detected ^{15}N-labeled contaminants to be assimilated into biomass was verified directly from cultures of *D. tertiolecta,* which acquired elevated δ^{15}N of PN in media equilibrated with a Sigma-Aldrich $^{15}N_2$ stock. Expectedly, media equilibrated with $^{15}N_2$ from a Cambridge Isotopes stock did not cause detectable ^{15}N-enrichment of biomass. At the given experimental conditions, however, the complete assimilation of the contaminant ^{15}N-nitrate/nitrite from the Sigma-Aldrich stock should have yielded greater $\delta^{15}N_{PN}$ values than those observed, of at least 56.3 ± 5.4‰ (*vs.* control $\delta^{15}N_{PN}$ values of ~1.9‰), notwithstanding the additional contribution of any ^{15}N-ammonium contaminant (^{15}N-ammonium was not measured explicitly in the *Sigma A3* stock). This discrepancy is difficult to reconcile. We tentatively posit that ^{15}N-*nitrite* comprises a substantial fraction of the trace ^{15}N-nitrate/nitrite contaminant, and

that *D. tertiolecta* may not be able to transport nitrite at nanomolar to sub-nanomolar concentrations. Indeed, such trace nitrite concentrations are likely below the thresholds achievable by micro-algal nitrite transport systems (e.g., Cordoba et al. 1986).

The contaminants in the $^{15}N_2$ stocks ostensibly derive from the method of $^{15}N_2$ gas production. $^{15}N_2$ gas is generally produced by the catalytic oxidation of ^{15}N ammonia ($^{15}NH_3$) gas with cupric oxide (e.g., Bergersen 1980). The bulk of the oxidation product is N_2 gas, although more oxidized N species are also produced in lesser quantities, specifically N_2O and NO (Il'chenko 1976). Thus, potential contaminants in a $^{15}N_2$ gas stock would expectedly consist of unreacted ammonia gas, N_2O, and nitric oxide (NO). In contact with any oxygen and water vapor, NO would inadvertently be oxidized to nitric and nitrous acid (Ashmore et al. 1962), which would, in turn, dissociate to nitrate and nitrite upon dissolution in water, respectively. Purification of the $^{15}N_2$ gas from unreacted ammonia and from the generated nitrogen oxides involves sequential acid and alkaline scrubbing, respectively (e.g., Ohyama and Kumazawa 1981) and/or cryo-trapping of ammonia and NOx gases. Upon personal communication, Cambridge Isotopes and Campro Scientific did not provide details on their method of $^{15}N_2$ production, whereas Sigma-Aldrich reported that the company's subsidiary, Isotec, produces $^{15}N_2$ gas by the catalytic oxidation of ^{15}N-ammonia gas with cupric oxide, followed by sequential rounds of cryo-trapping and alkaline scrubbing of the N_2 gas to increase purity.

In order to gauge the extent to which the observed ^{15}N-ammonium contamination of Sigma-Aldrich and Cambridge Isotopes $^{15}N_2$ gas could skew estimates of N_2 fixation in incubations with $^{15}N_2$ gas, we modeled a field incubation experiment in which microorganisms assimilate the ^{15}N-ammonium contaminant rather than reduce $^{15}N_2$ gas. A simple finite-differencing model of a 'typical' oceanic N_2 fixation assay was devised, in which 0.1 mL of $^{15}N_2$ gas was equilibrated in

two different water sample volumes, 0.25 L or 4.5 L, then incubated for 24 hours. Prescribed biomass and growth rates were characteristic of those at the oligotrophic surface ocean, namely, a particulate N stock of 0.2 μmol L^{-1} assimilating ammonium at a specific growth rate coefficient (μ) of 0.1 d^{-1} to 0.3 d^{-1}, with a recycling rate (the rate at which particulate N is returned to the ammonium pool) equivalent to the respective growth rate. The prescribed $\delta^{15}N$ of the initial particulate N was 0‰ (Altabet 1988), and the $\delta^{15}N$ of ambient ammonium was -2‰ (Fawcett et al. 2011). Incremental initial concentrations of ambient ammonium were prescribed, from 1 nmol L^{-1} to 1 μmol L^{-1}. Ammonium concentrations in surface oligotrophic waters are typically very low (≤ 10 nmol L^{-1}), however, ammonium is a pervasive contaminant that could easily be introduced during sample preparation, as well as leached from incubation vial septa. We note that the ^{15}N-ammonium introduced by the $^{15}N_2$ gas, while substantial in terms of the $^{15}N/^{14}N$ ratio of ammonium, is on the order of ~20 nanomolar *at most* (under the modeled conditions), and thus has minimal effect on ambient ammonium concentrations. ^{14}N-ammonium contamination is expected to be negligible, given the method of $^{15}N_2$ gas synthesis. Finally, ^{15}N-ammonium assimilation was simulated for the broad range of ^{15}N-ammonium contaminant concentrations observed among Sigma-Aldrich and Cambridge Isotopes lecture bottles. N_2 fixation rates inferred from the simulated $\delta^{15}N$ increase of particulate N were computed based on the formulation of Montoya (1996):

$$\frac{[\mathrm{PN}]_{\Delta}}{[\mathrm{PN}]_{\mathrm{f}}} = \frac{A_{\mathrm{PNf}} - A_{\mathrm{PN0}}}{A_{\mathrm{N2}} - A_{\mathrm{PN0}}}$$

$$V = \frac{1}{\Delta t} * \frac{[PN]_{\Delta}}{[PN]_{f}}$$

$$\rho = \frac{\mathrm{V}}{2} * [\mathrm{PN}]_{\mathrm{f}}$$

$[PN]_\Delta$ is the change in particulate nitrogen concentration, $[PN]_f$ is the final particulate nitrogen concentration, A_{PNf} is the final ^{15}N enrichment of particulate nitrogen, A_{PN0} is the initial ^{15}N enrichment of particulate nitrogen, A_{N2} is the ^{15}N enrichment of the N_2 available for fixation, V is the specific rate of N_2 uptake, and ρ is the volumetric rate of N_2 fixation.

The model-derived 'N_2 fixation rates' resulting from Sigma-Aldrich ^{15}N-ammonium contaminant levels ranged from undetectable, < 0.01 nmol N L^{-1} d^{-1}, to as high as 530 nmol N L^{-1} d^{-1} under the modeled conditions (Table 6). Rates were clearly sensitive to the concentration of ^{15}N-contaminant, the ambient ammonium concentration, the incubation volume, and the specific growth rate. At the lower level of ^{15}N-ammonium contaminant observed in the Sigma-Aldrich stocks, N_2 fixation rates were comparable to rates observed *in situ* for nearly all parameter permutations, from < 0.01 to 9 nmoles N L^{-1} d^{-1}. N_2 fixation rates reported for marine environments cover a broad range, from 0.01 nmoles L^{-1} d^{-1} to tens of nmoles N L^{-1} d^{-1} (e.g., Dore et al. 2002, Montoya et al. 2004, Needoba et al. 2007). Rates simulated with the highest observed level of contaminant, in smaller incubation volumes at given $^{15}N_2$ additions, and/or with low ambient ammonium concentrations, tended to surpass rates observed *in situ* by 10 to 100 fold. The N_2 fixation rates modeled using the minute contaminant level detected in a Cambridge Isotopes stock ranged from undetectable to 0.02 nmoles N L^{-1} d^{-1} (Table 6), approximating the lower limit of some N_2 fixation rates reported in the literature (e.g., Dore et al. 2002, Fernandez et al. 2011, Hamersley et al. 2011, Blais et al. 2012, Halm et al. 2012, Dekaezmaker et al. 2013). These simulated rates can be deemed conservative since the model does not account for any assimilation of contaminant ^{15}N-nitrate/nitrite, and the 0.1 mL $^{15}N_2$ injection volume used in the model is on the lower end of $^{15}N_2$ injection volumes typically used in open ocean N_2 fixation rate measurements.

Based on the simulations above, the likelihood of N_2 fixation rates being inflated when using contaminated $^{15}N_2$ gas stocks is high. It is surprising, then, that contamination of the $^{15}N_2$ stocks has not been reported previously. While growth solely upon N from N_2 fixation would eliminate the effect of ^{15}N-labeled bioavailable contaminants, it is expected that nitrate and ammonium assimilation would be rapid relative to N_2 fixation due to the prohibitive energetic cost of N_2 fixation (Stam et al. 1987). A review of pertinent literature reveals that soil scientists were once aware of the possible contamination of $^{15}N_2$ with bioavailable N, and took steps to mitigate it (De-Polli et al. 1977, Ohyama and Kumuzawa 1981). However, to the best of our knowledge, there is no mention of potential contamination of $^{15}N_2$ stocks in the marine literature, or in more recent terrestrial literature. The fact that this issue has gone unnoticed could mean that major contamination of $^{15}N_2$ gas stocks, such as that observed here in Sigma-Aldrich stocks, could be limited to the current lots. Supporting the notion that contamination is rare is the observation of undetectable N_2 fixation rates at the surface ocean, where phytoplankton readily assimilate ammonium (e.g., Dekaezemacker et al. 2013) – even in investigations utilizing the Sigma-Aldrich (Isotec) $^{15}N_2$ gas (e.g., Dore et al. 2002). However, a representative at Isotec stated that their procedures for synthesis and purification of $^{15}N_2$ gas have not changed in past decades, which suggests that ^{15}N-contaminants may have been pervasive in previous lots. Failure to detect interferences from ^{15}N-contaminants in previous studies may then stem from incubation conditions conspiring to yield expected rates of *apparent* N_2 fixation in spite of the presence of ^{15}N contaminants (Table 6). Interference of ^{15}N contaminants on N_2 fixation rate measurements may then be relatively minor in systems where bioavailable N assimilation rates are low and/or where ambient nitrate and ammonium concentrations are relatively elevated ($\geq$ 100 nmol L^{-1};

Table 6), as ambient assimilable N effectively diminishes ^{15}N enrichment resulting from ^{15}N-labeled contaminants.

It is difficult, if not impossible, to discern whether N_2 fixation rate estimates in previous studies may have been confounded due to the assimilation of ^{15}N contaminants in $^{15}N_2$ gas stocks. Given that $^{15}N_2$ stocks from only one of the three suppliers tested here contained contaminants to an extent that would interfere with any but the lowest reported N_2 fixation measurements, there is a strong likelihood that published estimates performed with $^{15}N_2$ from the other two suppliers have not been significantly inflated by labeled contaminants. In fact, many estimates may be lower than reality due to the incomplete equilibration of $^{15}N_2$ gas with the incubation medium, a pervasive problem with aqueous $^{15}N_2$ fixation assays that was diagnosed only recently (Mohr et al. 2010, Grosskopf et al. 2012, Wilson et al. 2012). Nevertheless, it is advisable at this point to analyze commercial $^{15}N_2$ stocks prior to their use to ensure their relative purity. In doing so, particular attention must be paid to the lower limit of detection for N_2 fixation rates. In recent years, workers have reported estimates of very low rates ($\leq$ 0.1 nmol L^{-1} d^{-1}) in environments where N_2 fixation is otherwise unexpected, which include oxygen-deplete regions of the water-column at Pacific margins (Fernadez et al 2011, Hamersley et al. 2011, Dekaezmacker et al. 2013), as well as in the Beaufort Gyre of the Arctic Ocean (Blais et al. 2012). Such minimal rates are questionable, considering that the relatively clean Cambridge Isotopes $^{15}N_2$ gas was found to contain enough ^{15}N-ammonium to infer N_2 fixation rates of up to 0.02 nmoles N L^{-1} d^{-1}. Campro Scientific and other commercially available $^{15}N_2$ gas stocks could similarly contain minute, but significant, concentrations of ^{15}N-nitrate or ammonium. Therefore, it behooves investigators to not only verify the purity of their commercial $^{15}N_2$ prior to use, but

also to generate constraints as to the lower limit of detection, allowing for the possibility that a trace-level ^{15}N-contaminant could interfere with the detection of diminutive N_2 fixation rates.

Steps toward mitigation

The catalytic synthesis of $^{15}N_2$ gas from ^{15}N-ammonia gas invariably entails the incidence of ^{15}N-ammonium and ^{15}N-NOx contaminants, the removal of which is dependent on the stringency of scrubbing procedures to which a given batch is subjected. The consistency of ^{15}N-nitrate/nitrite measurements among bottles from an individual lot from Sigma-Aldrich (*Sigma A1-A3*), in contrast to the lower ^{15}N-nitrate/nitrite detected in a subsequent lot (*Sigma B*), supports the premise that the levels of ^{15}N-contaminants are associated with discrete batch syntheses, identified by lot numbers, rather than with individual lecture bottles. The variability in ^{15}N-ammonium among lecture bottles of the same lot suggests that ammonia gas does not disperse homogeneously in compressed N_2 gas. In any case, large-scale batch syntheses of $^{15}N_2$ occur relatively infrequently, on the order of every 2 years at Isotec (subsidiary of Sigma-Aldrich). We currently have a verbal agreement with Isotec to perform nitrate and ammonium isotopic analyses of $^{15}N_2$ batches, toward providing a certificate of analysis ensuring adequate purity for N_2 fixation assays. In the meantime, we advise that workers procure low-contaminant stocks from lots that we tested here. The very high purity of the batches from these suppliers suggests stringent and efficacious purification protocols, such that batches synthesized by these groups in the future are likely to be equally pure, notwithstanding the potential for human error during synthesis or subsequent purification.

Regardless of 'expected' purity, we recommend that workers explicitly test new batches availed by respective suppliers for ^{15}N-nitrate and ammonium prior to using them in N_2 fixation assays, and actively disseminate the results to targeted web-based forums. To test a given batch, $^{15}N_2$ gas can be equilibrated with nitrate and ammonium solutions following protocols akin to the low and high sensitivity equilibrations herein. A number of laboratories perform commercial nitrate isotope analyses routinely at a modest cost per sample. Ammonium isotope analyses are substantially more involved, but are also performed routinely by a number of laboratories.

We further recommend that pertinent publications include not only the brand of $^{15}N_2$ stock, but also the associated lot number, and references to reported contaminants. With continued testing, our understanding of the prevalence of commercial $^{15}N_2$ contamination will grow and shed light on this problem, which may have plagued N_2 fixation estimates in the past.

Acknowledgements

We wish to thank Moritz Lehmann for providing data on Campro Scientific contamination, Nicole Chang for assistance with $^{15}N_2$ measurements, David Cady at the University of Connecticut for assistance with particulate nitrogen and carbon $\delta^{15}N$ and $\delta^{14}C$ measurements, and Mark Rollog and Thomas Kuhn for assistance in the lab at the University of Basel.

References

Addison SL, McDonald IR, Lloyd-Jones G. 2010. Identifying diazotrophs by incorporation of nitrogen from $^{15}N_2$ into RNA. Appl Microbiol Biotechnol 87(6): 2313-22.

Altabet M. 1988. Variations in nitrogen isotopic composition between sinking and suspended particles - implications for nitrogen cycling and particle transformation in the open ocean. Deep-Sea Research Part A-Oceanographic Research Papers 35(4): 535-54.

Ashmore PG, Burnett MG, Tyler BJ. 1962. Reaction of nitric oxide and oxygen. Trans Faraday Soc 58: 685-691.

Belay N, Sparling R, Choi B, Roberts M, Roberts J, Daniels L. 1988. Physiological and ^{15}N-Nmr analysis of molecular nitrogen fixation by methanococcus-thermolithotrophicus, methanobacterium-bryantii and methanospirillum-hungatei. Biochim Biophys Acta 971(3): 233-45.

Bergersen FJ. 1980. Measurements of nitrogen fixation by direct means. In: Bergersen FJ, editor Methods for evaluating biological nitrogen fixation. Wiley-Interscience, Chichester, p. 5-110.

Blais M, Tremblay J, Jungblut AD, Gagnon J, Martin J, Thaler M, Lovejoy C. 2012. Nitrogen fixation and identification of potential diazotrophs in the Canadian Arctic. Global Biogeochem Cycles 26: GB3022.

Böhlke J, Gwinn C, Coplen T. 1993. New reference materials for nitrogen-isotope-ratio measurements. Geostand Newsl 17(1): 159-64.

Böhlke JK, Coplen, TB. 1995. Interlaboratory comparison of reference materials for nitrogen isotope ratio measurements. Proceedings of a consultants meeting held in Vienna, 1 - 3. Dec. 1993, IAEA-TECDOC-825, 51-66.

Böhlke J, Mroczkowski S, Coplen T. 2003. Oxygen isotopes in nitrate: new reference materials for ^{18}O:^{17}O:^{16}O measurements and observations on nitrate-water equilibration. Rapid Commun Mass Spectrom 17(16): 1835-46.

Braman R and Hendrix S. 1989. Nanogram nitrite and nitrate determination in environmental and biological-materials by vanadium(III) reduction with chemi-luminescence detection. Anal Chem 61(24): 2715-8.

Burris RH and Miller CE. 1941. Application of N^{15} to the study of biological nitrogen fixation. Science 93(2405): 114-5.

Casciotti K, Sigman D, Hastings M, Böhlke J, Hilkert A. 2002. Measurement of the oxygen isotopic composition of nitrate in seawater and freshwater using the denitrifier method. Anal Chem 74(19): 4905-12.

Cordoba F, Cardenas J, Fernandez E. 1986. Kinetic characterization of nitrite uptake and reduction by chlamydomonas-reinhardtii. Plant Physiol 82(4): 904-8.

Dekaezemacker J, Bonnet S, Grosso O, Moutin T, Bressac M, Capone DG. 2013. Evidence of active dinitrogen fixation in surface waters of the eastern tropical South Pacific during El Nino and La Nina events and evaluation of its potential nutrient controls. Global Biogeochem Cycles 27(3): 768-79.

De-Polli H, Matsui E, Döbereine J, Salati E. 1977. Confirmation of nitrogen fixation in two tropical grasses by $^{15}N_2$ incorporation. Soil Biol and Biochem 9: 119–123

Dore J, Brum J, Tupas L, Karl D. 2002. Seasonal and interannual variability in sources of nitrogen supporting export in the oligotrophic subtropical North Pacific Ocean. Limnol Oceanogr 47(6): 1595-607.

Fawcett SE, Lomas M, Casey JR, Ward BB, Sigman DM. 2011. Assimilation of upwelled nitrate by small eukaryotes in the Sargasso Sea. Nat Geosci 4(10): 717-22.

Fernandez C, Farias L, Ulloa O. 2011. Nitrogen fixation in denitrified marine waters. PLoS One 6(6): e20539.
Giller KE. 1987. Use and abuse of the acetylene-reduction assay for measurement of associative nitrogen fixation. Soil Biology & Biochemistry 19(6): 783-4.
Gonfiantini R. 1984. Report on an advisory group meeting on stable isotope reference samples for geochemical and hydrochemical investigations. Vienna, 19 - 21 Sept. 1983. IAEA, Vienna.
Grosskopf T, Mohr W, Baustian T, Schunck H, Gill D, Kuypers MMM, Lavik G, Schmitz RA, Wallace DWR, LaRoche J. 2012. Doubling of marine dinitrogen-fixation rates based on direct measurements. Nature 488(7411): 361-4.
Guillard RRL and Ryther JH. 1962. Studies of marine planktonic diatoms: I. Cyclotella nana Hustedt, and Detonula confervacea (cleve) Gran. Can. J. Microbiol. 8: 229-239.
Halm H, Lam P, Ferdelman TG, Lavik G, Dittmar T, LaRoche J, D'Hondt S, Kuypers MMM. 2012. Heterotrophic organisms dominate nitrogen fixation in the South Pacific Gyre. Isme Journal 6(6): 1238-49.
Hamersley MR, Turk KA, Leinweber A, Gruber N, Zehr JP, Gunderson T, Capone DG. 2011. Nitrogen fixation within the water-column associated with two hypoxic basins in the Southern California Bight. Aquat Microb Ecol 63(2): 193-205.
Hardy RWF, Holsten RD, Jackson EK, Burns RC. 1968. The acetylene-ethylene assay for N_2 fixation: laboratory and field evaluation. Plant Physiol 43(8): 1185-207.
Hardy RWF, Burns RC, Holsten RD. 1973. Applications of the acetylene-ethylene assay for measurement of nitrogen fixation. Soil Biol Biochem 5(1): 47-81.
Holmes R, Aminot A, Kerouel R, Hooker B, Peterson B. 1999. A simple and precise method for measuring ammonium in marine and freshwater ecosystems. Can J Fish Aquat Sci 56(10): 1801-8.
Il'chenko N. 1976. Catalytic-oxidation of ammonia. Usp Khim 45(12): 2168-95.
Kendall C and Grim E. 1990. Combustion tube method for measurement of nitrogen isotope ratios using calcium-oxide for total removal of carbon-dioxide and water. Anal Chem 62(5): 526-9.
McIlvin MR and Casciotti KL. 2011. Technical updates to the bacterial method for nitrate isotopic analyses. Anal Chem 83(5): 1850-6.
Mohr W, Grosskopf T, Wallace DWR, LaRoche J. 2010. Methodological underestimation of oceanic nitrogen fixation rates. PLoS One 5(9): e12583.
Montoya JP, Voss M, Kahler P, Capone DG. 1996. A simple, high-precision, high-sensitivity tracer assay for N_2 fixation. Appl Environ Microbiol 62(3): 986-93.
Montoya J, Holl C, Zehr J, Hansen A, Villareal T, Capone D. 2004. High rates of N_2 fixation by unicellular diazotrophs in the oligotrophic Pacific Ocean. Nature 430(7003): 1027-31.
Needoba JA, Foster RA, Sakamoto C, Zehr JP, Johnson KS. 2007. Nitrogen fixation by unicellular diazotrophic cyanobacteria in the temperate oligotrophic North Pacific Ocean. Limnol Oceanogr 52(4): 1317-27.
Ohyama T and Kumazawa K. 1981. A simple method for the preparation, purification and storage of $^{15}N_2$ gas for biological nitrogen fixation studies. Soil Sci Plant Nutr 27(2): 263-5.
Park J and Lee Y. 1988. Solubility and decomposition kinetics of nitrous-acid in aqueous-solution. J Phys Chem 92(22): 6294-302.

Qi H, Coplen T, Geilmann H, Brand W, Bohlke J. 2003. Two new organic reference materials for $\delta^{13}C$ and $\delta^{15}N$ measurements and a new value for the $\delta^{13}C$ of NBS 22 oil. Rapid Communications in Mass Spectrometry 17(22): 2483-7.

Scharff A, Egsgaard H, Hansen P, Rosendahl L. 2003. Exploring symbiotic nitrogen fixation and assimilation in pea root nodules by in vivo ^{15}N nuclear magnetic resonance spectroscopy and liquid chromatography-mass spectrometry. Plant Physiol 131(1): 367-78.

Sigman D, Casciotti K, Andreani M, Barford C, Galanter M, Bohlke J. 2001. A bacterial method for the nitrogen isotopic analysis of nitrate in seawater and freshwater. Anal Chem 73(17): 4145-53.

Staal M, Lintel-Hekkert ST, Harren F, Stal L. 2001. Nitrogenase activity in cyanobacteria measured by the acetylene reduction assay: A comparison between batch incubation and on-line monitoring. Environ Microbiol 3(5): 343-51.

Stam H, Stouthamer A, Vanverseveld H. 1987. Hydrogen metabolism and energy costs of nitrogen-fixation. FEMS Microbiol Lett 46(1):73-92.

Stewart WDP, Fitzgerald GP, Burris RH. 1967. In situ studies on N_2 fixation using the acetylene reduction technique. Proc Natl Acad Sci USA 58(5): 2071-8.

Wilson ST, Boettjer D, Church MJ, Karl DM. 2012. Comparative assessment of nitrogen fixation methodologies, conducted in the oligotrophic North Pacific Ocean. Appl Environ Microbiol 78(18): 6516-23.

Zhang L, Altabet MA, Wu T, Hadas O. 2007. Sensitive measurement of NH_4^+ $^{15}N/^{14}N$ ($\delta^{15}NH_4^+$) at natural abundance levels in fresh and saltwaters. Anal Chem 79(14): 5297-303.

Table 5. The quantity of ^{15}N-labeled contaminants detected relative to $^{15}N_2$ additions

	μmoles $^{15}N_X$ per mole $^{15}N_2$		
	$^{15}NO_3^-/NO_2^-$	**$^{15}NH_4^+$**	**$^{\underline{46}}N_2O$**
Sigma A1 lot # SZ1670V	420 ± 110	34 ± 11	≥ 21 ± 3
Sigma A2 lot # SZ1670V	420 ± 40	520 ± 30	109 ± 5[§]
Sigma A3[†] lot # SZ1670V	350 ± 80	N/A	≥ 63 ± 15
Sigma B[†] lot # MBBB0968V	1.8 ± 0.6	1900 ± 560	≥ 49 ± 17
Cambridge A lot # I1-11785A	n.d.[*]	0.052 ± 0.020	n.d.[*]
Cambridge B[†] lot # I-16727	0.024 ± 0.006	0.014 ± 0.004	≥ 0.81 ± 0.24
Campro Scientific[†] lot # EB1169V	n.d.[*]	N/A	≥ 11 ± 3

The μmoles of ^{15}N contaminants (NO_3^- + NO_2^-, NH_4^+, and N_2O) detected per mole of $^{15}N_2$ gas from lecture bottles provided by different suppliers. N/A = not available; n.d. = not detected.

*Not explicitly tested in high sensitivity $^{15}N_2$ dilutions

[†]Moles of $^{15}N_2$ estimated from the injection volume rather than direct measurements

[§] ^{46}N2O measured directly.

Table 6. Inferred N_2 fixation rates (nmoles N L^{-1} d^{-1}) resulting from ^{15}N-labeled contaminants

Ambient $[NH_4^+]$	Cambridge Isotopes *Cambridge A* Lot # I1-11785A 0.52 µmol $^{15}NH_4^+$/mol $^{15}N_2$			Sigma-Aldrich *Sigma A1* Lot # SZ1670V 25 µmol $^{15}NH_4^+$/mol $^{15}N_2$			Sigma-Aldrich *Sigma B* Lot # MBBB0968V 1900 µmol $^{15}NH_4^+$/mol $^{15}N_2$			Incubation Volume (L)
(µmol L^{-1})	µ = 0.1	µ = 0.2	µ = 0.3	µ = 0.1	µ = 0.2	µ = 0.3	µ = 0.1	µ = 0.2	µ = 0.3	
0.001	0.019	0.019	0.019	9.0	9.0	9.0	310	460	530	**0.25**
0.01	0.014	0.016	0.016	7.5	8.5	8.6	250	400	470	
0.1	n.d.	n.d.	n.d	1.6	2.7	3.6	90	170	220	
1	n.d.	n.d.	n.d.	0.17	0.32	0.45	13	24	34	
0.001	n.d.	n.d.	n.d.	0.50	0.50	0.50	38	38	38	**4.5**
0.01	n.d.	n.d.	n.d.	0.42	0.47	0.48	30	35	36	
0.1	n.d.	n.d.	n.d.	0.08	0.15	0.19	6.5	11	15	
1	n.d.	n.d.	n.d.	n.d.	0.012	0.017	0.7	1.4	1.9	

N_2 fixation rates that would be inferred from 24-h field N_2 fixation assays conducted with $^{15}N_2$ stocks containing the respective concentrations ^{15}N-ammonium contaminants detected in Sigma-Aldrich and Cambridge Isotopes $^{15}N_2$ gas. In the simulations, microbial plankton assimilate ^{15}N-ammonium rather than fix $^{15}N_2$. Incubations are simulated in volumes of 0.25 L or 4.5 L equilibrated with 0.1 mL of $^{15}N_2$ gas, with 2.0 x 10^{-7} µmol L^{-1} of plankton nitrogen (with a $\delta^{15}N$ = 0‰) assimilating at a range of specific growth rates, µ (d^{-1}), countered by equivalent recycling rates, at incremental concentrations of ambient ammonium ($\delta^{15}N_{NH4}$ = -2‰). Inferred rates of <0.01 nmoles N L^{-1} d^{-1} are considered undetectable (n.d.).

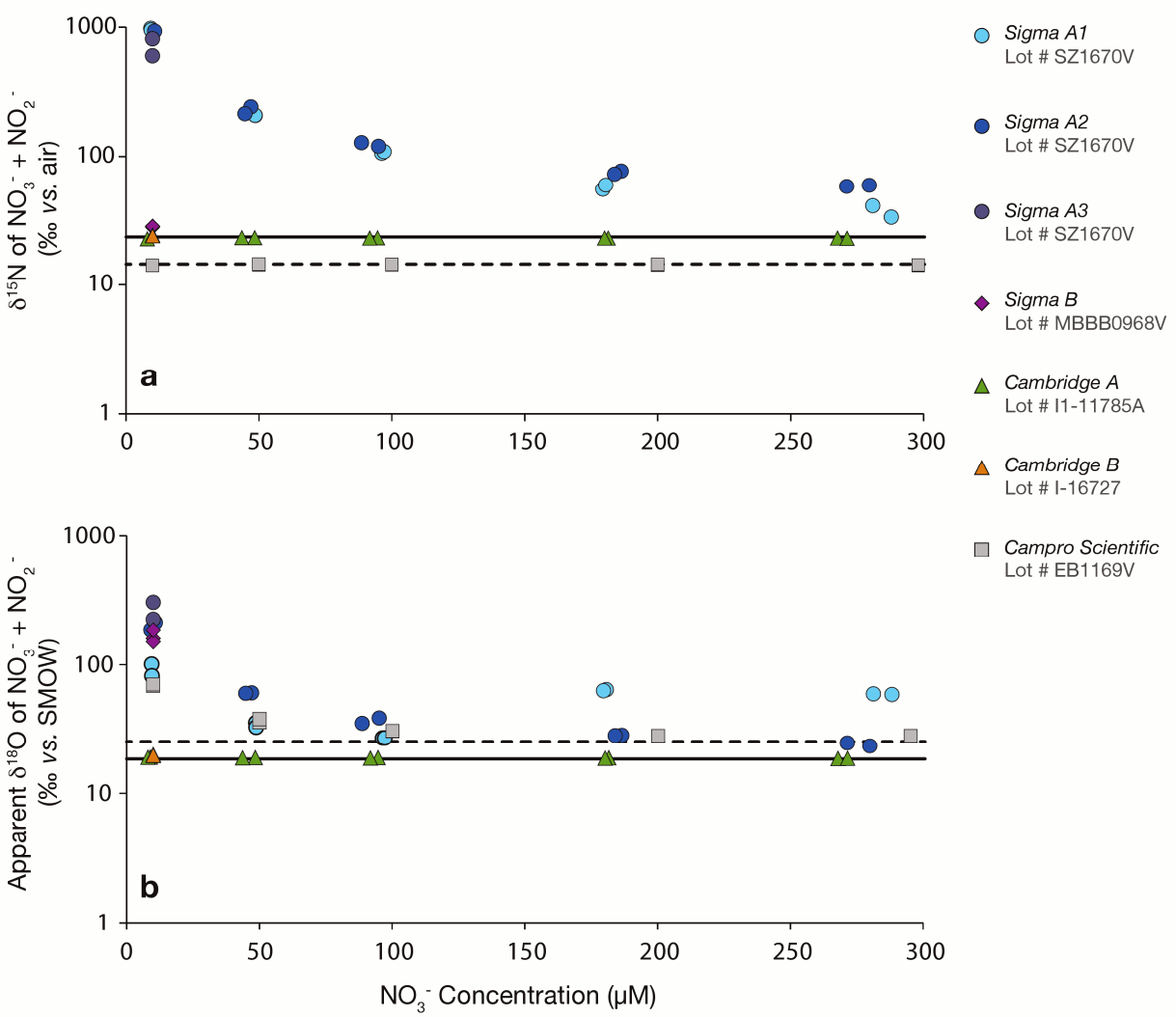

Figure 11. (a) $\delta^{15}N_{NO3+NO2}$ (log scale) of nitrate solutions (10-300 µmol L^{-1}) following equilibration with 0.1 mL $^{15}N_2$ gas from lecture bottles procured from three distributors. Solutions were 40 mL for Sigma-Aldrich and Campro Scientific equilibrations, and 100 mL for Cambridge Isotopes equilibrations. The solid line corresponds to the $\delta^{15}N_{NO3}$ of the control solutions for Sigma-Aldrich and Cambridge Isotopes experiments ($\delta^{15}N_{NO3}$ = 23.5 ± 0.5‰); the dashed line corresponds to controls for Campro Scientific experiments ($\delta^{15}N_{NO3}$ = 14.15 ± 0.1‰). Paired symbols identify replicate experimental treatments. **(b)** Corresponding apparent $\delta^{18}O_{NO3+NO2}$ of the experimental nitrate solutions. The solid line corresponds to the $\delta^{18}O_{NO3}$ of control solutions for the Sigma-Aldrich and Cambridge Isotope experiments ($\delta^{18}O_{NO3}$ = 18.9 ± 0.3‰); the dashed line corresponds to controls for Campro Scientific experiments (25.4 ± 0.3‰).

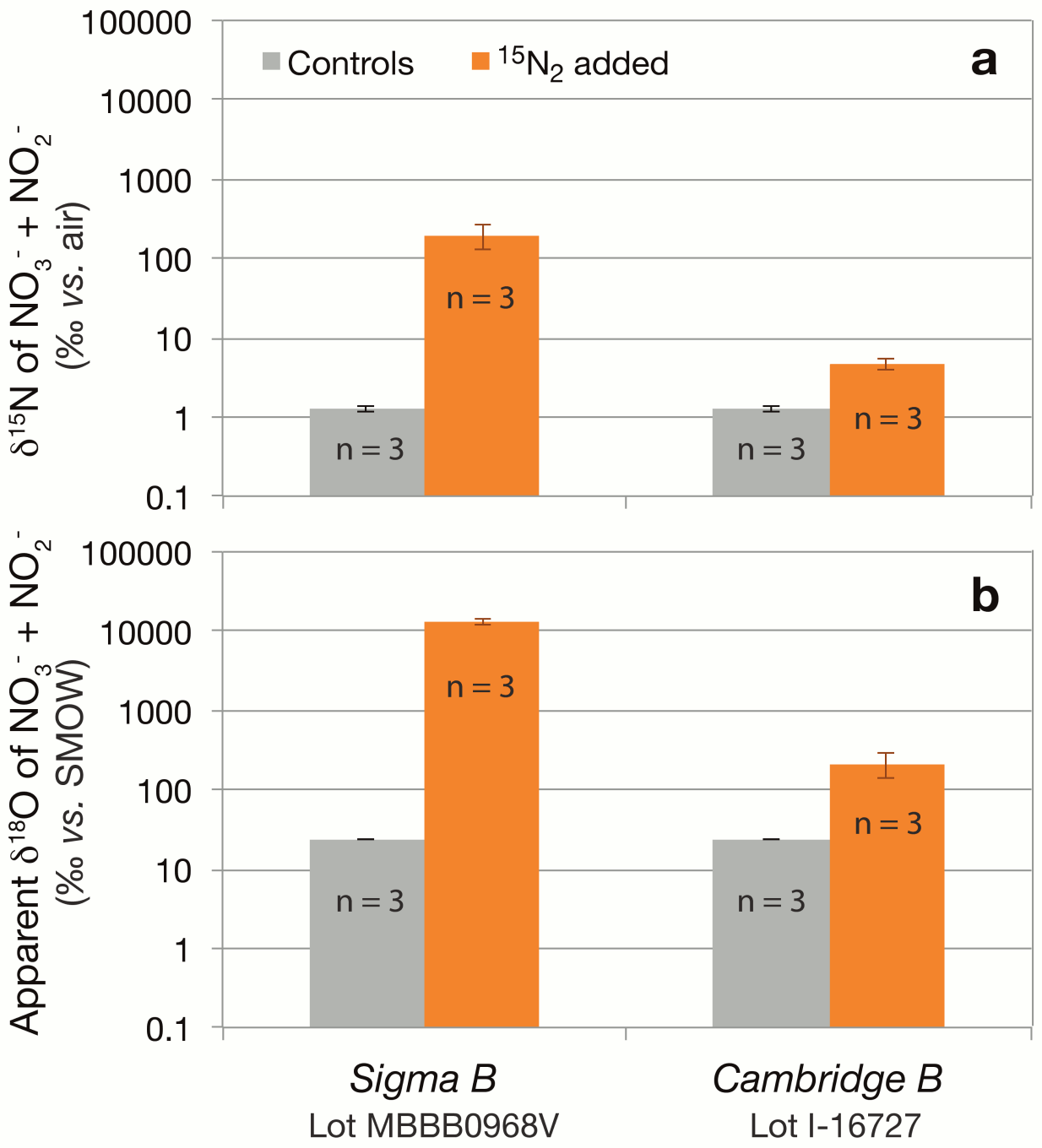

Figure 12. **(a)** $\delta^{15}N_{NO3+NO2}$ (log scale) of higher sensitivity equilibrations of 10 µmol L^{-1} nitrate solutions (10 mL) with 2 mL of $^{15}N_2$ gas from a Cambridge Isotopes or a Sigma-Aldrich bottle. **(b)** Corresponding apparent $\delta^{18}O_{NO3}$ (log scale) of higher sensitivity equilibrations of the two stocks. n = the number of experimental replicates.

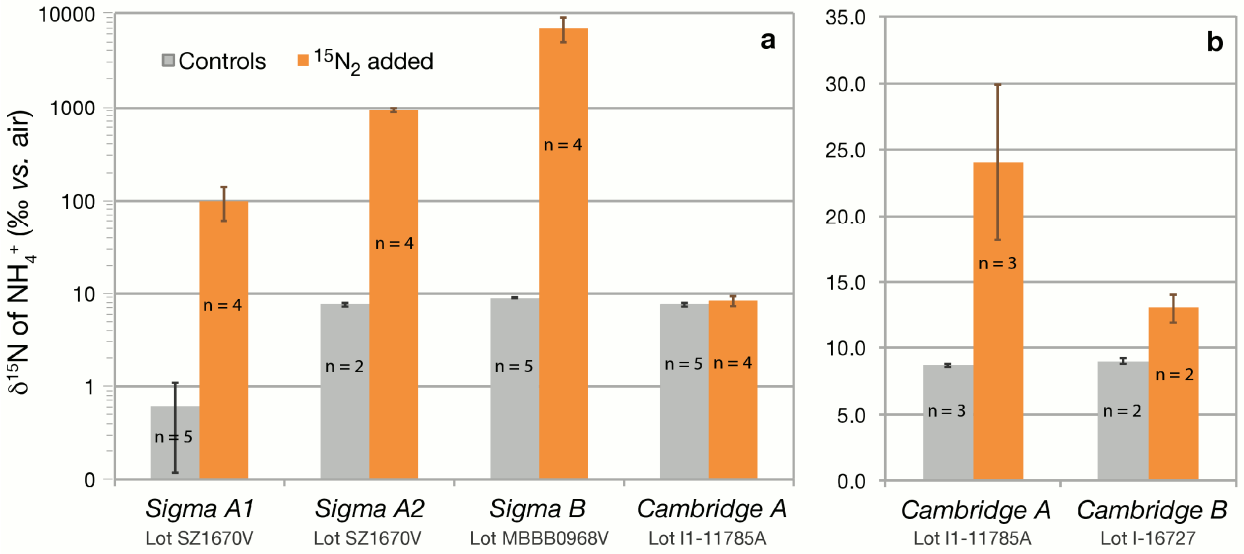

Figure 13. (a) $\delta^{15}N_{NH4}$ (log scale) of 5 µmol L^{-1} ammonium solutions after equilibration with 0.1 mL $^{15}N_2$ gas from respective Sigma-Aldrich and Cambridge Isotopes lecture bottles *vs.* control solutions. Sigma-Aldrich treatments utilized 40 mL ammonium solutions, whereas Cambridge Isotopes treatments utilized 100 mL ammonium solutions. **(b)** $\delta^{15}N_{NH4}$ of higher sensitivity equilibrations of 5 µmol L^{-1} ammonium solutions (10 mL) with 2.0 mL $^{15}N_2$ gas from Cambridge Isotopes lecture bottles *vs.* control solutions. n = the number of experimental replicates.

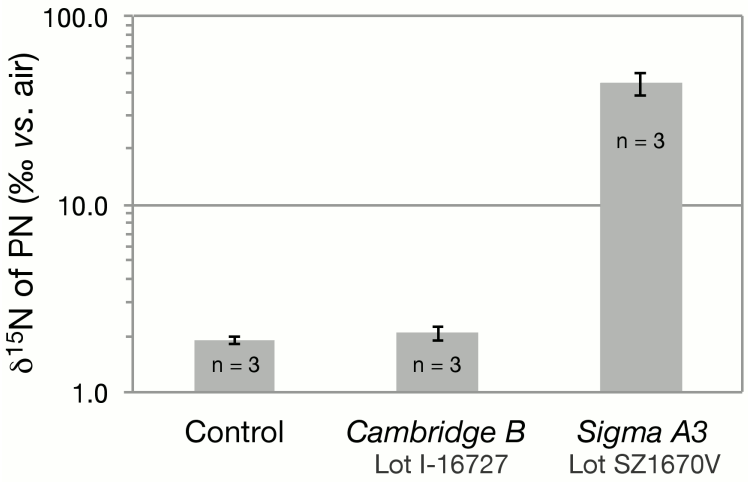

Figure 14. The $\delta^{15}N$ of particulate nitrogen ($\delta^{15}N_{PN}$) of *D. tertiolecta* harvested in stationary phase following growth in media containing sodium nitrate (and no ammonium) and equilibrated with $^{15}N_2$ gas from Sigma Aldrich or Cambridge Isotopes. n = the number of experimental replicates.